May 2015

A Study on the Synthesis - Structure - Property - Performance Relationship of Bulk Functionalized Polyurethane Foams for Water Filtration Applications

Subhashini Gunashekar
University of Wisconsin-Milwaukee

A STUDY ON THE SYNTHESIS – STRUCTURE – PROPERTY – PERFORMANCE RELATIONSHIP OF BULK FUNCTIONALIZED POLYURETHANE FOAMS FOR WATER FILTRATION APPLICATIONS

By

Subhashini Gunashekar

A Dissertation Submitted in

Partial Fulfillment of the

Requirements for the Degree of

Doctor of Philosophy

in Engineering

at

The University of Wisconsin-Milwaukee

May 2015

ABSTRACT

A STUDY ON THE SYNTHESIS – STRUCTURE – PROPERTY – PERFORMANCE RELATIONSHIP OF BULK FUNCTIONALIZED POLYURETHANE FOAMS FOR WATER FILTRATION APPLICATIONS

by

Subhashini Gunashekar

The University of Wisconsin-Milwaukee, 2015
Under the Supervision of Dr. Nidal H Abu-Zahra

Polymers, macromolecules made of repeat units, are one of the major building blocks of life. They exist naturally in the form of DNA, proteins, sugars, cellulose, natural rubber etc. However, it was only in the mid twentieth century man began to understand its true nature and developed a new class of materials called 'Plastics'. In recent years, the concept of a truly tailor made polymer has become a reality as a result of better understanding of the polymer structure-property relationships, newer polymerization techniques and due to the availability of new low cost monomers. Polymers from different elements with any desired property can be produced today. These polymers may be in the form of solid plastics, fibers, elastomers and foams. The endless possibilities of the structure – property – processing relationships, has led to fascinating applications of these materials.

The pliable nature of polymer materials render them lucrative for many applications. They are becoming prominent in the water industry as the need for water and waste water treatment products increase to solve the global water woes. Contamination of water sources

by lead has been a cause of concern for several decades. Stringent regulations to treat water or waste water from lead are in place throughout the world due to the harmful health effects of lead toxicity.

Polymer based, surface functionalized ion exchange resins can be fabricated to selectively prefer multiple heavy metal ions such as lead, arsenic etc. This advantage of tailor ability among various others outweigh the limitations of polymer resins, such as, fouling and high operational costs. It has been found that bulk functionalization of polymers compared to surface functionalization can improve the efficiency and lower the operation costs of heavy metal ion filtration systems. Hence research in this area to develop and analyze other ion exchange systems is vital for practical purposes.

This research is thus aimed at developing and understanding the merits and limitations of a bulk functionalized filtration system to overcome the above said limitations. Foams are usually preferred over monolithic forms for their increased surface area. Polyurethane (PU) foams have been considered by researchers for their adsorptive and ion exchange nature. The ease of processing PU foams has kindled the interest of many researchers to develop PU foam based, novel heavy metal ion filtration systems.

This research work focuses on synthesizing bulk functionalized PU foams using a suitable chain extender. A chain extender is usually multifunctional: one, as a low-molecular weight species it links linear chains or chain segments to obtain the final polymer; two, it provides functional

groups capable of reacting with other chemical species. N, N- bis (2-hydorxyethyl)-2-aminoethane-sulfonic acid (BES), is a chain extender containing sulfonic acid groups which are capable of exchanging lead ions from aqueous solutions. PU foam synthesized using BES will thus be bulk functionalized with selectivity to lead ions.

Bulk functionalized PU foams, have been synthesized by earlier researchers as a cation exchange media for continuous electro deionization (CEDI) process with an ion exchange capacity of 2.5 meq/L, though no understanding of the process – structure – properties – performance relations were investigated. The cation exchange nature of the aforesaid system is exploited in this research to selectively treat lead ions from water. The structure-property-process-performance relationship of this foam system are investigated thoroughly to determine the effect of the process and application variables on the lead ion removal performance of the foam at parts per billion levels. In the due course of the study, the optimum composition, foam structure and morphology, and the mechanism of lead removal were determined to identify the rate limiting factors for lead ion removal.

Results show that poly propylene glycol (PPG) and toluene diisocyanate (TDI) used in a molar ratio of 1:2 are best suited to produce open cell PU foams and the choice of this polyol and isocyanate system is suitable to incorporate the chain extender, BES by dissolving it in a solvent, dimethyl sulfoxide (DMSO). However, DMSO is the rate limiting factor in the foam formulation, as it is a strong solvent capable of dissolving PU foam. Higher amounts of this solvent in the foam formulation will affect the foam structure at a molecular level. Batch

adsorption isotherms and column tests indicate that the functionalized PU foam is capable of removing lead ions by both adsorption and ion exchange mechanisms. The lead ion removal efficiency of the foam depends on several parameters such as the initial concentration of lead ions in the solution, pre-conditioning of the foam, pore size, pore distribution and the foam formulation itself which determines the structure of the foam. The pH of the solution has little effect on the lead removal efficiency of the foam unlike other ion exchange resins. Batch and column tests show 87-88% lead removal efficiency of the functionalized PU foam.

The performance of the functionalized PU foams was benchmarked against commercial activated carbon and ion exchange resins. The results show that the efficiencies of the functionalized PU foam are comparable to that of the commercial media, until equilibrium is reached and soon after, it starts to drop as the foam surface is saturated by lead ions due to adsorption which limits the ion exchange ability of the functionalized PU foam. A case study on product development, suggests that the functionalized PU foam has the potential to be developed as a pre-filter to complement the existing reverse osmosis (RO), ultraviolet (UV), granulated activated carbon (GAC) and ion exchange systems by extending their life while serving as a multipurpose pre-filter, capable of removing lead ions and filtering sediment and silt from the influent.

To

My loving husband, for believing in me and supporting me since the day we met;

My precious son, for giving me a challenging and unforgettable grad school experience in his terrible 2's and 3's;

My parents, family and friends for their unconditional love and encouragement; and

The scientific community for nurturing my intellect and scientific curiosity!

TABLE OF CONTENTS

LIST OF FIGURES

LIST OF TABLES

NOMENCLATURE

PU – Polyurethane

TDI – Toluene Diisocyanate

PPG – Poly propylene Glycol

BES – N, N-bis (2-hydorxyethyl)-2-aminoethane-sulfonic acid

DMSO – Dimethyl Sulfoxide

DBTL – Dibutyl tin diluarate

CERT – Chain extender reaction time

ppb – parts per billion

ACKNOWLEDGEMENTS

I wish to express my sincere thanks to my mentor and adviser Dr. Nidal H. Abu-Zahra, for his able guidance throughout the course of my graduate studies at UWM. His profound knowledge and encouragement has molded me into a more confident individual with a clear vision for my future. I am also grateful to, Dr. Benjamin C. Church and Dr. Changsoo Kim, from the Materials Science and Engineering Department, Dr. Rani El-Hajjar from Civil Engineering and Dr. Stanislav D. Dobrev from the Lubar School of Business for serving on my doctoral committee. Their valuable time, patience and intellectual contributions have helped me complete my dissertation successfully. I place on record my sincere thank you to Dr. Krishna M. Pillai, from the Mechanical Engineering Department, for sharing his expertise and guiding me to understand and analyze the flow properties of the tailor-made polyurethane foams discussed in this research work.

I am extremely thankful to Dr. Ernie Lee from AO Smith, for agreeing to be my industrial consultant and mentor and sharing his expertise on water chemistry and water treatment media. His valuable feedback and inputs were significant in this research work to understand the practical aspects of developing a media for water filtration applications. I would be remiss if I do not place on record, his generosity for extending the column test equipment at the Global Water Center, in Milwaukee, to study the performance of the tailor-made polyurethane foams. I would like to place on record my thanks to Mr. Chris Genthe, from Rockwell automation for accommodating our request and assisting me with image analysis via optical microscopy.

I am greatly indebted to Sue Krezoski, from the Chemistry and Biochemistry Department at UWM for scheduling and setting-up the ICP-MS which was significant for the performance analysis in this research work. I wish her a joyous retirement and thank her for her kind services. I am also grateful to Dr. Marianna Orlova and Dr. Shongding Liu, from the Biological Sciences Department at UWM, for their guidance and assistance in the GPC analysis. I am very grateful to Dr. Henry Tomasiewicz, from the Bioengineering Imaging and Testing Lab, at the Innovation Campus in Wauwatosa, for his valuable time and sharing his expertise with the Micro-CT analysis. I would also like to thank Betty Warras, Penelope Stiglitz and Shelly Fowler, for their guidance, support and encouragement throughout my Graduate studies. I take this opportunity to express my gratitude to all of the Department faculty members and the teachers and staff of the dragonfly room at the UWM Children's center for their help and support.

I would like to extend my profound thanks and gratitude to my dear friends and neighbors, Kala and Kannan for lending me a hand with my son when needed the most. Their unconditional support has been crucial in the completion of my dissertation on time. I would like to express my gratitude to one and all, who directly or indirectly, have lent their hand in this venture.

Chapter I: Introduction and Theoretical Background

1.1 Lead in Water: An Overview

The progress of our society, since the pre-historic ages, has been measured by our ability to use metals. Metals have not only made our lives easier but are also vital for our well-being. Metal ions such as iron (II), calcium, potassium and magnesium are essential for the health of human beings and other organisms. These ions are obtained primarily from the foods we consume as well as the water we drink.

However, not all metal ions which are present in our waters are beneficial for our wellbeing. Some heavy metal ions[1], such as lead, mercury, and arsenic are harmful as they bind to proteins in biological systems and prevent them from performing their intended tasks. Heavy metal poisoning is usually due to bioaccumulation, which is a process by which organisms can take up contaminants more rapidly than their bodies can eliminate them. Their accumulation in biological systems can damage the nervous system, kidneys, liver and even cause death. Figure 1 provides a brief insight on the effects of heavy metal toxicity on human beings [1]. The toxicity of heavy metals and the specific symptomatology varies according to the metal, the total dose absorbed, and whether the exposure was acute or chronic. The age of the person can also influence toxicity. For example, young children are more susceptible to the effects of lead exposure because they absorb several times the percent ingested compared with adults and because their brains are more plastic, even brief

[1] Heavy metals are called so due to their atoms, which have a greater mass than the masses of essential metallic elements.

exposures may influence developmental processes [2]. Hence an understanding of heavy metal ions and their chemistry is important and vital for our survival.

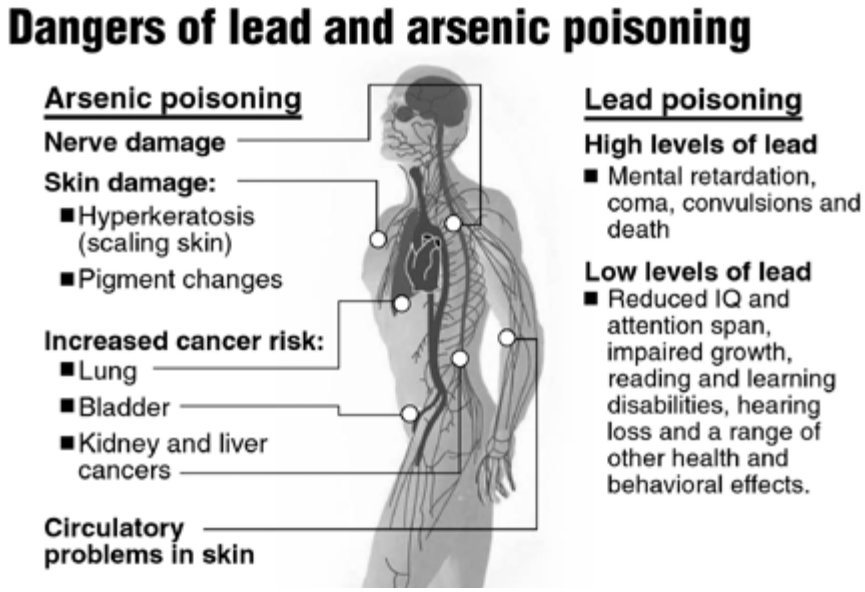

Figure 1: Health hazards of Heavy Metal Poisoning [1]

Most elements found in nature are in the form of ions. An ion is an atom or a molecule, which has lost or gained an electron and thus acquired an electrical charge. These ions are of two types; cations and anions based on the charges they carry. Positively charged ions are called *cations* and negatively charged ions are called *anions* [3].

Lead is one of the most familiar toxic heavy metal ions. Lead exposure to biological systems can be by air, water, soil, food or consumer products. Occupational exposure is also one of the causes of lead exposure in adults. Some of the major sources of lead contamination are: lead paints, lead solder used in plumbing, lead pipes, leaded brass faucets, lead containing gasoline, pesticides

(used in the past), cosmetics, foundries automobile electrical storage batteries, cooing vessels etc. Lead from air and soil can end up in water bodies. Lead can also be in drinking water, corrosion of the old plumbing lines and the fixtures can contaminate water. Another major cause for concern is the quality of water; some places have a higher water acidity which accelerates the breakdown of lead from plumbing lines. By increasing the pH of the water this process can be slowed to a certain extent.

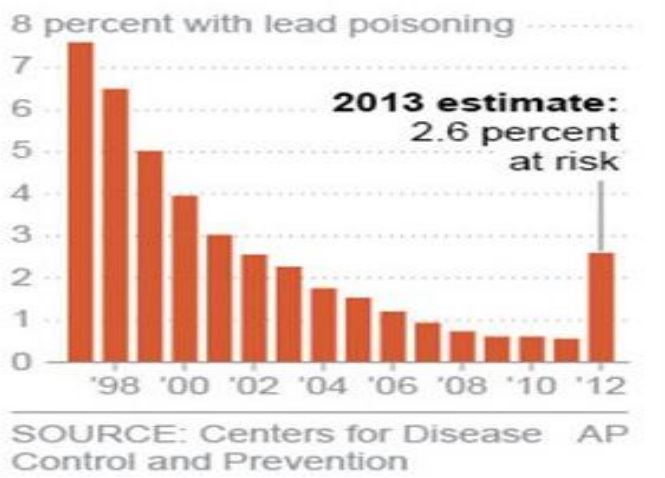

Figure 2: Statistics on Lead Poisoning in Children [3]

Lead poisoning used to be a much larger concern in the United States, but it has declined significantly as lead was removed from paint and gasoline and other sources. However, recent statistics show that more than half a million U.S. children are now believed to have lead poisoning, roughly twice the previous high estimate, as reported by health officials, as shown in Figure 2. The increase is the result of the EPA lowering the threshold (0 ppb) for lead poisoning in 2012, so now more children are considered at risk. The new number translates to about 1 in 38

young children. This estimate suggests a need for more testing and preventive measures to avoid lead poisoning [4].

The main issue with heavy metal ions such as lead ions, is that they are hard to detect in water at very low concentrations and are even more difficult to remove [5]. Adequate measures are being taken since the issue was first identified to minimize or avoid heavy metal ions reaching the ground water and other water bodies. However, on a large scale, this task proves to be challenging. Methods to remove these heavy metal ions from aqueous solutions have been developed since the early 1900's.

It started with the need to soften hard water by exchanging ions causing hardness in water and since then various materials have been developed to function as ion exchange media for various purposes such as dealkalization, deionization or demineralization etc. Some of the conventional methods available for heavy metal ions removal from aqueous solutions are:

- Chemical precipitation
- Chemical oxidation
- Chemical reduction
- Ion exchange
- Filtration
- Electrochemical treatment
- Evaporation

Significant disadvantages in all these procedures such as incomplete removal, high energy requirements, production of toxic sludge or waste products, which require disposal and the cost have led to the need for research and development in this field to identify other alternative methods or materials to overcome these limitations [6].

1.2 Ion Exchange

The ion exchange mechanism is a perfect tool to remove or exchange contaminants present in low concentrations. An ion exchange reaction is a reversible chemical reaction where ions are exchanged from a solution for similar ions attached to an immobilized solid phase. This solid ion exchange phase can be in the form of particles such as naturally occurring inorganic zeolites or synthetically produced organic resins. Ion exchange materials can be classified as cation exchange materials and anion exchange materials based on the charge of the mobile ion available for exchange as shown in Figure 3 [7, 8].

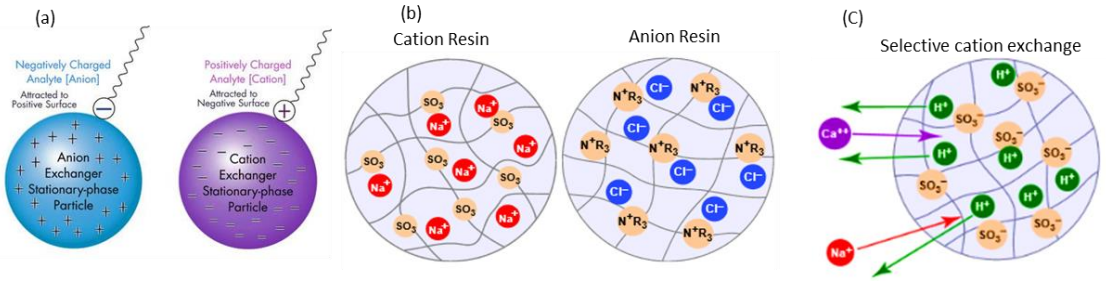

Figure 3: (a) Schematic of cation and anion exchangers [7] (b) Cation (Na^+) and Anion (Cl^-) exchange resin beads with SO_3 and N^+R_3 functional groups, respectively (c) Selective cation exchange [8]

The major ion exchange materials used in deionization are synthetic resins made by the polymerization of various organic compounds. An organic ion exchange resin is composed of high-molecular-weight polyelectrolytes, which can exchange their mobile ions for ions of similar charge from the surrounding medium. Each resin has a distinct number of mobile ion sites, which set the maximum quantity of exchangers per unit of resin. Both anion and cation resins are produced from the same basic organic polymers. They differ in the ionizable group attached to the hydrocarbon network as shown in Figure 3b. It is this functional group which determines the chemical behavior of the resin. Thanks to differences of affinity for different ions, common ion exchange resins can be used to remove selective ions from water, Figure 3c [8]. A broader classification of ion exchangers is shown in Figure 4 [9].

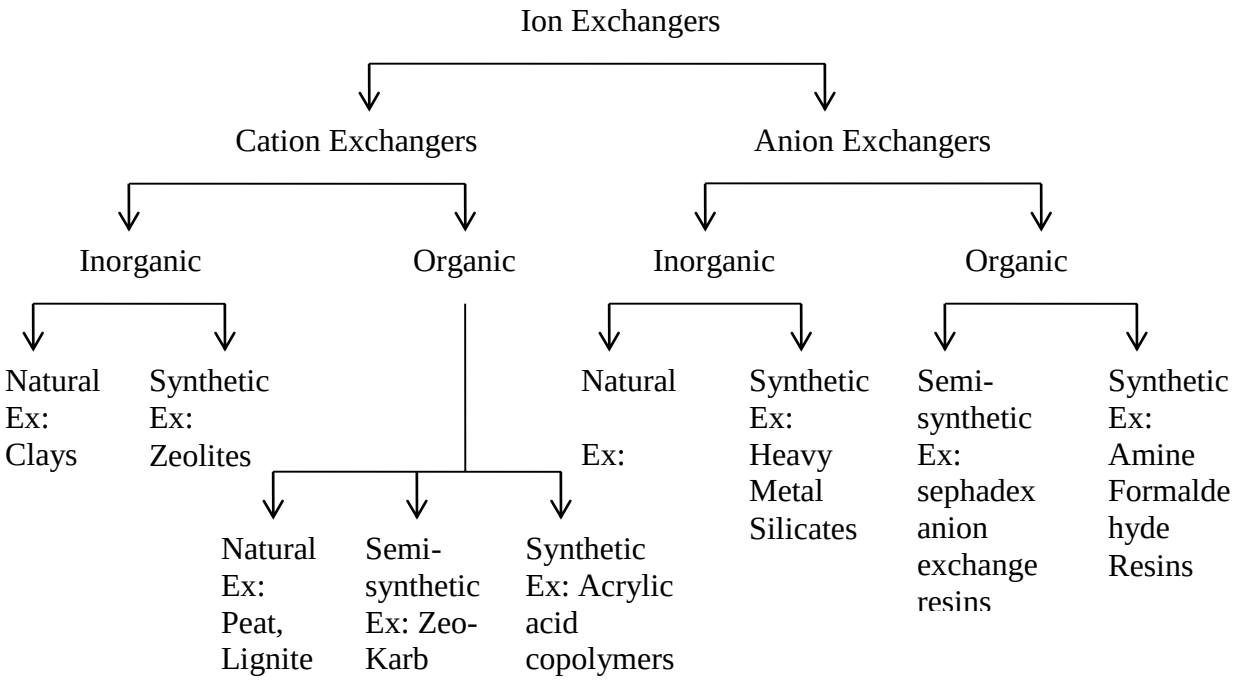

Figure 4: General classification of ion exchange materials

1.2.1 Ion Exchange Mechanism

Deionization (or demineralization) simply means the removal of ions. Ions are electrically charged atoms or molecules found in water, which has either a net negative or positive charge. For many applications, which use water as a rinse or ingredient, these ions are considered impurities and must be removed from the water. Ions with a positive charge are called "Cations" and ions with a negative charge are called "Anions". Ion exchange resins are used to exchange non desirable cations and anions with hydrogen and hydroxyl ions; respectively, forming pure water (H_2O), which is not an ion as shown in Figure 5. Table 1 shows a list of ions commonly found in municipal water: [10]

Table 1: Ions found in Municipal water

Cations (removed by cation resins)	**Anions (removed by anion resins)**
Calcium (Ca^{2+})	Chlorides (Cl^-)
Magnesium (Mg^{2+})	Sulfates (SO_4^{2-})
Iron (Fe^{2+})	Nitrates (NO_3^{2-})
Manganese (Mn^{2+})	Carbonates (CO_3^{2-})
Sodium (Na^{2+})	Silica (SiO_2^-)
Hydrogen (H^+)	Hydroxyl (OH^-)

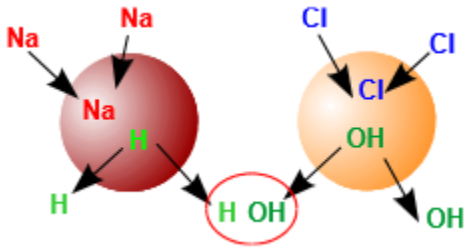

Figure 5: Ion exchange summary [9]

Ion exchange mechanism is thus based on the principle of electro-neutrality. Ion exchange in demineralization takes place with equilibrium reactions. They may be expressed in simple terms by the following two equations:

$$\underline{\text{Cation exchange}}: Z_s.a^+ + b^+ = Z_s.b^+ + a^+$$

Where $\mathbf{Z_s}$ is the matrix and anionic fixed site of the cationic exchanger, $\mathbf{a}^+$ and $\mathbf{b}^+$ are two cations.

$$\underline{\text{Anion exchange:}}\ A_s.c^- + d^- = A_s.d^- + c^-$$

Where $\mathbf{A_s}$ is the matrix and cationic fixed site of the anionic exchanger, $\mathbf{c}^-$ and $\mathbf{d}^-$ are two anions.

Ion exchange equilibria are strongly affected by interactions of the counter ions with other components in the external solution. Interactions with the co-ion are particularly important because the co-ion is rather efficiently excluded from the resin phase, so that the effect of interactions in the solution is not compensated by that of similar interactions in the ion exchanger. The counter ions may form weakly dissociated aggregates or complex ions with the

co-ions. Application of Le Chatelier's principle[2] to the ion exchange equilibrium, shows that reverse exchange is favored when the species B is sequestered in the solution by reaction with the co-ion. Thus the ion exchanger prefers the counter ion which associates less strongly with the co-ion. [11]

$$\bar{A} + B \leftrightarrow \dot{B} + A$$

Ion exchange resins are classified as strong and weak acid or base cation or anion resins, respectively based on the type of functional groups attached to them and their reactivity. Strong cation exchange resins usually contain sulfonic acid ($-SO_3H$) groups or their corresponding salts and behave as strong acids. Consequently, the exchange capacity of strong acid resins is independent of solution pH. These resins would be used in the hydrogen form for complete deionization. Weak acid cation resin behave similar to weak organic acids, which are weakly dissociated and the ionizable group is a carboxylic acid (COOH). Weak acid resins exhibit a much higher affinity for hydrogen ions than strong acid resins. Strong base cation resins are highly ionized and can be used over the entire pH range. These resins are used in the hydroxide (OH) form for water deionization. They will react with anions in solution and can convert an acid solution to pure water. Weak base resins are similar to weak acid resins, in which the degree of ionization is strongly influenced by pH. Consequently, weak base resins exhibit minimum exchange capacity above a pH of 7.0

[2] Le Chatelier's principle states that if a dynamic equilibrium is disturbed by changing the conditions, the position of equilibrium moves to counteract the change. [12]

Regeneration of the exhausted exchange material to its original state is another important aspect of the ion exchange mechanism. Regeneration is generally initiated after most of the active sites have been used and the ion exchange is no longer effective. The properties of the regenerant used are similar to those of a weak acid resin; the ion exchange resin can be converted to the hydrogen form with slightly greater than stoichiometric doses of acid because of the fortunate tendency of the heavy metal complex to become less stable under low pH conditions. Regeneration of a fixed-bed column usually requires between 1 to 2 hours. The regeneration frequency depends on the volume of resin in the exchange columns and the quantity of heavy metals and other ionized compounds in the wastewater. [13]

Commercial ion exchange resins are very small plastic beads, with a diameter of about 0.6 mm as shown in Figure 6a. These beads are porous and contain invisible water inside the beads, measured as “humidity” or “moisture content”. The structure of the resin is a polymer on which a fixed ion has been permanently attached. This ion cannot be removed or displaced; it is part of the structure. To preserve the electrical neutrality of the resin, each fixed ion must be neutralized with a counter ion. This counter ion is mobile and can get into and out of the resin bead as shown in Figure 6b.

Polystyrene is the most frequently used ion exchange resin synthesized using styrene and divinylbenzine. Styrene forms a liner polymer chain and divinylbenzine holds the long polymer chain by cross-linking it. The synthesis involves the mixing of both compounds with peroxide and a stabilizing agent. This mixture is then added to water and then agitated which leads to the

formation of droplets. Application of heat until polymerization begins, and then cooling the mixture increases the viscosity of the droplets, once polymerization is completed these droplets take the form of beads. The beads thus formed constitute the polystyrene matrix.

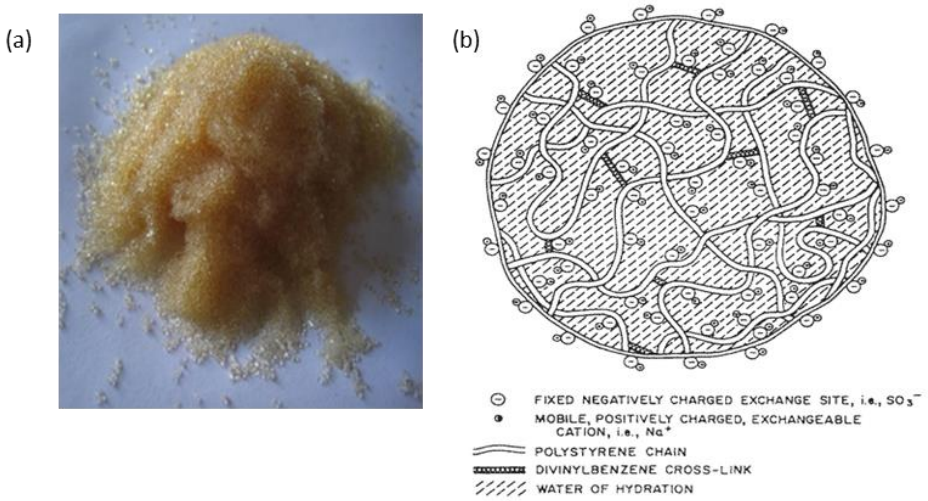

Figure 6: (a) Commercial polystyrene ion exchange resin bead (b) Schematic of a single ion exchange resin bead [14]

Treating the polystyrene beads with concentrated sulfuric acid attaches the $–SO_3H$ functional groups to the hydrocarbon chain and makes them strong acid cation exchangers. These sulfonic functional groups provide the fixed SO_3^- anions and the mobile H^+ cations, which can be exchanged with other heavy metal cations. On the other hand, if the matrix is chloromethylated and aminated they can be used as anion exchangers. The resin beads shrink when they are dry and the chains are closely intertwined together, this avoids the penetration of ions into the beads. However when placed in water the resin beads take on water and start swelling. This leads to the spreading of chains and permits the diffusion of ions. [8, 9, 15]

1.3 Adsorption

Adsorption is a process which occurs when a solute accumulates on the surface of an adsorbent, forming a molecular or atomic film (the adsorbate). Adsorption is operative in most natural physical, biological, and chemical systems, and is widely used in industrial applications such as activated charcoal, synthetic resins and water purification [16]. The most common industrial adsorbents are activated carbon, silica gel, and alumina, because they present enormous surface areas per unit weight. However, the available surface area is also a limitation in the adsorption process as a surface already heavily contaminated by adsorbates is not likely to have much capacity for additional binding [17].

Similar to surface tension, adsorption is a consequence of surface energy. In a bulk material, all the bonding requirements (ionic, covalent or metallic) of the constituent atoms of the material are filled. But atoms on the surface experience a bond deficiency, because they are not wholly surrounded by other atoms. Thus it is energetically favorable for them to bond with whatever is available in its immediate surroundings. The exact nature of the bonding depends on the species involved, but the adsorbed material is generally classified as exhibiting physisorption or chemisorption [16].

Physisorption or physical adsorption is a type of adsorption in which the adsorbate adheres to the surface only through weak intermolecular interactions or bonds called Van der Waals bonds. On the other hand, chemisorption is a type of adsorption whereby a molecule adheres to a surface through the formation of a chemical bond, these bonds are usually stronger in nature compared to

the bonds formed by physisorption [16]. A schematic of the heavy metal ion adsorption process by physisorption and chemisorption is shown in Figure 7 [18].

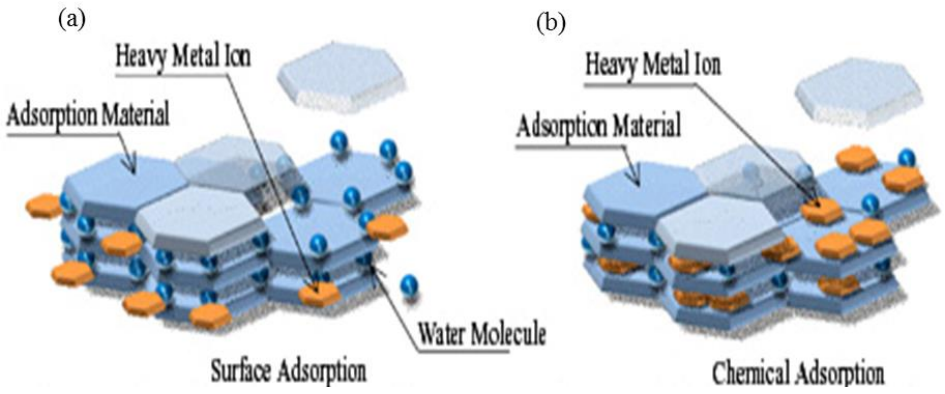

Figure 7: Schematic Diagram of (a) Physisorption and (b) Chemisorption processes [18]

Adsorption mechanism is usually described through isotherms using functions, which connect the amount of adsorbate on the adsorbent, with its pressure in case of gases or, its concentration in case of liquids. Several models namely Freundlich isotherm, Langmuir isotherm, BET isotherm, etc. are available in literature to describe the adsorption process [16].

1.3.1 Adsorption Mechanism and Isotherms

Adsorption is a useful filtration process when the contaminant is in very dilute concentrations. If the adsorbent and adsorbate are contacted long enough, an equilibrium will be established between the amount of adsorbate adsorbed and the amount of adsorbate in solution. The equilibrium relationship is described by adsorption isotherms. An adsorption isotherm is a curve relating the equilibrium concentration of a solute on the surface of an adsorbent, q_e, to the

concentration of the solute in the liquid, C_e, with which it is in contact. In general, an adsorption isotherm relates the volume or mass adsorbed to the concentration of the adsorbate in the main stream at a given temperature. Adsorption on a surface can be physical, chemical, monolayer or multilayer depending on the ratio of the equilibrium concentration of the solute on the surface of the adsorbent to the concentration of the solute in the liquid (q_e/C_e). The concept of the adsorption isotherm is very important, because the amount loaded to the surface at equilibrium depends on how much is left in the water [19].

Adsorption isotherms are generated by simple batch experiments. Varying amounts (loading) of the adsorbent is exposed to a fixed amount of the adsorbate/solute with an initial conetration, C_o in mg/L, in a solution as shown in Figure 8. The equilibrium concentration, C_e in mg/L, is determined by the remaining amount of the solute/adsorbate in the solution by analytical methods. The equilibrium concentration of the solute on the surface or the adsobate on the adsorbent, q_e in mg/g, is determiend by equation 1:

$$q_e = \frac{(C_o - C_e)V}{M} \qquad (1)$$

Where V is the volume of the solution in liters and M is the mass of the adsorbent in grams. A plot of q_e as a function of C_e is then used to determine the adsorption mechanism.

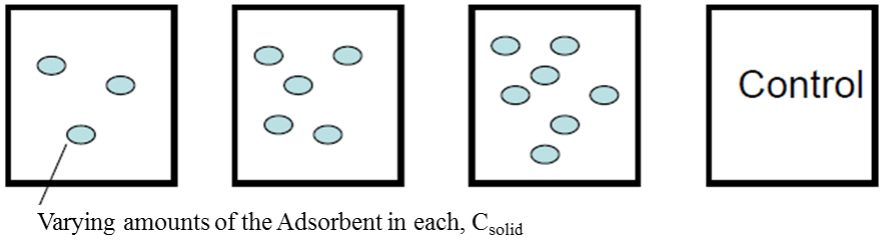

Figure 8: Batch test to determine the adsorption isotherms [20]

There are several models to predict the adsorption equilibrium based on the q_e/C_e relationship, among them the following four are predominant: Linear, Langmuir, BET and Freundlich.

The *linear* function is the simplest and most widely used adsorption isotherm equation as shown in equation 2 and in Figure 9; respectively:

$$q_e = K\,C_e \qquad (2)$$

Where K is the distribution co-efficient which is widely used in describing the contaminant adsorption in flowing systems.

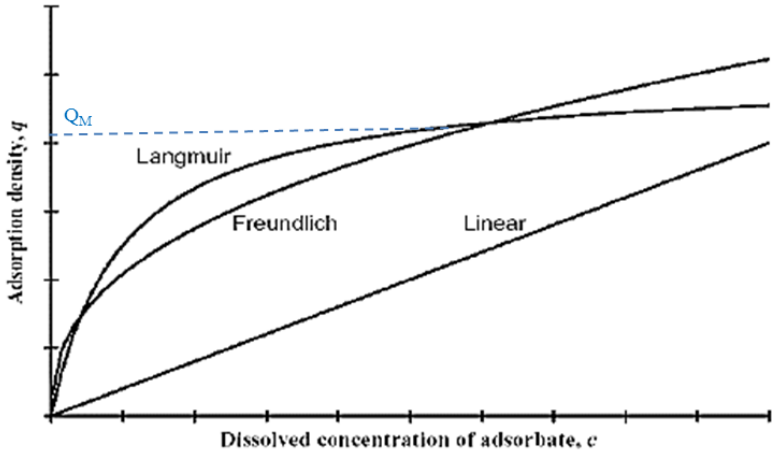

Figure 9: Adsorption Isotherms [20]

The *Langmuir* adsorption isotherm is a second order reaction, it assumes monolayer coverage of the adsorbate on the adsorbent surface with an equal probability of adsorption on all the sites and is represented by equation 3:

$$q_e = \frac{Q_M K_C}{1 + K_C} \qquad (3)$$

Where, Q_M is the maximum adsorption per unit mass and K is the affinity parameter.

Freundlich isotherm is an empirical equation, which is more widely used. It is also the oldest of the nonlinear isotherms and its use implies heterogeneity of adsorption sites. The Freundlich adsorption isotherm equation is:

$$q_e = K_F {C_e}^{1/n} \qquad (4)$$

Where, K_F is an indicator of adsorption capacity and 1/n is a measure of intensity of adsorption. The adsorption is usually favorable at higher 1/n values (n < 1). In other terms 1/n is also called the heterogeneity parameter. The expression reduces to a linear adsorption isotherm when n=1.

BET (Brunauer, Emmet and Teller) is a more general multi-layer adsorption isotherm (Figure 10) model, which assumes a Langmuir isotherm for each layer with no transmigration between the layers. It also assumes that each layer, has the same adsorption energy except the first layer.

The BET isotherm equation is:

$$q_e = \frac{K_B C_e Q_M}{(C_s - C_e)\left\{1 + (K_B - 1)\left(\frac{C_e}{C_s}\right)\right\}} \qquad (5)$$

Where, K_B is a parameter relating to the binding intensity of all the layers in L/mg, C_e is the equilibrium concentration of solute in the solution in mg/L, Q_M is the maximum amount of solute adsorbed per unit weight of the solid at equilibrium in mg/g and C_s is the solubility limit of the

solute in mg/L. The BET isotherm approaches the Langmuir isotherm when $C_e << C_s$ and $K_B > 1$ [21].

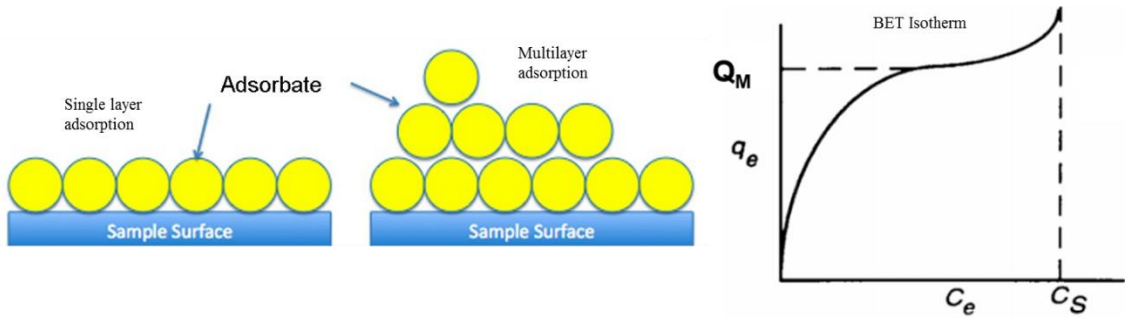

Figure 10: Schematic diagrams of single and multilayer adsorption and BET isotherm

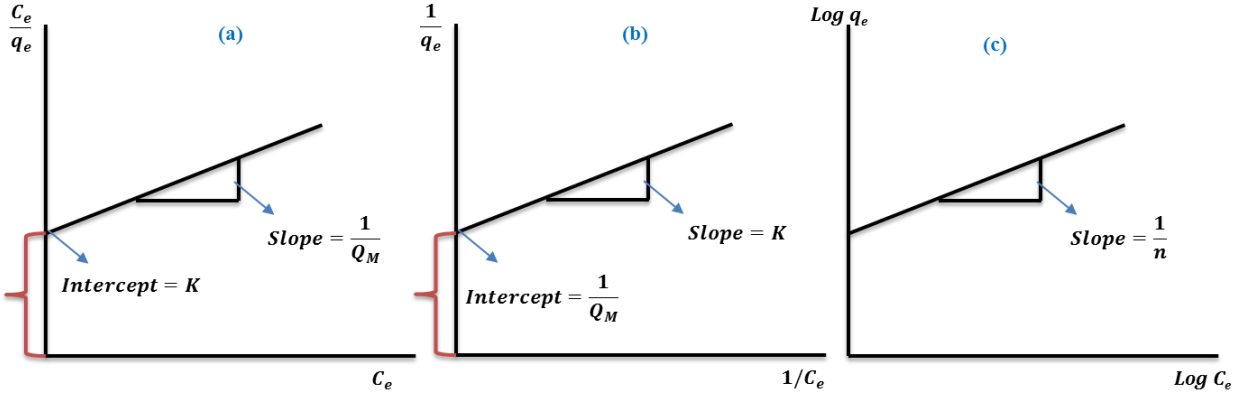

Figure 11: Adsorption isotherm analysis, plots (a) and (b) are linearization of Langmuir and (c) is linearization of Freundlich isotherm models respectively

The data from the batch experiments are analyzed by linearizing the models to determine which model can be used to determine the adsorption mechanism of a particular adsorbent/adsorbate system. For example, a plot of C_e/q_e *versus* C_e or $1/q_e$ *versus* $1/C_e$ from the linearization of the Langmuir model or the *logarithmic* plot of q_e *versus* C_e will give a straight line, the slope and

intercept of which can be used to determine the maximum adsorption capacity and the binding or affinity constants respectively as shown in Figure 11 [20, 21].

Activated carbon (AC) is the most commonly used adsorption media for most water filtration applications as it has an extremely large amount of adsorption surface area, generally around 73 acre/lb (650 m^2/gram) to 112 acre/lb (1000 m^2/gram). AC is made of tiny clusters of carbon atoms stacked upon one another, and is produced by heating the carbon source (coal, lignite, wood, nutshells or peat) in the absence of air which produces a high carbon content material. Based on its form, AC is termed granular activated carbon (GAC) or powdered activated carbon (PAC) as shown in Figure 12a. The contaminants are usually adsorbed on the microporous surface of AC physically or chemically (Figure 12b). GAC and PAC are used predominantly in the water industry to treat several organic and inorganic contaminants either in the form of small scale filter cartridges or large filtration tanks as shown in Figure 12c [22-24].

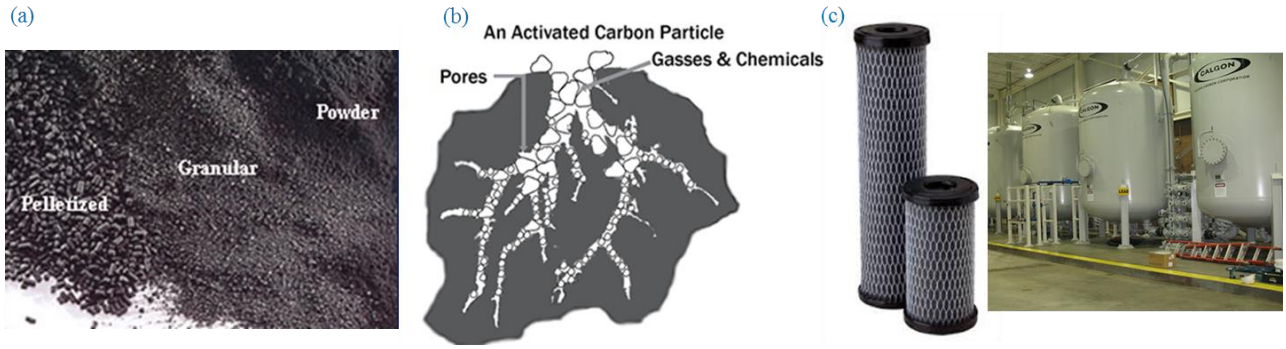

Figure 12: (a) Different forms of activated carbon (b) Porous structure of an activated carbon particle (c) GAC filter cartridges and filtration tanks [20-22]

1.4 Polyurethane Foams

Polymer foams are produced by the dispersion of a gaseous phase in a solid phase. The gas used for foaming changes some of the properties of the polymer, and the foam usually reflects the properties and limitations of its base polymer. This has led to characteristic applications of foams produced by various processing techniques. The foam properties, however, depend on the physical and chemical structure of the foam. Foaming mechanism plays a very crucial role in determining the physical characteristics of the foam [23].

Polyurethane (PU) foams are considered to be one of the best commercially available insulation materials. They have good thermal insulating properties, low moisture-vapor permeability and high resistance to water absorption, relatively high mechanical strength and low density. One of the advantages of PU foam systems is that the synthesis, can be tailored to any specific application. The major components are an isocyanate and a polyol (or a mixture of polyols). A blowing agent and a catalyst are commonly used to accelerate the foam formation process. The foams can be synthesized as open-cells or as closed-cells based on their initial raw material concentration. Open cell PU foams have shown to exhibit a reasonable amount of ion exchange capacity and hence are more suitable as ion exchange media for heavy metal ions removal [24]. The following characteristics of PU foams make them attractive for commercial ion exchange systems:

- Low cost and simple preparation methods
- Resistance to pH changes and reliable resistance to swelling in organic solvents

- Convenient handling for large scale CEDI (continuous electro-deionization) applications
- Lower fouling by hydrophobic macro ions due to their macro porous structure [25, 26].

1.4.1 Polyurethane Chemistry

Polyurethanes are organic polymers which contain the urethane group in the structure. The basic components of the PU foam system are isocyanates and polyols along with a suitable blowing agent. PU foam synthesis is based on the reaction of an Isocyanate (-NCO) group with a polyol $(-OH)_n$ group to form the urethane species as shown in Figure 13a.

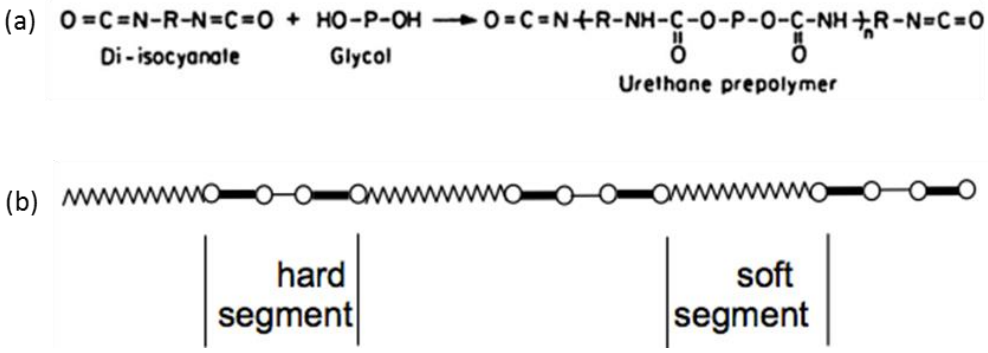

Figure 13: (a) Reaction between a diisocyanate and a polyol to form a urethane prepolymer (b) urethane pre-polymer containing hard and soft segments [27]

The pre-polymer formed by this reaction is a repeating unit of soft segments from the polyol and hard segments from the isocyanate as shown in Figure 13b. Based on the ratio of the polyol and isocyanate, two types of pre-polymers are obtained. A true pre-polymer, is

obtained when the polyol is processed with an excess of isocyanate molar ratio of 1:2. This forms an isocyanate terminated pre-polymer which is reasonably stable and has less handling hazards than free isocyanates. This has the advantage of low exotherms and greater flexibility in design of compounds. If the molar ratio of polyol and isocyanate is more than 1:2, a quasi-pre-polymer is formed. It has a low molecular weight and has low viscosity. However, this has high exotherms and free isocyanates which make handling hazardous [28].

The polymer foam can be formed by reacting water with the viscous pre-polymer. Addition of water to the pre-polymer initially forms an unstable carbamic acid intermediate which decomposes to form carbon-di-oxide. The carbon-di-oxide gas causes cell formation and foam expansion. Figure 14 shows the schematic of the gelling reaction (top) between the polyol and isocyanate and the blowing reaction (bottom) between water and isocyanate. The process to make flexible PU foams requires a precise control over these two competing reactions.

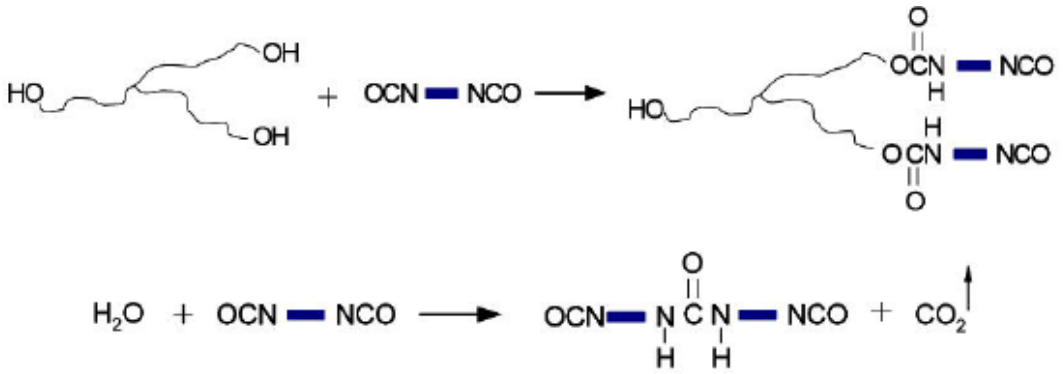

Figure 14: Gelling (top) and blowing (bottom) reactions in PU foam synthesis [29]

If the blowing reaction is faster than the gelling reaction, the foam will likely collapse early on, and if the gelling reaction is faster than the foaming reaction, it will entrap the gas and suppress bubble formation. Therefore it is an intricate, and yet, critical step before manufacturing to find a kinetic balance point for the foaming process. Catalysts are usually used in industries to provide kinetic leverages [30].

In the case of polyurethanes, two types of additives can be used, chain extenders and/or cross linkers. Chain extenders are multifunctional low molecular weight compounds, which can modify the backbone structure of the polymer and link linear pre-polymer chains. The schematic in Figure 15 shows the reaction of a tri functional chain extender with an isocyanate terminated pre-polymer. The final polymer is thus, formed by the reaction of the pre-polymer with the chain extender or curing agent. The chain extender links the pre-polymer molecules together, which increases the molecular weight, and then the cross-linker reacts forming a complete polymer network. The chain extender has a direct influence on the distribution of both hard and soft segments in the polyurethane polymer. The degree of crystallinity and crosslinking are also affected, depending on the structure of the chain extender and whether it is amino- or hydroxyl- functional [31].

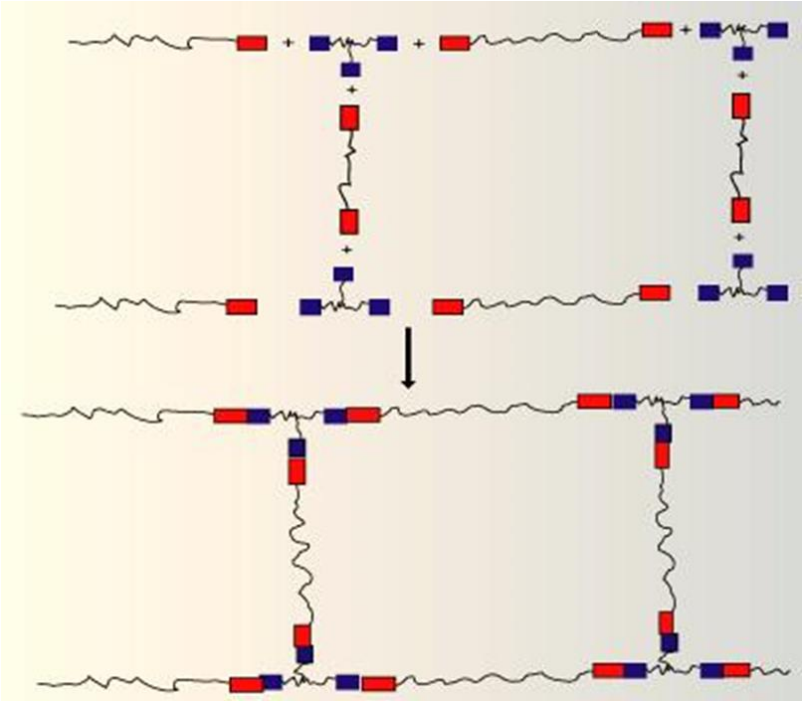

Figure 15: Functionalization of polyurethane pre-polymer using a tri functional chain extender [32]

1.4.2 Foaming Mechanism

The production of foamed polymers includes three stages within the polymer: (1) Implementation of gas, (2) Expansion of gas, and (3) Stabilization of the polymer as shown in Figure 16. Different mechanisms occur and they sometimes overlap during these stages. Changes in the surrounding conditions and, competing mechanisms appear to make the kinetic processes more complex during foaming [33, 34].

The solubility limit of the gas in the polymer is the predominant factor during the implementation stage. It usually depends on the surrounding pressure, temperature, and

interaction with the polymer. The amount of gas blended or generated during the reaction into the polymer is a controllable processing parameter. This affects the melt solution homogenization, foaming dynamics, and stabilization. When the gas solubility limit is met, the gas phase tends to separate from the polymer phase. Based on the stability of the separated phases, nucleation (Nu) and spinodal decomposition (SD) are the two mechanisms which initiate the foaming process.

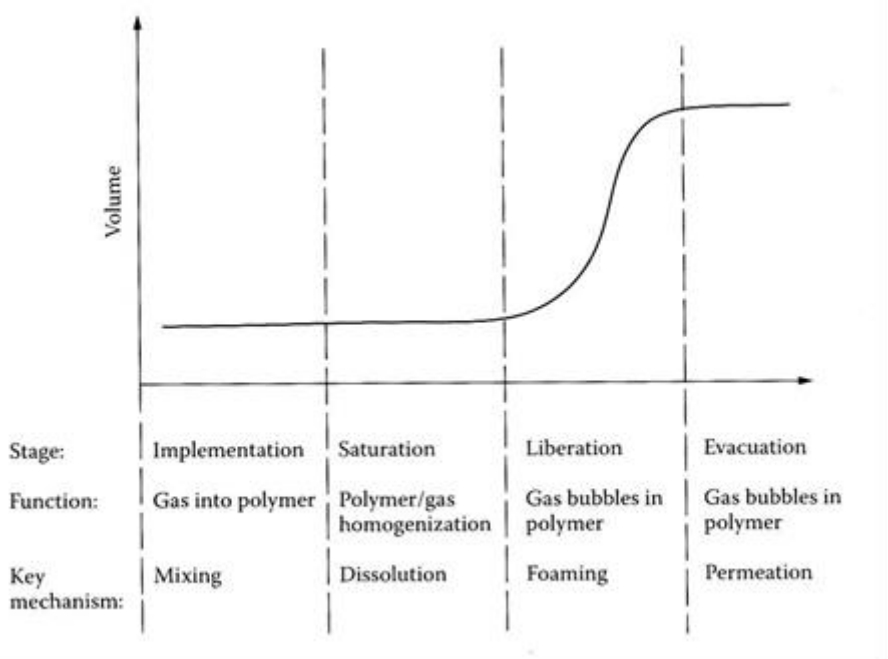

Figure 16: Foaming mechanism and the stages involved in foaming

Nucleation leads to the formation of gas bubbles inside the polymeric phase during foaming. A nucleated bubble so formed is termed a critical bubble, which is intrinsically unstable and grows further. The bubble growth creates a concentration gradient in the system leading to the diffusion of gas from the polymeric solution, which in turn feeds the growth process. Since nucleation is an unstable phenomenon, growth is imminent, therefore expansion and gas diffusion occur

simultaneously. Bubble growth is a complex process involving mass, momentum, and heat transfer. On the other hand, SD is a mechanism by which a solution of two or more components can separate into distinct phases with distinctly different chemical compositions and physical properties. This mechanism differs from the classical nucleation as phase separation due to spinodal decomposition is much more defined, and occurs uniformly throughout the material and not just at discrete nucleation sites. The difference between foaming through SD and Nu are shown in Figure 17a.

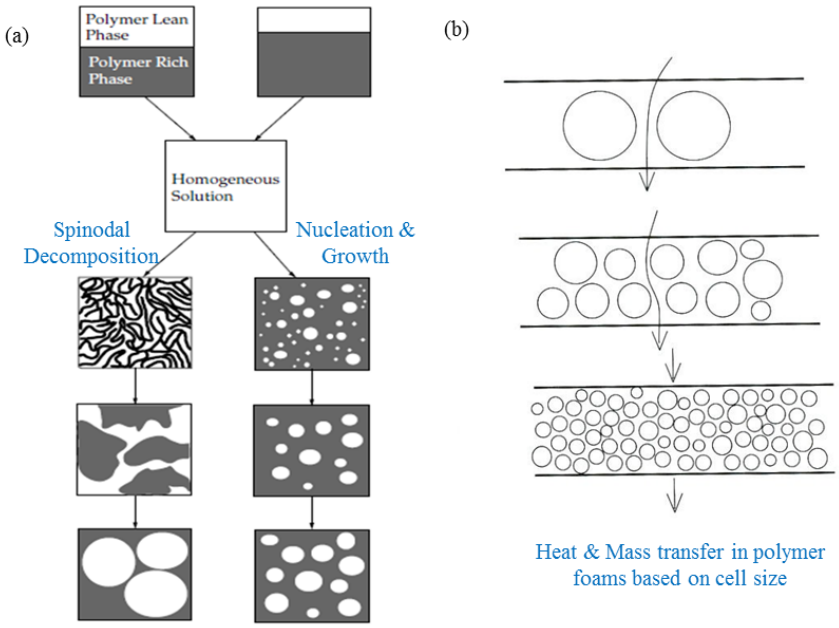

Figure 17: (a) Cell growth during foaming by spinodal decomposition and nucleation processes (b) Heat and mass transfer channels as a function of cell size in polymer foams

The cell size and number in foams, depends on the nucleation process. This is an energy controlled step where the stable nuclei gains energy to offset the opposing forces in order to

grow. Unlike spinodal decomposition, nucleation does not occur uniformly across the polymeric phase; it begins earlier at some points than at others [35-37] which lead to a cell size distribution which alters the paths available for heat and mass transfer through the foam as shown in Figure 17b.

The foaming mechanism in PU foams has been reviewed by research scientists extensively to understand the foaming models due to the ease of processing at room temperature and the absence of visual barriers to observe the foaming process. Agitating the pre-polymer mixture creates sites for nucleation and the polymerization reaction simultaneously, the blowing agent starts bubble formation. Suitable catalysts and surfactants can lower the rate of the gelling and blowing reactions which can produce a stable foam. The ratio of the polyol and isocyanates dictate the final foam property. PU foams are produced by casting to obtain sheets or blocks and by reaction injection molding processes to produce rigid, flexible or integral skin PU foams [38].

1.5 Literature Review: Polyurethane Foams for Water Filtration

The basic structure of segmented polyurethane is based on the chemical nature, molar mass and distribution of hard and soft segments, their size and degree of crosslinking. These structures determine the secondary structure, such as configuration of the polymeric chain, crystallinity, and ultimately the morphology of the polyurethanes. The final properties of the polyurethanes are thus dependent on its chemical structure [39], tailoring the synthesis is hence an effective way to alter its chemical structure to get the desired properties for a particular application.

PU foams have thus intrigued researchers to device novel applications based on the above said properties and their ease of processing. One other unique application of open pore PU foams emerged from its ability to sorb contaminants in water. Ever since, the foam polymer has been considered in sorption processes and it dates back to the 1970's. Considerable work has been done on PU foams for water treatment since then to explore other applications in the water industry. The first paper reporting sorption and recovery of some inorganic and organic compounds from aqueous solution using this sorbent was published in 1970 by Bowen [40]. One year later, Gesser et al. [41] proposed the use of untreated PU foams for sorption of organic contaminants from water using a batch technique. Braun and Farag [42, 43] published the first applications of PU foams for chromatographic separation in 1972. Farag et al. [44] showed that open-pore PU microspheres exhibit low cation exchange capacity. Their research on foams prepared by chemical bonding of specific functional groups (-SH) was used to adsorb mercury ions from mercury (II) chloride and methyl mercury (II) chloride in the range of 0.4 to 400 ppb. These studies resulted in a number of papers, involving the use of unloaded and loaded PU foams (polyether and polyester type) in separation and pre-concentration procedures for the determination of inorganic and organic species.

The use of chemical reagents to modify the physical and chemical structure of the PU led to the development of unloaded and loaded PU foams. Unloaded PU foams were not treated in any reagents whereas loaded PU foams were the ones which had undergone some kind of chemical treatment suck as the ones shown in Figure 18. Unloaded PU foams only adsorbed metal ions after complex formation. Organic and inorganic ligands can be used for this operation. Several

batch and on-line procedures have been established this way. In a batch method, for example, molybdenum (VI) ions were quantitatively extracted with unloaded PU foams after formation of thiocyanate complexes [45]. An on-line system was proposed for determination of zinc in biological matrices, where zinc (II) ions reacted on-line with thiocyanate ions and the complexes were adsorbed in a minicolumn packed with unloaded PU foams [46].

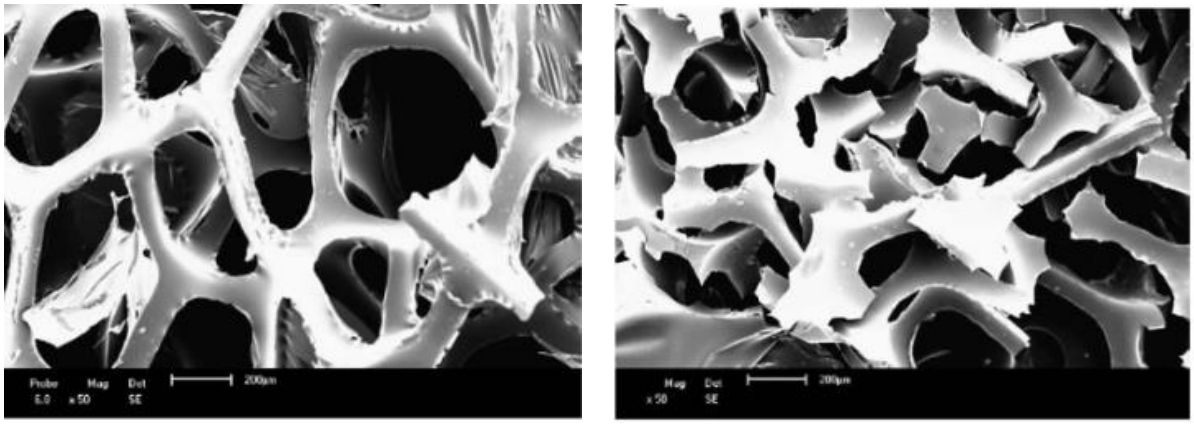

Figure 18: SEM images of PU foam: (L) untreated (R) after grinding with ethanol [45]

Loaded PU foams offer a wider field of applications than unloaded PU foams. The loaded ligand can determine if an extraction process is selective or non-selective, i.e., multi-element. Loaded PU foams can also be used in batch or on-line operations. PU foam loaded with dimethylglyoxime was, for example, proposed for the selective extraction of nickel [47].
A multi-element procedure was proposed for simultaneous pre-concentration and determination of cadmium, cobalt, copper, manganese, nickel, lead and zinc in water using PU foams loaded with piperidine dithiocarbamate [48]. Both procedures were based on batch operation.

These led to the development of functionalized polyurethane foams in the late 90's. Research shows that functional groups such as hydroxyl, ketone and carboxylic acids have been found to adjust the surface energy and improve the hydrogen binding in polymers [49]. This made them capable of effectively eliminating heavy metal ions either by adsorption or pre-concentration mechanisms. Functionalizing PU foams either by surface or structural modification has generated a lot of interest among researchers since then.

Functionalization of polyurethane foams by surface modification has led to systems capable of adsorbing heavy metal and trace metal ions. [50-54] Surface modification of PU foam by coupling chromotropic acid through an AZO group has been used to pre-concentrate and detect Co and Ni in lettuce samples [51]. In another study, composite ion exchange PU foam was prepared by coating copper-ferrocyanide (CFC) and hydrous manganese oxide (HMO) powders using polyvinyl acetate/acetone as the binding agent. This composite foam was used to treat low level radioactive liquid wastes such as cesium and strontium. The ion exchange column and the composite foam cartridge used for this purpose are shown in Figure 19 [52]. It was found that the HMO-PU foam had a higher exchange capacity for strontium compared to the CFC-PU foam for Cesium. Based on their ion exchange capacities it was decided to include higher amounts of CFC-PU foams in the cartridge.

Figure 19: (L) Ion exchange column and (R) CFC-PU and HMO-PU foam cartridge [52]

In another study by Meligi [55], PU foams were modified by grafting acrylo nitrile and acrylic acid by gamma irradiation method. It was found that the adsorption of heavy metal ions such as Zn (II), Fe (II), Ca (II), Ni (II), Cu (II) and Pb (II) were affected by pH, atomic weight and initial contaminant concentration. A SEM image of the grafted PU foam before and after exposing to heavy metal ions is shown in Figure 20. The figure to the left shows the interphase between the PU and acrylo nitrile and acrylic acid comonomers after grafting and the figure on the right shows the metals loaded onto the graft foam with the interphase between the two phases. Results showed that the adsorption capacity of the grafted PU foam was highest for Pb^{2+} ions among all the other metal ions considered in the study. The degree of adsorption affinity observed was Pb > Ni > Co > Zn > Cu > Fe. The variation in the degree of adsorption affinity of the metal ions to different adsorbents can usually be explained as a function of ionic radii, ionic charge, electronic structure and some hydration capacity.

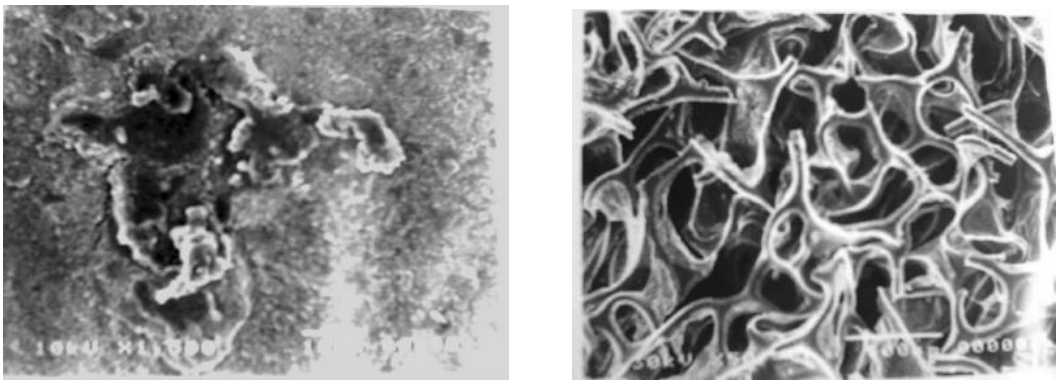

Figure 20: SEM images of graft PU foam before (L) and after heavy metal absorption (R) [55]

In a study by Jang et al. [56], hydroxyapatite (HAp) - polyurethane foams were synthesized for Pb^{2+} ion adsorption. HAp is a major inorganic constituent of bones, teeth and a natural source of phosphate. It has a high removal capacity for divalent heavy metals. Immobilization of Pb^{2+} ions from soil and water using natural and synthetic HAp has simulated intensive research to understand the mechanism involved in Pb^{2+} removal and its application for filtration. The PU-HAp composites were synthesized by mixing different weight percent's of HAp into a commercial PU pre-polymer. The SEM image of the PU-HAp composite foam at 20 wt. % and 50 wt. % loading is shown in Figure 21. The image confirmed that the foam exhibited well developed open pore structure, independent of the HAp content. The image, also showed that the HAp dispersion was uniform at 20 wt. % compared to 50 wt. %. The resultant composite foam was capable of a maximum adsorption capacity of 150 mg/g (150000 ppm) for the composite with 50 wt. % HAP for an exposure of 48 hours as shown in Figure 22.

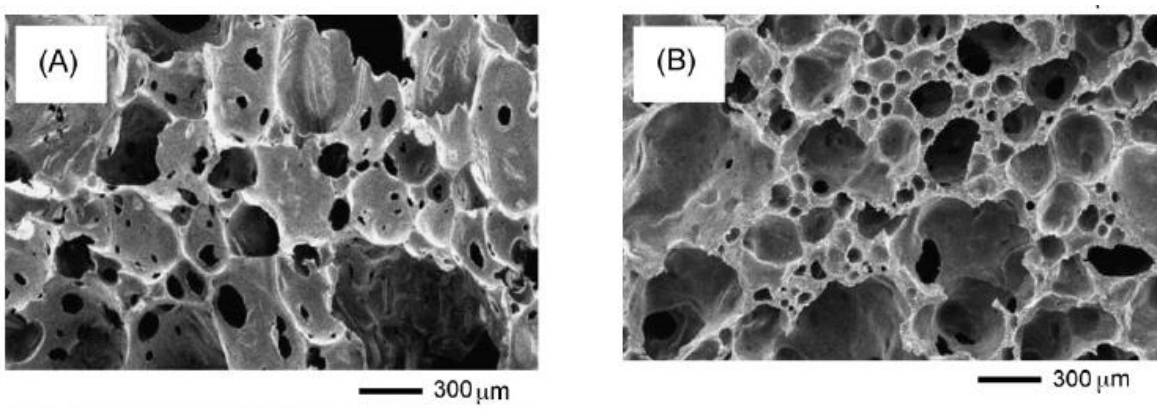

Figure 21: SEM image of HAp/PU foam composite at (A) 20 wt. % (B) 50 wt. % Hap [56]

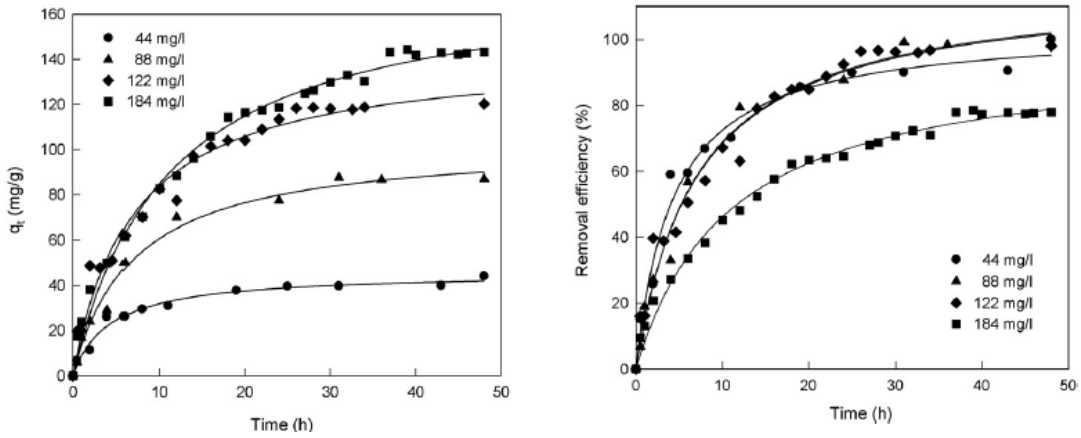

Figure 22: Pb^{2+} removal capacity of HAp/PU composite foams based on initial solution concentration [56]

The study also concluded that higher HAP concentration exhibited higher Pb^{2+} ion adsorption capacity. Less uniform dispersion of HAP in the foam led to slower adsorption and adsorption was dominant at higher pH levels.

Another type of polyurethane composite foam containing alginate was synthesized by Sone et al. [57], which had a structure similar to that of a weak cation exchanger. Alginate is the main component of brown algae which has carboxyl functional groups. A commercial pre-polymer mixture was mixed with aqueous sodium alginate to produce the foam. Figure 23 shows the SEM image along with an image of the bulk foam. The results show that the capacity of the PU-alginate foam to adsorb Pb^{2+} ions was 16 µmol/g (3.3 ppm) over a period of 2 hours as shown in Figure 23c. The adsorption capacity was found to be highly sensitive to the pH of the sample solution. Competing ions such as Mg^{2+}, Ca^{2+} and Cd^{2+} were found to decrease the selectivity and adsorption capacity of Pb^{2+} ions.

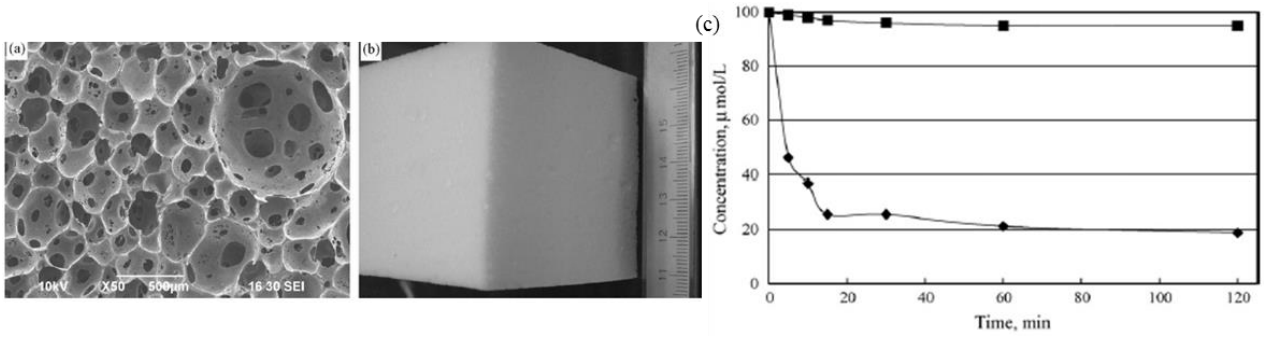

Figure 23: PU-Alginate composite foam (a) SEM image (b) Actual foam (c) Lead removal capacity of (■) plain PU and (♦) PU-alginate foam [57]

Likewise, researchers have developed several adsorption and ion exchange media based on polyurethane foams by altering the surface chemistry or by modifying the chemical structure of the PU foams. However, the literature summary described above does not address bulk functionalization of polyurethane foams to eliminate heavy metal ions such as lead. To address

this the current work is focused on the development of a bulk functionalized PU foam system using a chain extender.

Moon et al. [58], synthesized a polyurethane foam with a sulphonic functional group by chemically modifying the structure of the polymer backbone. BES was chosen as a functionalizing agent due to the presence of two hydroxyl groups and a sulfonic acid group in its chemical structure. The hydroxyl groups in BES will react with the remaining isocyanate groups in the polyurethane pre-polymer resulting in a chain extended pre-polymer. The sulfonic acid group, present in BES is thus available for reaction at a later time. This functional group was utilized to deionize water for a continuous electro deionization (CEDI) process. The ion exchange capacity of the functionalized PU foam was determined as 2.5 meq/g and the PU foam synthesized using BES was determined to be a cation exchange media.

1.6 Overview of the Thesis

Chapter 1 outlines the significance and need for the development of new water treatment products, by reviewing the adverse health effects of lead in drinking water, the current state of the art, and the current state of knowledge. Chapter 2 outlines the research objectives along with its significance and novelty based on the discussion in chapter 1. Chapter 3 presents the experimental procedures and materials involved in the synthesis of functionalized PU foam according to the design of experiments to study the effect of various process parameters on the foam synthesis.

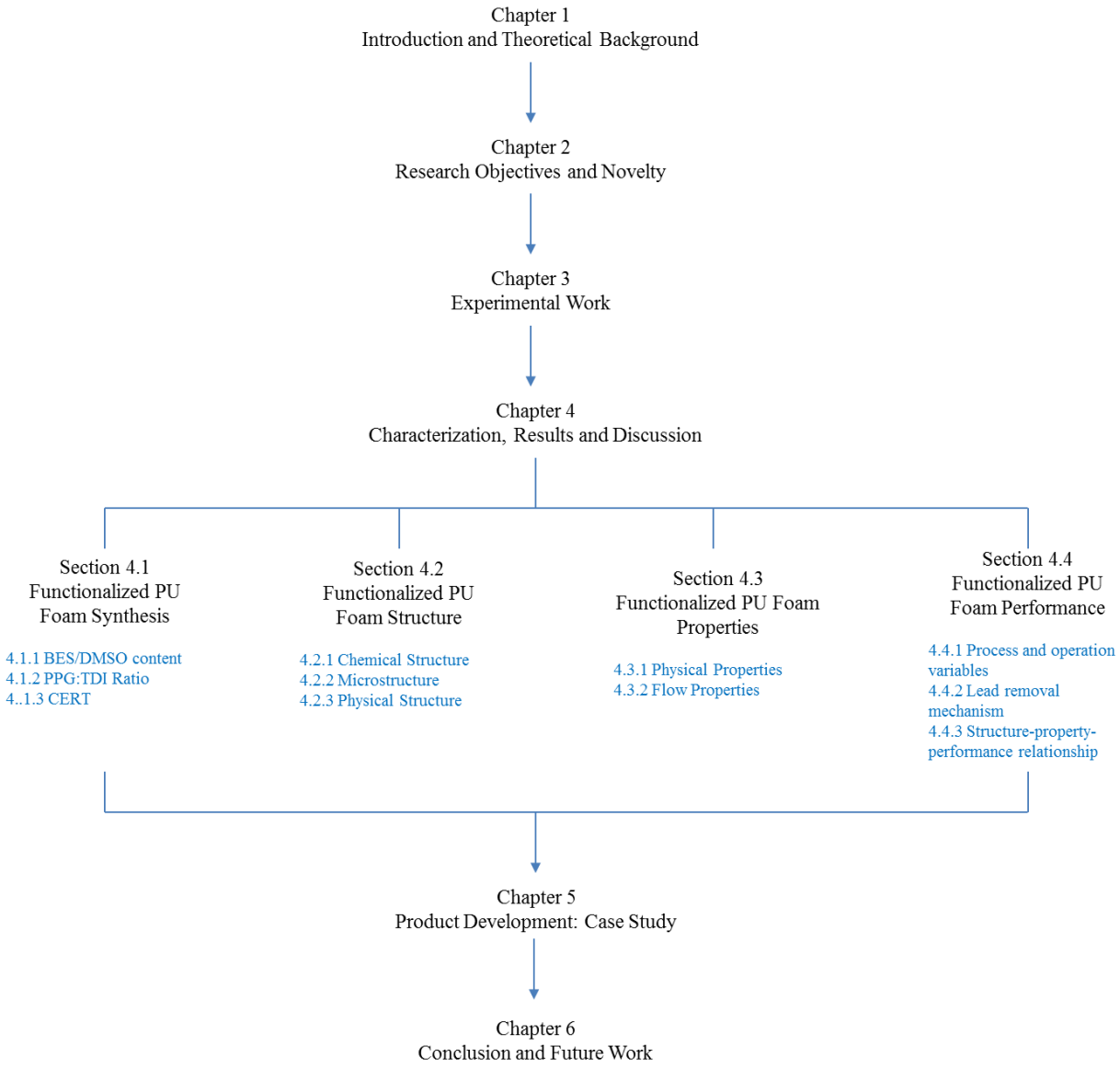

Figure 24: Thesis Overview

Chapter 4 reviews the characterization methods and techniques to determine the structure, properties and performance of the functionalized PU foam. The results from the structure, property, performance characterization are discussed to identify the relationship between the process and application parameters on the structure, property and lead removal efficiency of the

functionalized PU foam. Chapter 5 reviews the current state of the water industry in general and water treatment sector in particular while discussing strategies and implementation models to develop the functionalized PU foam into a new product. Chapter 6 summarizes the research findings and contributions and concludes by recommending directions for future research.

Chapter II: Research Objectives and Novelty

2.1 Research Motivation

The new guidelines set by the EPA in 2012 for lead in drinking water (0ppb) and the limitations of the commercial ion exchange resin beads, in terms of operational costs and regeneration costs, has opened a gateway to research and develop new polymer based filtration systems.

The overall purpose of this research is to address the aforementioned issues in existing water filtration systems by developing bulk functionalized PU foam filtration system to selectively eliminate lead ions from drinking water. The outcomes of this research work answer the following questions:

- What are the materials and processing variables which will affect the bulk functionalization of PU foam?
- How does the PU foam synthesis chemistry affect the physical structure and performance of the functionalized PU foam?
- What is the relationship between the structure, property, process and the performance of the functionalized PU foam?
- How does the functionalized Pu foam eliminate lead ions from water and what are its limitations?
- What will be the production and operating costs of the functionalized PU foam in comparison to the commercial water treatment products?

2.2 Research Objectives

The objectives of this research work are:

1. To synthesize a chain extended PU foam capable of exchanging and/or adsorbing lead ions from water at ppb levels.

2. To study the effect of the following processing variables on the physical and chemical structure, flow properties and performance of the functionalized PU foam:

- Chain extender and Solvent content
- Polyol and Isocyanate ratio
- Chain Extender Reaction Time (CERT)

3. To study the effect of the following application parameters on the performance of the functionalized PU foam:

- Solution pH
- Pressure drop and flow properties
- Adsorption isotherms
- Flow through column tests
- Competing cations

4. To determine if regeneration is viable and to identify a suitable regenerant if applicable.

5. To benchmark the cost and evaluate the parameters for product realization through a case study on industrial practices.

The outcome of this study will hence provide a clear understanding on the effect of composition and processing variables; i.e., the isocyanate and polyol contents, the chain extender content and

the chain extender reaction time, on the performance of the bulk functionalized PU foam. The optimum process conditions and composition required to synthesize stable foam will be determined during the course of this study. Analyzing the foam at the molecular level by various characterization techniques will provide an insight on the mechanism(s) involved in removing lead ions and will help understand the effect of processing parameters on the consistency and repeatability of the lead removal efficiency of the foam.

Batch and column test experiments, in line with real world applications along with benchmarking the production and operational costs against the efficiency of the functionalized PU foam will help us understand the challenges or issues which need to be addressed to take this applied research to the next level for product realization.

2.3 Research Novelty and Significance

This work was inspired by the literature published by Moon et al [58], which describes the development of a CEDI (continuous electro deionization) medium to deionize aqueous media to a high level without the need for chemical regeneration by synthesizing a functionalized polyurethane foam. A chain extender containing sulfonic acid groups was used during synthesis to functionalize the pre-polymer. This led to the bulk functionalization of polyurethane foam with an increase in ion exchange capacity as the number of sulfonic acid groups increased.

However, no further work was done on this system to prove the aforesaid cation exchange media is capable of exchanging other cations. In addition, based on an extensive literature search and

review, there is no published work on the synthesis-structure-property relationship of functionalized open cell polyurethane foams for water filtration applications.

The novelty of our work lies in providing a detailed analysis of the lead ion removal mechanism and the relationship between the foam formulation and its physical and molecular structure, properties to the lead ion removal efficiency.

The significance of this research work is manifested by its ability to create a uniform, bulk medium for lead ion exchange by incorporating the functionality into the foam formulation, which is accomplished using a chain extender with a sulfonic acid group. The experimental design and data analysis is significant to the scientific community, and is rudimentary for the water industry, as it provides knowledge necessary for developing alternative water filtration media using PU foams as shown in Figure 25.

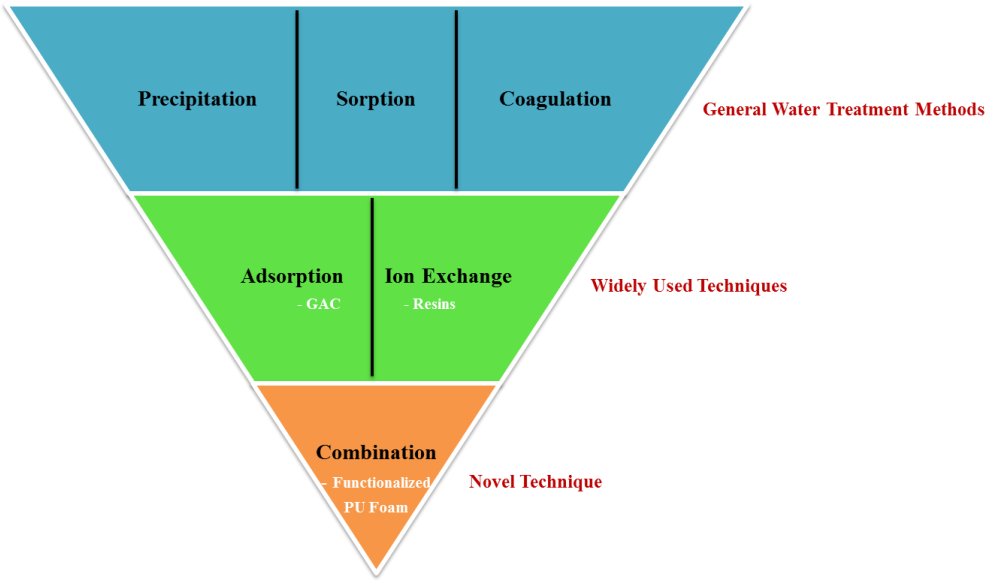

Figure 25: Novelty of functionalized PU Foam filter media

Chapter III: Experimental Work

3.1 Materials

3.1.1 Toluene Diisocyanate (TDI)

Isocyanates are the unique and basic monomers in polyurethane foams which can be either aromatic or aliphatic. Previous studies have shown that aromatic isocyanates are more reactive than aliphatic isocyanates [59, 60]. These are specific towards special properties which can be produced in the final product. The aromatic isocyanates are less stable than aliphatic isocyanates in the light. So, aliphatic isocyanates are utilized to develop the polyurethane coatings. Moreover, the reactivity of an isocyanate group also depends on the stereochemistry; structure, substituents, and steric effect of the isocyanates which is evenly different for the same class. For example, in 2,4-toluene diisocyanate (TDI), the -NCO group at para position is 25 times more reactive than the -NCO group at the ortho position. Reactivity of the second -NCO group can change as a result of the initial reaction. The most important aromatic isocyanates which are used in polyurethane industry are TDI and methylene diphenyl diisocyanate (MDI) [61-64].

TDI contains two isocyanate groups. Each of the isocyanate functional groups in TDI can react with a hydroxyl group to form a urethane linkage. It exists in two isomers, 2,4-TDI (CAS: 584-84-9) and 2,6-TDI (CAS: 91-08-7). 2,4-TDI is produced in the pure state, but TDI is often marketed as 80/20 and 65/35 mixtures of the 2,4 and 2,6 isomers respectively. The structure of 2,4-TDI is:

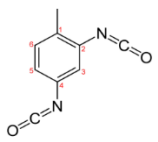

Figure 26: Toluene-2, 4-diisocyanate [65]

2,4-TDI is an asymmetrical molecule and thus has two isocyanate groups of different reactivity. The 4-position is approximately four times more reactive than the 2-position. 2,6-TDI is a symmetrical molecule and thus has two isocyanate groups of similar reactivity, similar to the 2-position on 2,4-TDI. However, since both isocyanate groups are attached to the same aromatic ring, reaction of one isocyanate group will cause a change in the reactivity of the second isocyanate group.

3.1.2 Poly Propylene Glycol (PPG)

Polyols determine the properties of the final PU polymer. There are many types of polyols which have made polyurethanes the most versatile family of polymeric materials. Chemically these polyols are the compounds which have hydroxyl (-OH) groups which react with diisocyanate to produce PU polymer. Typically, polyols are produced with 2 and 8 reactive groups having average molecular mass in the range of 200-8000g mol^{-1}. Selection of polyols is based on the end use application and cost. The types of polyols used are hydroxyl terminated polyester polyols, hydroxyl terminated polyether polyols and miscellaneous polyols [66].

PPG is a polymer of propylene glycol and chemically, it is a polyether. The term polypropylene glycol or PPG is reserved for low to medium range molar mass polymers when the nature of the end-group, which is usually a hydroxyl group, still matters. The term "oxide" is used for high molar mass polymer when end-groups no longer affect polymer properties. The generic structure of PPG is shown in Figure 27:

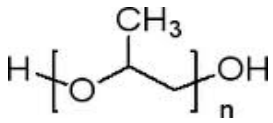

Figure 27: Polypropylene glycol; n = number of repeating units [66]

Polypropylene glycol is produced by anionic ring-opening polymerization of propylene oxide. The type of initiator used for polymerization determines the final structure of PPG. The presence of hydroxyl groups makes PPG the most sought-after raw material for polyurethanes. It is used as a rheology modifier. In this work, PPG was used as the sole polyol to react with TDI to control and alter the chemistry of the pre-polymer by using a chain extender to functionalize the final PU foam.

3.1.3 N, N- bis (2-hydorxyethyl)-2-aminoethane-sulfonic acid (BES)

BES is a chain extender used to functionalize the polyurethane foam for selective heavy metal ion exchange. The structure of BES is shown in Figure 28. [67]

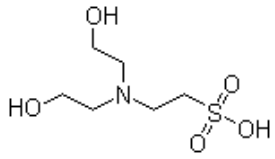

Figure 28: BES chain extender [67]

The presence of hydroxyl groups in BES leads to the reaction between remaining isocyanate groups in the polyurethane pre-polymer. The sulfonic group thus becomes the functional group

for ion exchange which can exchange the hydrogen ion for a lead ion and form a lead sulfate complex.

3.1.4 Dimethyl Sulfoxide (DMSO)

DMSO is an organosulfur compound with the formula $(CH_3)_2SO$. This colorless liquid is an important polar aprotic solvent, which dissolves both polar and nonpolar compounds and is miscible in a wide range of organic solvents as well as water [68-k70]. In the synthesis of polyurethane foam, it is used to dissolve the chain extender, BES.

3.1.5 Dibutyl Tin Diluarate (DBTL)

DBTL is an organo tin catalyst used in the production of polyurethane foam. It promotes the polymerization or gelation reaction between the isocyanate and the polyol.

3.2 Design of Experiments

To determine the optimum chain extender (BES) composition, the optimum molar ratio of PPG and TDI, and the optimum chain extender reaction time (CERT), a set of experiments were designed to study the effect of these parameters on the physical and lead ion exchange capacity of the foam. These variables were divided into 3 categories, as shown in Table 2, and the number of experiments required to study these parameters were determined.

For ease of processing, the weight of PPG is maintained constant in all the experiments. The moles and hence the amount of TDI required can be determined based on the amount of PPG

used. For ex: 50g of PPG-1000 is equal to 0.05 moles, and the required moles of TDI are twice that of PPG which is equal to 0.1 moles. Using the molecular weight of TDI, we can determine the amount of TDI as 18.3g, which is the weight of 0.1 moles of TDI.

Table 2: Design of Experiments Overview

Variables	**Parameters**	**# Experiments required**
BES/DMSO content	2	$2^2 = 4$
PPG/TDI molar ratio	1	$2^1 = 2$
CERT	1	$2^1 = 2$

BES has three functional groups, of which, two are hydroxyl groups (-OH) and one is a sulfonic acid group (SO_3H). The two -OH groups will readily attach to the –NCO ends of TDI in the pre-polymer, linking two linear chains. The -SO_3H functional group will be available for ion exchange and will also cross link any available –NCO groups in the polymer chain. This means that we will need one third moles of BES during the reaction. Based on 0.1 moles of TDI, 0.03 moles of BES is required during the reaction. Using the molecular weight of BES, 0.03 moles accounts to 6.7g.

The amount of DMSO used is determined based on the solubility limit of BES in 1ml DMSO. This value can be scaled to determine the amount of DMSO needed to dissolve 6.7g of BES in DMSO. The amount of catalyst, surfactant, and distilled water is kept constant based on the

amount of PPG used. An excess of 0.5% moles of TDI is added to stabilize the foam structure. Tables 3 and 4 summarize the foam composition in moles and grams; respectively.

Table 3: Molar Composition of the foam based on DOE

Variable	Expt. # or Sample Code	PPG (moles)	TDI (moles)	BES (moles)	DMSO (moles)	CERT (min)
BES/DMSO	A1	0.05	0.105	0	0	40
	A2	0.05	0.105	0.02	0.10	40
	A3,B6,C8	0.05	0.105	0.03	0.20	40
	A4	0.05	0.105	0.05	0.30	40
PPG/TDI	B5	0.05	0.052	0.03	0.20	40
	B7	0.05	0.157	0.03	0.20	40
CERT	C9	0.05	0.105	0.03	0.20	60
	C10	0.05	0.105	0.03	0.20	90

Table 4: Foam composition in grams based on DOE

Variable	Expt # or Sample Code	PPG (g)	TDI (g)	BES (g)	DMSO (g)	DBTL (g)	Surfactant (g)	Water (g)	CERT (min)
BES/ DMSO	A1	50	18.3	0	0	2	0.25	6	40
	A2	50	18.3	3.4	7.8	2	0.25	6	40
	A3,B6,C8	50	18.3	6.7	15.7	2	0.25	6	40
	A4	50	18.3	10.1	23.5	2	0.25	6	40
PPG/TDI	B5	50	9.1	6.7	15.7	2	0.25	6	40
	B7	50	27.4	6.7	15.7	2	0.25	6	40
CERT	C9	50	18.3	6.7	15.7	2	0.25	6	60
	C10	50	18.3	6.7	15.7	2	0.25	6	90

3.3 Functionalized PU Foam Synthesis

3.3.1 Experimental Setup

The experimental setup consists of a 3 necked round bottom reaction flask fitted with a mechanical stirrer and a water cooled condenser at the center neck. The second neck is fitted with a nitrogen gas inlet and outlet to create an inert atmosphere. The third neck is fitted with a drop funnel to charge the materials during the reaction as shown in Figure 29. A stopper will be used to cork the third neck after removing the drop funnel. An oil bath with a magnetic stirrer is used to maintain uniform heat throughout the reaction. High vacuum grease is used to seal the necks of the round bottom flask. The experiment is carried out under a fume hood to allow for sufficient ventilation. TDI is handled carefully to prevent contamination by moisture and atmospheric oxygen. The reaction is carried out at 70-75^{o} C in an oil bath in nitrogen atmosphere.

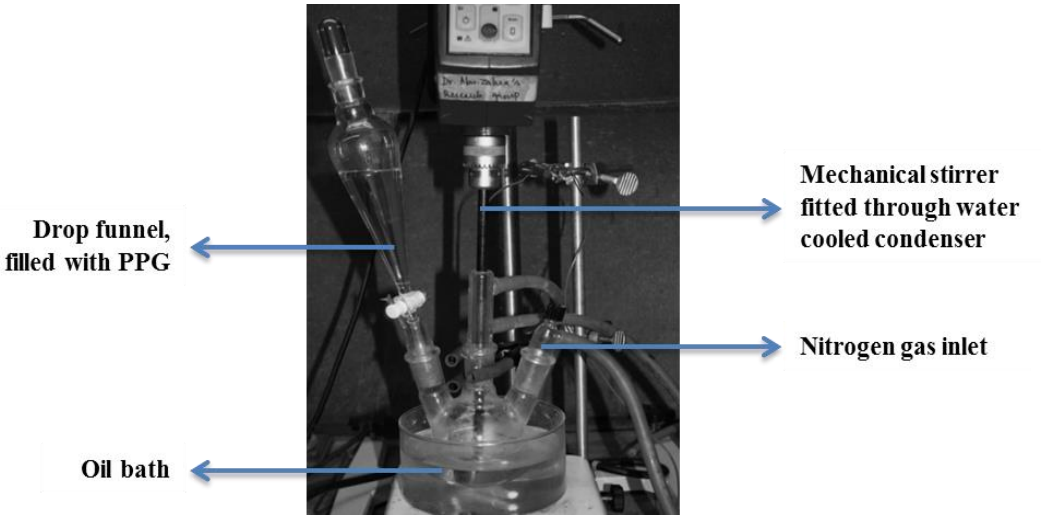

Figure 29: Experimental setup for functionalized PU foam synthesis

3.3.2 Functionalized PU Foam Synthesis

Two moles of TDI based on the molecular weight of PPG is weighed precisely and decanted into the 3–neck round bottom reaction flask. The dropping funnel is filled with 1 mole of PPG and fitted to the left neck of the round bottom flask, the glassware are sealed using high vacuum grease to prevent oxidation during the reaction. PPG is added drop-wise into the round bottom flask to react with TDI while the reaction mixture is stirred constantly at 175-200 rpm. Once x all the PPG is charged into the reaction flask, a sample is pipetted out to determine the Isocyanate content of the pre polymer according to ASTM D 5155, di-n-butyl amine method. The reaction is continued until the pre-polymer reaches a theoretical isocyanate content of 11% as determined by the di-n-butyl amine method. This may take anywhere between 3 to 20 hours, or more, depending on the molecular weight of PPG used. In this case, it took almost 4 hours to obtain a pre-polymer with an isocyanate content of 11%.

In the meantime a pre-weighed amount of the BES chain extender is dissolved in DMSO at a temperature of 70^{o} C. The amount of chain extender is calculated based on the remaining isocyanate groups available for reaction as explained in section 3.2. The dissolved chain extender is then added drop-wise into the reaction mixture followed by the tin catalyst; DBTL. The contents are allowed to react further until a theoretical isocyanate content of 7% is obtained in the pre-polymer.

Once the theoretical isocyanate content is 7%, the contents of the round bottom flask are decanted into a mold coated with a suitable release agent. Surfactant and distilled water is added

to the contents and stirred vigorously for 60 seconds using a mechanical stirrer. This will initiate foaming process as the water starts to react with the remaining isocyanate groups forming an intermediate compound, as was described earlier, and eventually releasing CO_2 gas to form the cellular structure, as shown in Figure 30.

Figure 30: (a) Functionalized PU pre-polymer (b) Initiating the foaming and polymerization reactions by mechanical mixing using water as a blowing agent (c) PU foaming in progress (d) Released functionalized PU Foam

Chapter IV: Characterization, Results and Discussion

4.1 Process Evaluation

In general, the structure of polyurethane foams depends on the isocyanate and the polyol content as they act as the hard and soft segments; respectively, in the urethane linkage. DMSO has been used as a solvent to dissolve BES in the synthesis of polyurethanes without significantly affecting the polyurethane chemistry, as shown in Figure 31 [58]. However, higher amounts of DMSO can affect the foam structure as it is a strong organic solvent capable of dissolving polyurethane [71]. This limits the use of higher amounts of BES which can provide more functional groups for ion exchange.

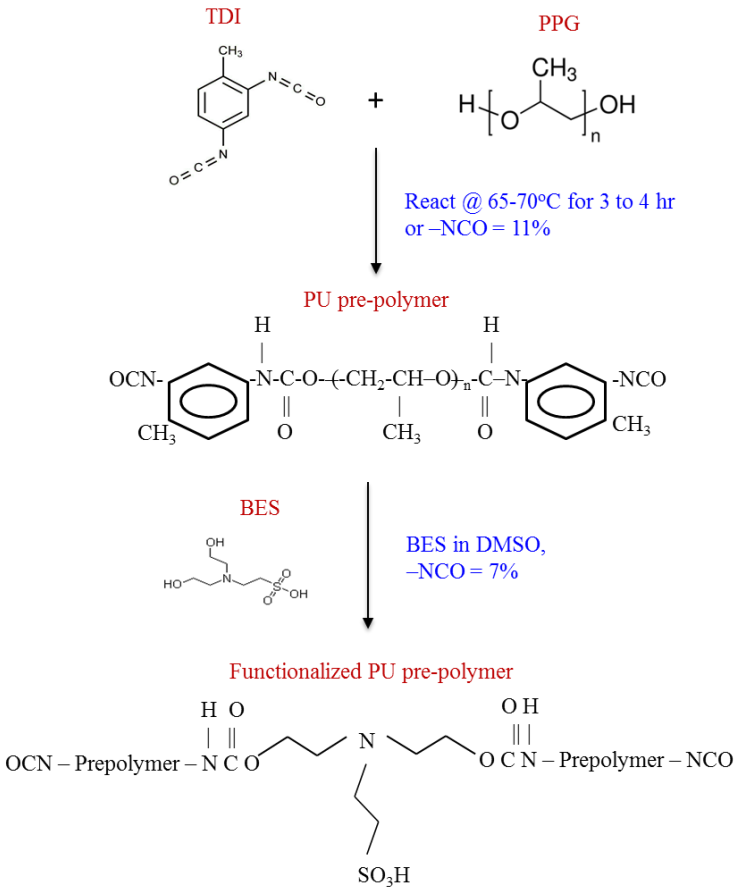

Figure 31: Chemical reaction scheme of functionalized PU foam synthesis [58]

4.1.1 Effect of BES and DMSO concentration on PU foam synthesis

The first set of foam samples from experiments A1 to A4 were synthesized with a constant PPG to TDI mole ratio and CERT of 40 minutes. The amounts of PPG and TDI used were 50g and 18.3g; respectively. The amounts of BES and DMSO were increased in each experiment. A1 had no BES in its composition and the synthesized foam had a uniform pore distribution with open pore structure and good flexibility. In sample A2, 3.4g BES was dissolved in 7.8g of DMSO. Some BES recrystallized in the prepolymer prior to foaming. This may be due to the reaction of DMSO with TDI [72] lowering the –NCO groups to bond with BES. The foam was flexible with uniform open pore structure.

In sample A3, 6.7g of BES was dissolved in 15.7g of DMSO. Some BES recrystallized in the pre-polymer and the foam flexibility increased compared to A1 and A2 with uniform open pore structure. Sample A4 had the highest amounts of BES and DMSO in its composition. 10.1g of BES was dissolved in 23.5g of DMSO and was added drop wise to PPG/TDI pre-polymer. After 15 minutes, some BES started to recrystallize in the pre-polymer. The pre-polymer turned dark brown during the reaction and the addition of water led to small foaming in the pre-polymer. The foam collapsed in the mold due to excess DMSO. The foam samples also had uneven open pore distribution in the foam with the highest flexibility.

4.1.2 Effect of PPG and TDI molar ratio on PU Foam Synthesis

The second process variable was the TDI content. The amount of PPG was maintained at 50g in the three experiments B5 to B7. The amounts of BES and DMSO were also maintained constant

with 6.7g of BES dissolved in 15.7g DMSO along with a CERT of 40 minutes. A 9.1g of TDI was used in the mole ratio of 1:1 (TDI: PPG) to synthesize the B5 foam sample. However; the addition of water to the prepolymer led to gel formation instead of foaming, due to the presence of excess –OH groups from PPG as fewer –NCO groups in TDI are available to react. This indicates that fewer hard segments are not suitable for foam synthesis.

The foam sample of B6 with a TDI: PPG mole ratio of 2:1 was similar to that of A3 with 18.3g of TDI in the composition. The highest amount of TDI used was in the B7 foam sample with a TDI: PPG mole ratio of 3:1, which had 27.4g of TDI in its composition. During synthesis, some BES recrystallized and the foam collapsed a couple of times before setting. This may be due to higher gas evolution during foaming as more –NCO groups are available from TDI in the composition. The resulting foam was more rigid and brittle compared to other foam samples.

4.1.3 Effect of CERT on PU Foam Synthesis

Chain extender reaction time (CERT) was set to increase from 40 to 60 and 90 minutes in samples C8, C9 and C10; respectively. The composition of C9 and C10 foam samples had 50g PPG, 18.3g TDI, and 6.7g BES dissolved in 15.1g DMSO. Foam sample C8 had a similar composition with a CERT of 40 minutes; the structure of this foam was the same as sample A3 discussed earlier.

In the foam sample C9, some BES recrystallized during reaction. It was also observed that the flexibility of the foam increased and the foam looked much darker at a CERT of 60 minutes, as

this gives DMSO more time to react with TDI dissolving the urethane segments. The foam sample C10 with CERT of 90 minutes looked similar to C9 and had some BES recrystallization. The foam flexibility was the highest compared to all the other foam samples.

From the above observations, the foam synthesized with the A3 composition was identified to exhibit the best physical and structural characteristics.

4.2 Structure Evaluation

4.2.1 Chemical and Molecular Structure of Functionalized PU Foams

4.2.1.1 Chemical Structure Analysis by FTIR

FTIR is based on infrared energy absorption by molecular vibrations. A molecule is irradiated by electromagnetic waves in the IR frequency range and a certain frequency will match the vibrational frequency of the molecule. The vibration resulting from this, will be excited by the radiation and the energy of molecular vibration will increase. Thus, FTIR is useful to analyze the chemical structure of polymers by identifying the molecular composition of the polymer chains [73].

The functionalized polyurethane foam samples were characterized by a BRUKER vector 22 FTIR with a DTGS (deuterated triglycine sulfate) detector and a PIKE 3-12 multi-bounce Zn-Se variable angle ATR. The incidence angle was set to 80 during characterization tests. The foam samples were cut into strips of 3"x1"x0.5" and were washed in distilled water and dried in a

vacuum oven before testing. The IR spectrum was measured between 400 and 4000 cm^{-1} to confirm the presence of sulfonic acid groups in the polymer structure.

Some of the chain extender started to recrystallize in the pre-polymer during synthesis. To confirm that the recrystallized material was in fact the chain extender, the precipitate was characterized to determine its constituents by filtering it from the pre-polymer. Both the precipitate and the clear pre-polymer were characterized using a diamond ATR in the BRUKER vector 22 FTIR between 400 and 4000 cm^{-1}.

The FTIR spectrum of the foam samples A1 to A4 with varying BES/DMSO content is shown in Figure 32. Sample A1 shows a clear C-O-C peak at 1100 cm^{-1} as it does not contain any chain extender with the sulfonic groups. The O-S-O peaks start to appear at ~1060 cm^{-1} in other samples and this peak partially overlaps with the C-O-C band. The asymmetrically stretched S=O peak appears at 1350 cm^{-1}. The urethane carbonyl peaks appear at 1700 cm^{-1}. The NH band and H-NH band appear at 3000 cm^{-1} [58]. These indicate that the sulfonic acid functional groups were successfully integrated into the polyurethane backbone. The –CH stretching vibrations from the polyol appear at 2850-3000 cm^{-1} followed by the –OH and –NH stretching can be seen at 3200-3300 cm^{-1} [74] The –CH bending vibrations due to substitution groups in alkenes and aromatics is usually seen between 850-950 cm^{-1} [75]. The gradual appearance of a peak in this region as the BES content and the CERT is increased (Figure 33) confirms the substitution of the BES chain extender to the PPG-TDI pre-polymer.

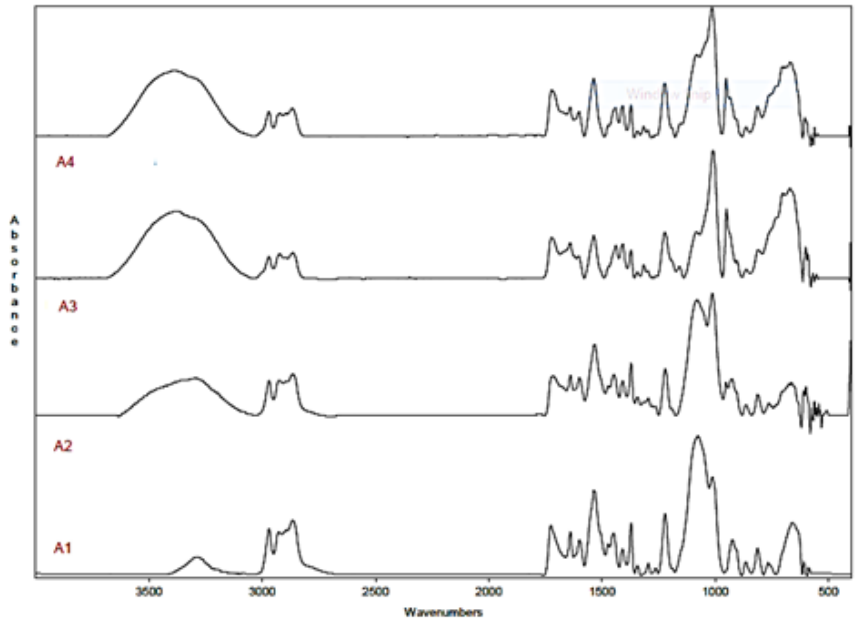

Figure 32: FTIR Spectrum of PU foam samples with varying BES/DMSO content

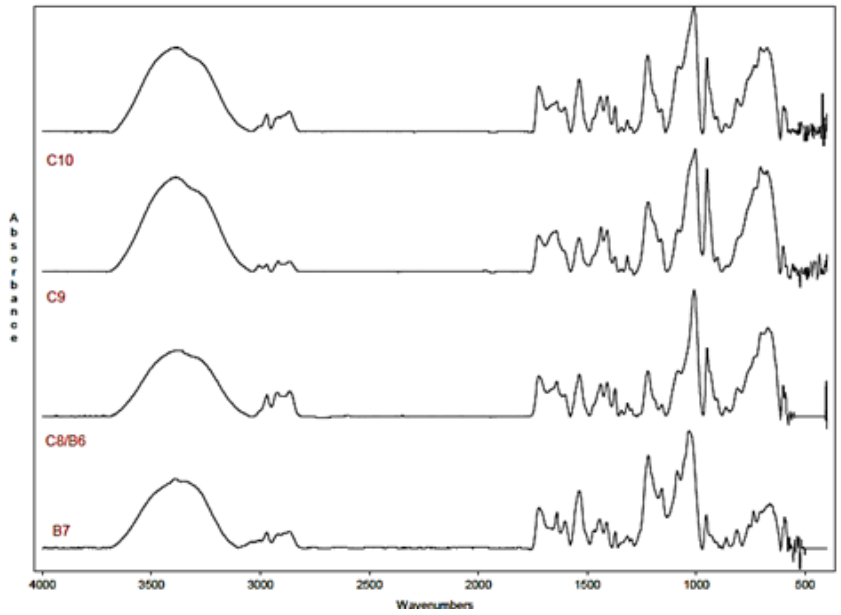

Figure 33: FTIR Spectrum of PU foam samples with varying TDI content and increasing CERT

The precipitate, mentioned earlier as recrystallized chain extender, was filtered and characterized. The clear prepolymer was also analyzed to compare the IR spectrum of the precipitate. The FTIR spectrums are shown in Figures 34 and 35.

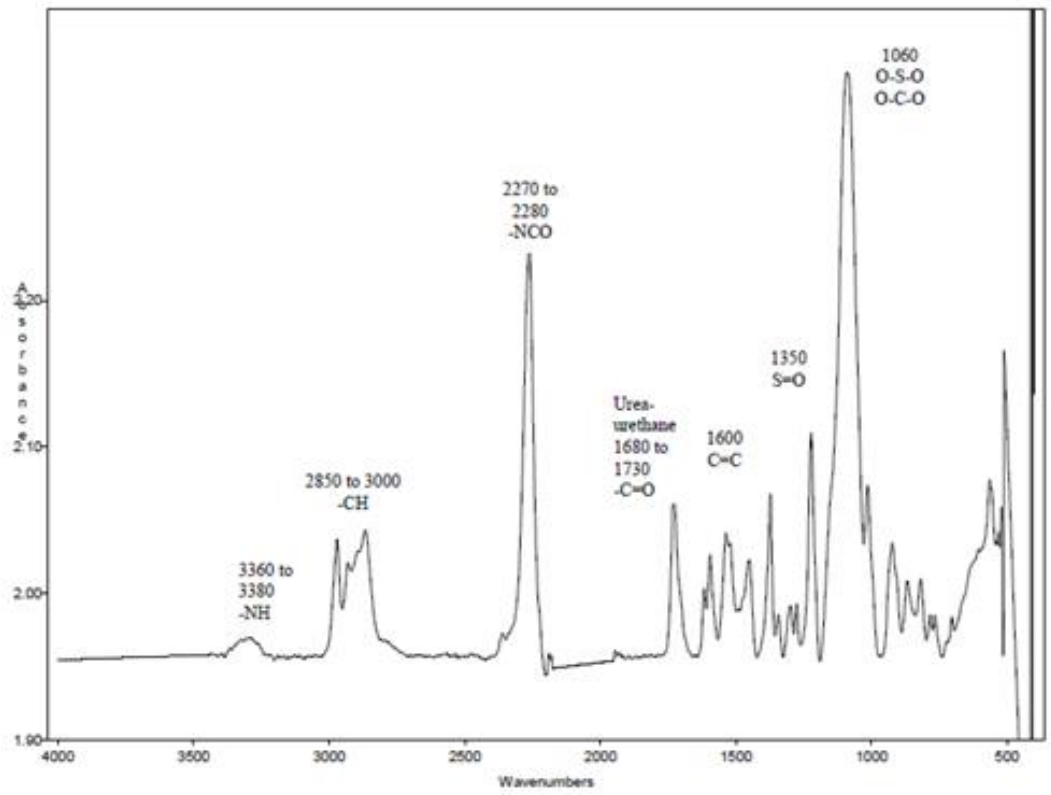

Figure 34: FTIR Spectrum of Clear Pre-polymer

The prepolymer shows the presence of O-S-O and S=O vibrations at 1060 and 1350 cm^{-1}; respectively, along with the urea-urethane and C=C and N-H vibrations at 1600 and between 3360 and 3380 cm^{-1}; respectively, confirming the addition of the sulfonic groups from the chain extender. The –NCO and –CH vibrations from unreacted isocyanate and polyol can be seen between 2270 to 2280 and 2850 to 3000 cm^{-1}.

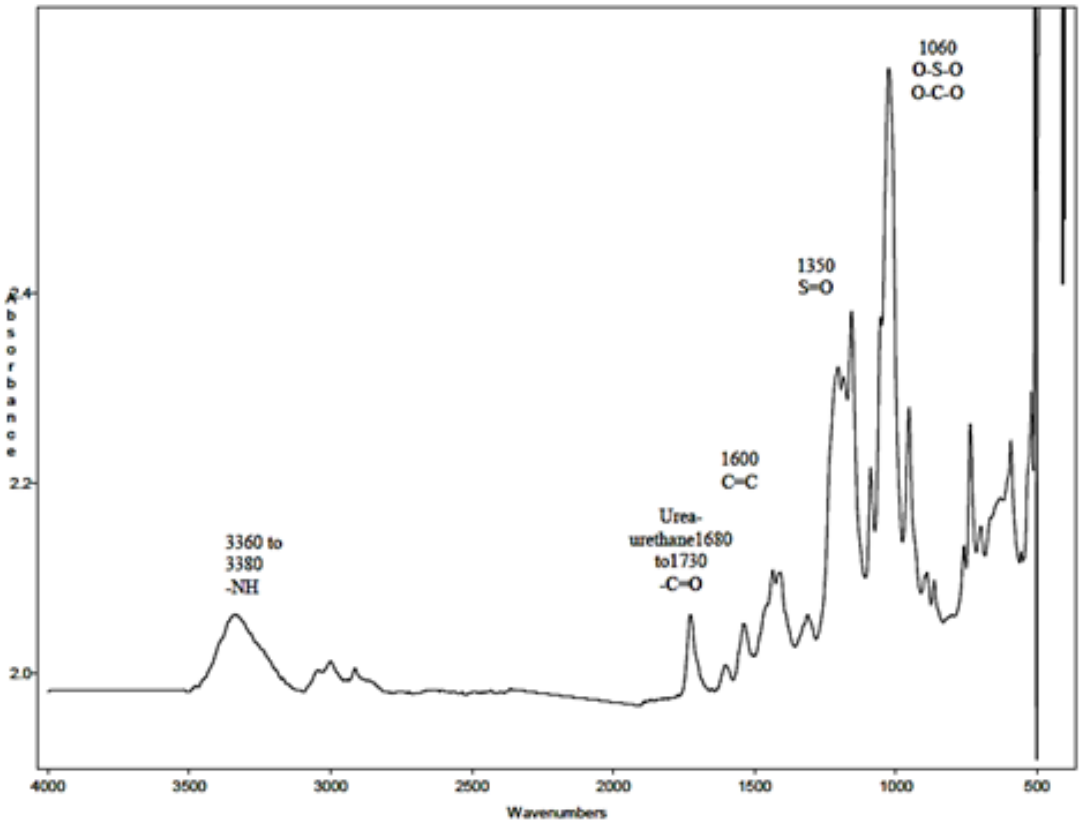

Figure 35: FTIR spectrum of precipitate formed during synthesis

The absence of the –NCO and –CH peaks in the precipitate suggests that the precipitate mainly contains recrystallized BES in the urethane pre-polymer [58, 76]. Unreacted –NCO reacts with water releasing carbon di oxide gas resulting in the foamed polymer. Further characterization of the foamed samples, as shown in Figures 34 and 35, reveals that the -NCO peak disappears as the remaining isocyanate groups are consumed during the foaming process.

4.2.1.2 Molecular Structure Analysis by GPC

GPC is one of the most powerful and versatile analytical techniques available to understand and predict the performance of polymers. It is the most convenient technique for characterizing the complete molecular weight distribution of a polymer. GPC separates molecules in solution by their effective size in solution as shown in Figure 31. Molecules of various sizes elute from the column at different rates. The column retains low molecular weight material longer than the high molecular weight material. The time it takes for a specific fraction to elute is called its retention time [77].

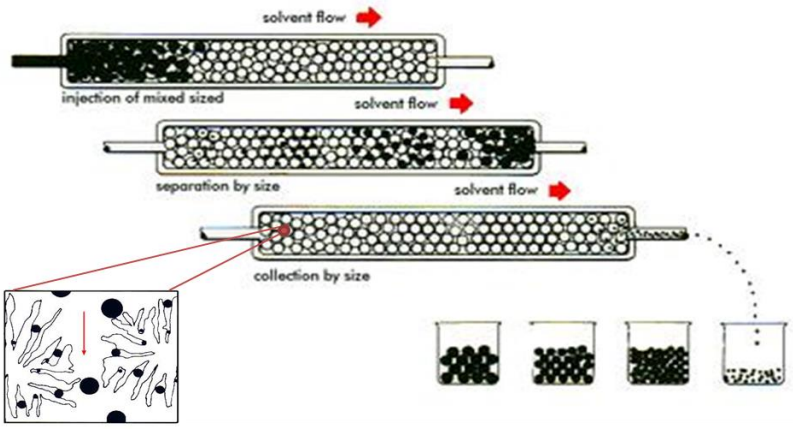

Figure 36: GPC column separating particles based on their size [77]

The polyurethane foam samples were analyzed using a Varian ProStar HPLC system using a PLgel 5mm mixed C column. HPLC grade dimethyl formamide (DMF) was used as the eluent with a flow rate of 1 ml/min. The UV detector was set to detect at 569 nm. Foam samples were dissolved in DMF to get a 0.5% w/v concentration and 25µl of the sample was injected into the column. The main purpose of this analysis was to determine the effect of the chain extender

(BES) and the solvent (DMSO) on the foam structure at a molecular level by analyzing the molecular weight of the PU foam samples.

BES is a chain extender which links the isocyanate groups in the linear polymer chains through its hydroxyl groups, thereby increasing the molecular weight of polyurethane. DMSO is a strong organic solvent which dissolves polyurethane as well as BES. Since BES is insoluble in other organic solvents, the use of DMSO cannot be eliminated from the foam synthesis process. Hence both BES and DMSO have an opposite effect on the molecular weight of the resulting polyurethane system.

GPC analysis shows that the retention time needed to elute higher molecular weight or larger molecules decreases as the DMSO content and CERT increase during synthesis. This can be seen in Figure 37 for samples A1-A4. Sample A1 has no DMSO and it elutes at 11.4 minutes. As the amount of DMSO increases in samples A2-A4, we can see larger molecules eluting earlier than 11.4 minutes followed by smaller molecules after 11.4 minutes. This can be attributed to the cleavage of polyurethane chains in samples with higher DMSO content. The peak retention times for all the tested samples are summarized in Table 5. Samples A2 and B7 seem to show a similar elution trend. A2 has a lower amount of DMSO and B7 has a higher TDI content in its composition. This provides additional isocyanate groups for functionalization; therefore lowering the ability of DMSO to break the polymer chains during synthesis. Hence increasing the TDI content in the foam composition without affecting the structural integrity of the foam may be a way to reduce the cleaving effect of DMSO [78].

Table 5: Retention times of foam samples

Sample	Peak Retention time (mins)				
A1	11.4				
A2	9.5	11.3			
A3	8.6	11.1	11.6		
A4	7.7	11.0	11.7	13.7	14.6
B7	9.2	11.4			
C9	9.4	11.0	11.4	13.9	
C10	9.4	9.7	10.6	11.7	15.3

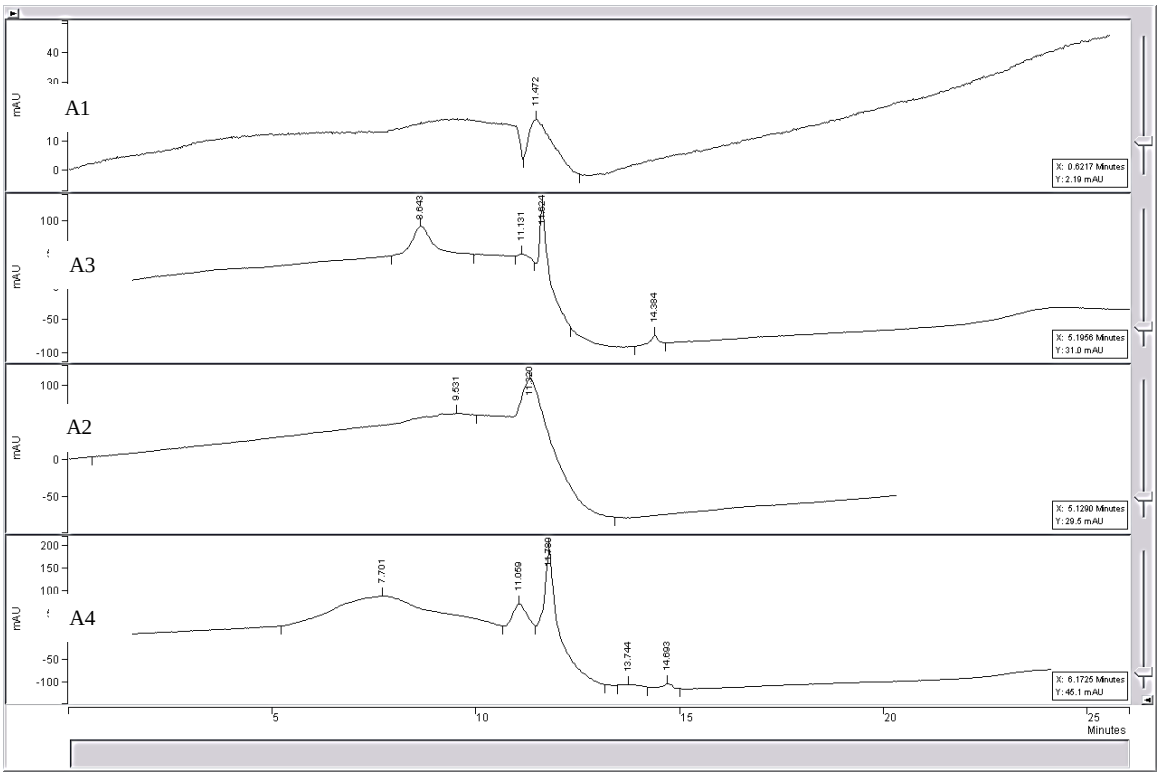

Figure 37: High and low molecular weight compounds of functionalized PU foam samples based on BES/DMSO content

Similarly; Figure 38 shows GPC analysis for samples B7-C10. It is evident that increasing CERT has the same effect in samples C9 and C10. Larger molecules start to elute after 9.4 minutes and with reasonable amounts of DMSO, higher CERT seems to cleave polymer chains to a greater extent resulting in a large molecular weight distribution in the foam sample. This is confirmed by the higher number of molecular segments which are seen to elute at 9.4, 9.7, 10.6, 11.7 and 15.3 minutes; respectively, in sample C10 which was prepared with the highest CERT. These factors influence the distribution of the functional group in the foam and affect the Pb^{2+} ion removal capacity of the foam.

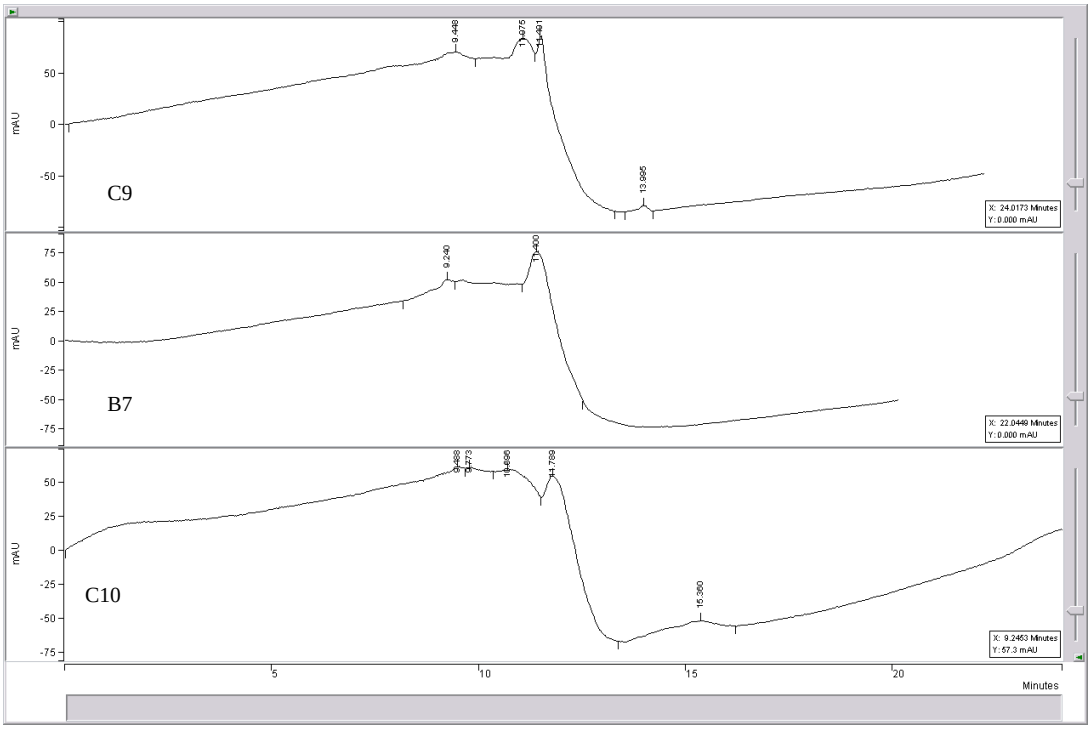

Figure 38: High and low molecular weight compounds of functionalized PU foam samples based on TDI content and increasing CERT

4.2.1.3 Morphological Structure Analysis by XRD

XRD is a nondestructive technique; it is widely applied to identify crystalline phases and orientation, structural properties, strain, grain size, phase composition, and even measure thickness of thin films and multi-layers, etc. In polymers, this information is very useful to determine the percent crystallinity of the polymer or the effect of crystalline materials on an amorphous polymer [79]. When an X-ray beam hits an atom, the electrons around the atom start to oscillate with the same frequency as the incoming beam. Because the wavelength of x-rays is comparable to the size of atoms, they are ideally suited for probing the structural arrangement of atoms and molecules in a wide range of materials. The energetic x-rays can penetrate deep into the materials and provide information about the bulk structure. When X-rays interact with a crystalline substance (Phase), one obtains a specific diffraction pattern [80].

Table 6: XRD Parameters for Bruker and Scintag XRD's

Parameter	**Scintag XDS 2000**	**Bruker D8 Discover**	**Function**
Source	Cu Kα	Cu Kα	- Produce x-rays
Detector	Ge	(VÅNTEC-500) Linxeye XE	- Detects diffracted x-rays - Records diffraction intensity as a function of 2θ
Slits (slit size)	X-ray tube: 2/3 Detector: as required [ex: 4/1 or 0.5/0.3 or 0.3/0.1]	Soller	- Collimates the X-ray beam - Converges the diffracted x-ray beams
Filter	Ni	-	- Suppresses wavelengths other than Kα - Decrease background radiation from sample

Scintag XDS 2000 and Bruker D8 Discover X-ray diffractometers were used to analyze the PU foam samples to determine the effect of the crystalline chain extender on the structure and morphology of the PU foam. In addition, after exposure to lead solution, dried foam samples were analyzed by XRD to identify the location of lead ions in the bulk functionalized PU foam. The XRD parameters for both Scintag and Bruker are shown in Table 6. XRD Spectra of the PU foam samples were recorded between 5^{o} and 40^{o}, major peaks were observed between 11^{o} and 25^{o} in the XRD spectrum.

The XRD spectrum of unfunctionalized PU foam sample A1, shows a highly amorphous structure. The addition of BES appears to slightly increase the crystallinity of the foam samples, as shown in Figure 39, since sharp crystalline peaks start to appear as the BES content is increased in the foam formulation. Sample A2, which has only 3.4g of BES, has a lower peak intensity and one can see the appearance of some crystalline peaks in comparison to the control sample, A1. The crystalline peaks start to increase in samples A3 and A4 which have a higher amount of BES. This can be attributed to the crystallinity of the chain extender, BES, a crystalline salt of sulfonic acid.

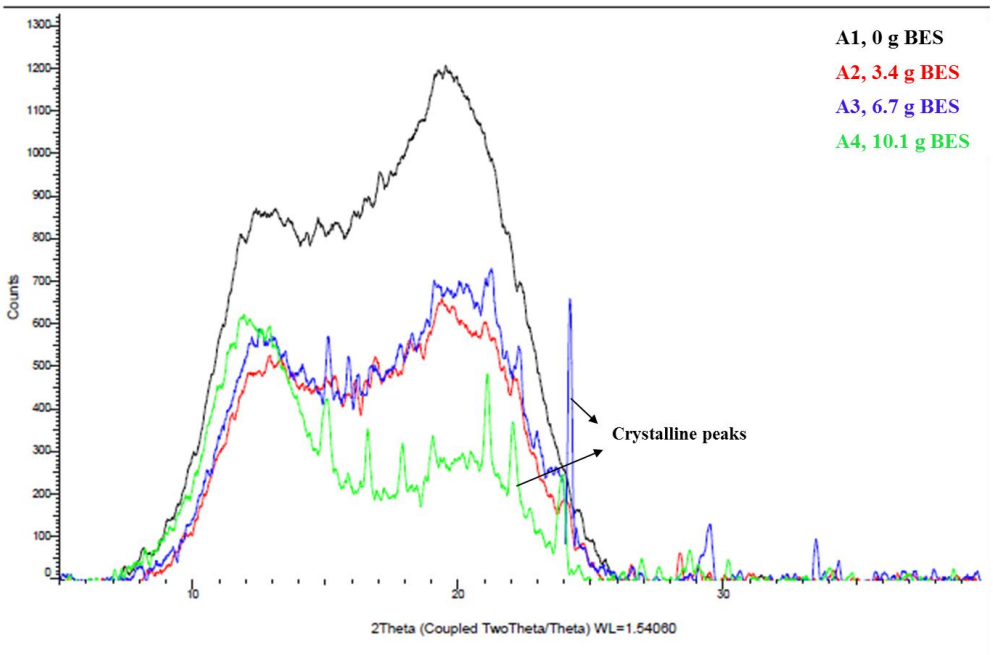

Figure 39: XRD spectrum showing the effect of BES/DMSO content on the morphological structure of PU foams

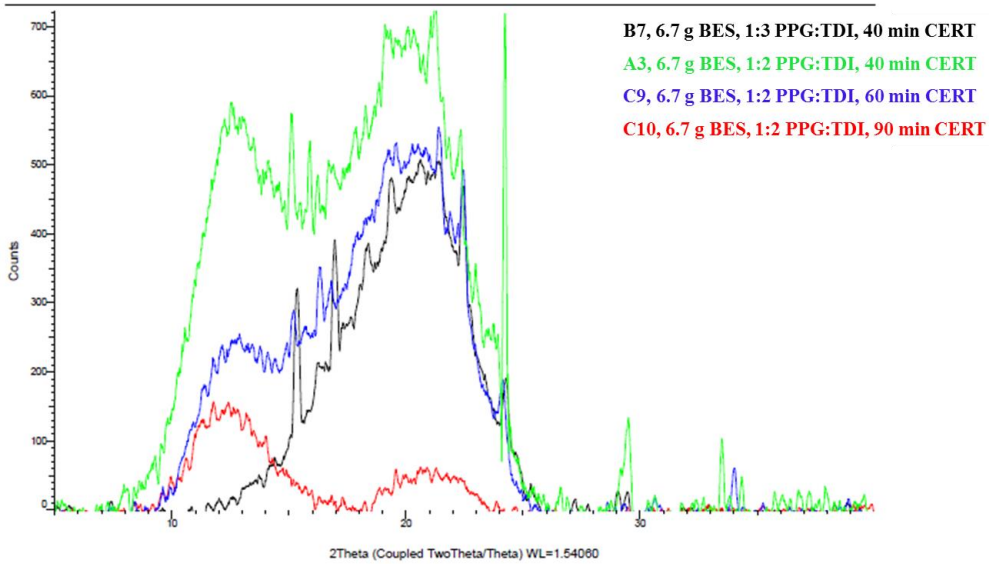

Figure 40: XRD Spectrum showing the effect of TDI content and CERT on the morphological structure of the PU Foams

On the other hand, maintaining the composition of BES as in A3 and increasing the TDI content does not seem to significantly increase the crystallinity in the samples as shown in Figure 40. TDI forms hard segments in the polymer backbone and, as a general correlation between hardness and crystallinity, one would expect the crystallinity to increase as the hard segments increase in the polymer. However, the XRD spectrums confirm that the hard segments in the polyurethane backbone do not contribute to the crystallinity of the polymer; this also explains the high amorphous nature of the control foam sample, A1. Increasing the CERT while maintaining the amount of BES in the foam formulation, seems to negatively affect the polymer morphology as the crystalline peaks are no longer visible in the XRD spectrum of foam samples C9 and C10. This is in line with the findings from the GPC analysis and confirms the deterioration of the PU foam morphology at the molecular level.

XRD is an analytical technique which can provide a plethora of information on the structure and composition in the bulk of a material. To confirm that the bulk of the PU foam was indeed functionalized, in other words, the sulfonic acid groups exist in the bulk of the material, the chemical composition of sample A3 was searched against the XRD database. The search returned several complex chemical compounds containing carbon, hydrogen, nitrogen, oxygen and sulfur. These elements are the basic building blocks of the functionalized PU foam based on the reaction scheme shown in Figure 41. Since the XRD database does not contain all polymeric materials and chemical compounds, the sample spectrum could not be directly matched to polyurethane or BES, which has the molecular formula of $\mathbf{C_6\,H_{15}\,N\,O_5\,S}$. However, the compound matching a majority of the crystalline peaks in sample A3 was selected from the

database match to confirm the presence of the elements present in both PU and BES as shown in Figure 41. This reaffirms the FTIR results confirming the presence of sulfonic acid groups in the bulk of the PU Foam sample indicating that the bulk of the PU foam was functionalized.

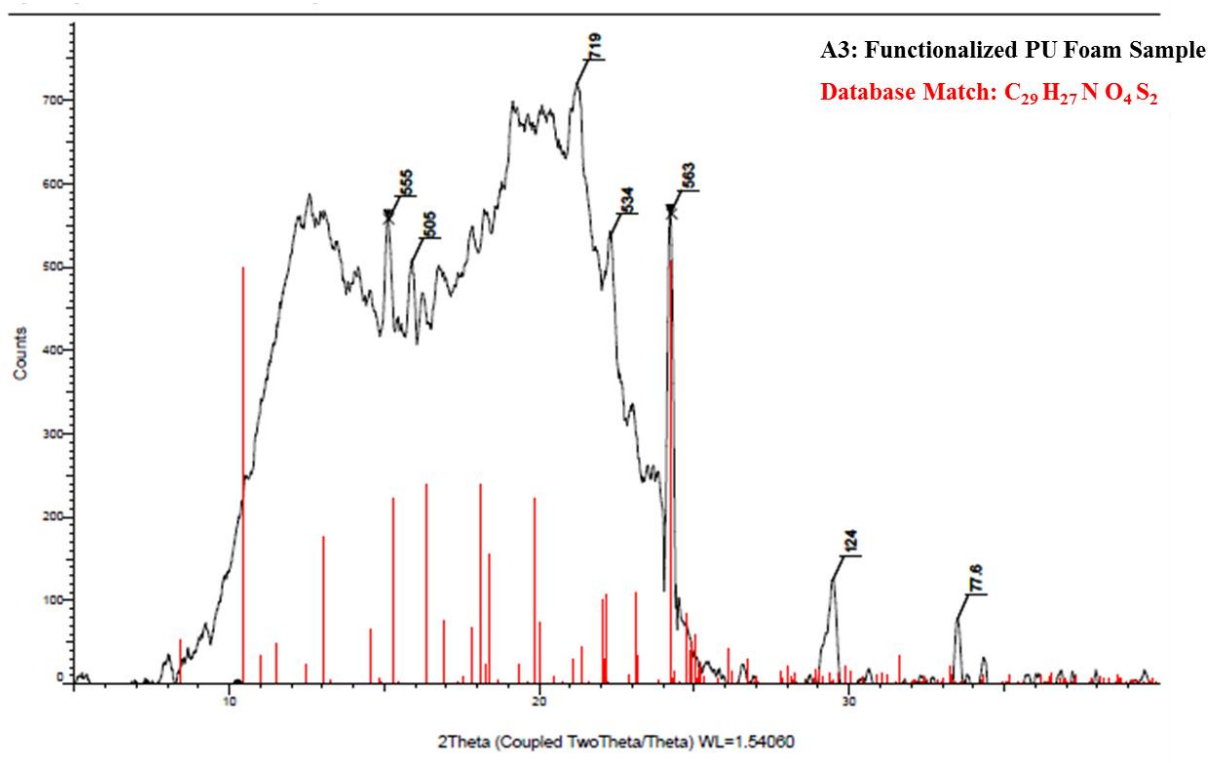

Figure 41: XRD Spectrum indicating the elements found in sulfonic acid groups (-SO_3H) confirming the bulk functionalization of the PU foam sample

4.2.2 Microstructure of the Functionalized PU Foam

4.2.2.1 Foam microstructure analysis by SEM

Scanning electron microscope (SEM) uses a focused beam of high-energy electrons to generate a variety of signals at the surface of solid specimens. The signals, which derive from electron-

sample interactions, reveal information about the sample including external morphology (texture), chemical composition, and crystalline structure and orientation of materials making up the sample [81]. Foam samples were analyzed using a Topcon SM-300 SEM/EDX instrument. The samples were coated using a sputter coater before SEM analysis. The elemental composition of the foam samples exposed to lead solution were analyzed by EDS to confirm the presence of lead in the bulk of the foam samples.

SEM micrographs of A3 foam sample at different magnifications and views are shown in Figure 42. The micrographs show a broad and non-uniform pore size distribution and also show some recrystallized BES (Figure 42b) in the foam. The large pore size of the foam samples made it difficult to obtain SEM micrographs with better resolution at lower and higher magnifications; hence other microscopic methods were considered to analyze the pore size distribution of PU foam samples. The SEM images were however, used for EDS analysis to detect the presence of lead ions after using the foams as filter media to remove lead ions from standard solutions spiked with lead.

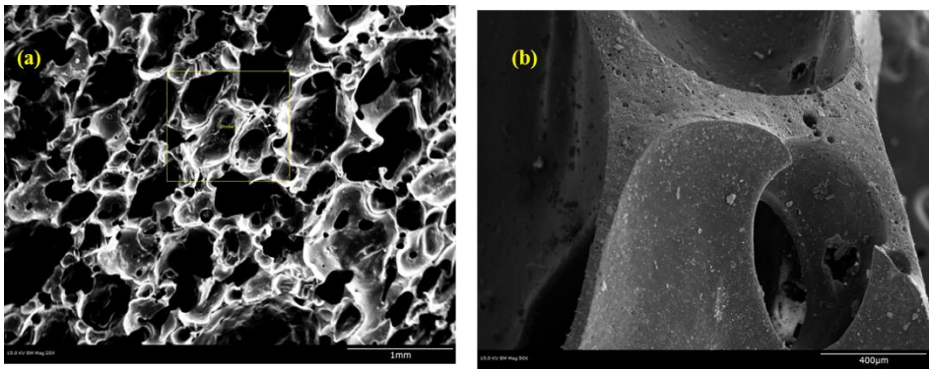

Figure 42: SEM micrographs of A3 foam sample at (a) 20X and (b) 50X

4.2.2.2 Foam Pore Size Analysis by Optical Microscopy

A Keyence VHX digital microscope was used to obtain optical micrographs of the PU foams. Two field of views were obtained from each foam sample without regard to orientation. The pore size was then measured using an image analysis software called ImageJ, by fitting circles to the pores in each image and measuring the diameters of the fitted circles. Histograms based on pore diameters (i.e., the diameters corresponding to the largest circles fitted inside various pores in the micrograph) were generated from two different field of views for each foam sample.

The optical micrographs of the foam samples show that the foam structure is different compared to the completely open cells of reticulated foams (Figure 43) due to the presence of cell membranes between cells [82] as seen in Figures 44a-44c. From the micrographs, it can also be seen that the foam contains several large pores, with smaller pores distributed on the walls of the larger ones. Moreover, the pore distribution is not uniform in the foams and the pores seemed to be denser at the core. In polyurethane foam production, the foaming and gelling reactions are critical for cell nucleation, growth, distribution, and collapse [83]. The foam composition, polyurethane chemistry, and foaming process are the main factors which determine the foam structure [83-85].

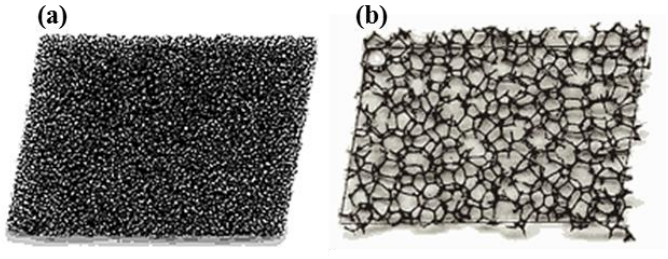

Figure 43: Reticulated commercial PU foams (a) 45 pores per inch (b) 10 pores per inch [13]

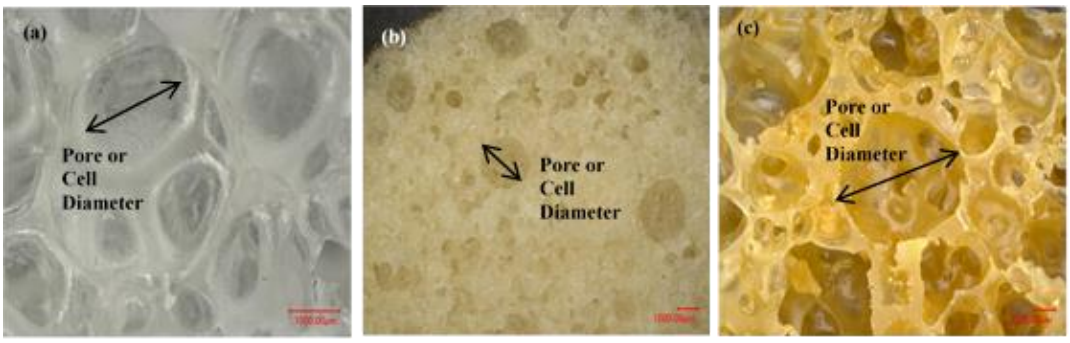

Figure 44: Optical Micrographs of (a) Control PU foam A1, (b) Functionalized flexible PU foam A3, and (c) Functionalized rigid PU foam B7

Histograms generated using the pore diameters of two sections of A1 foam (Figure 45a) show a very broad and a very narrow pore size distribution curve. This indicates that A1 sample has a non-uniform pore size distribution. In comparison, two different sections of A3 foam sample (Figure 45b) have similar bell-shaped curves indicating a more uniform pore size distribution.

If the pore size distribution of these two foam samples were compared based on the process parameters, one could say that the lack of BES and DMSO in A1 sample may have led to a non-uniform pore size distribution. In terms of the physical properties, the foam was also slightly rigid compared to the A3 foam sample. The flexibility of the foam may be another reason for the observed differences in pore size distributions. On studying the foam compositions for an explanation, it can be seen that the solvent DMSO used in A3 acts as a plasticizer imparting flexibility of the foam. The lack of DMSO in A1 may have restricted the distribution of pores during foaming; thus leading to a slightly rigid matrix and a non-uniform pore distribution in the foam.

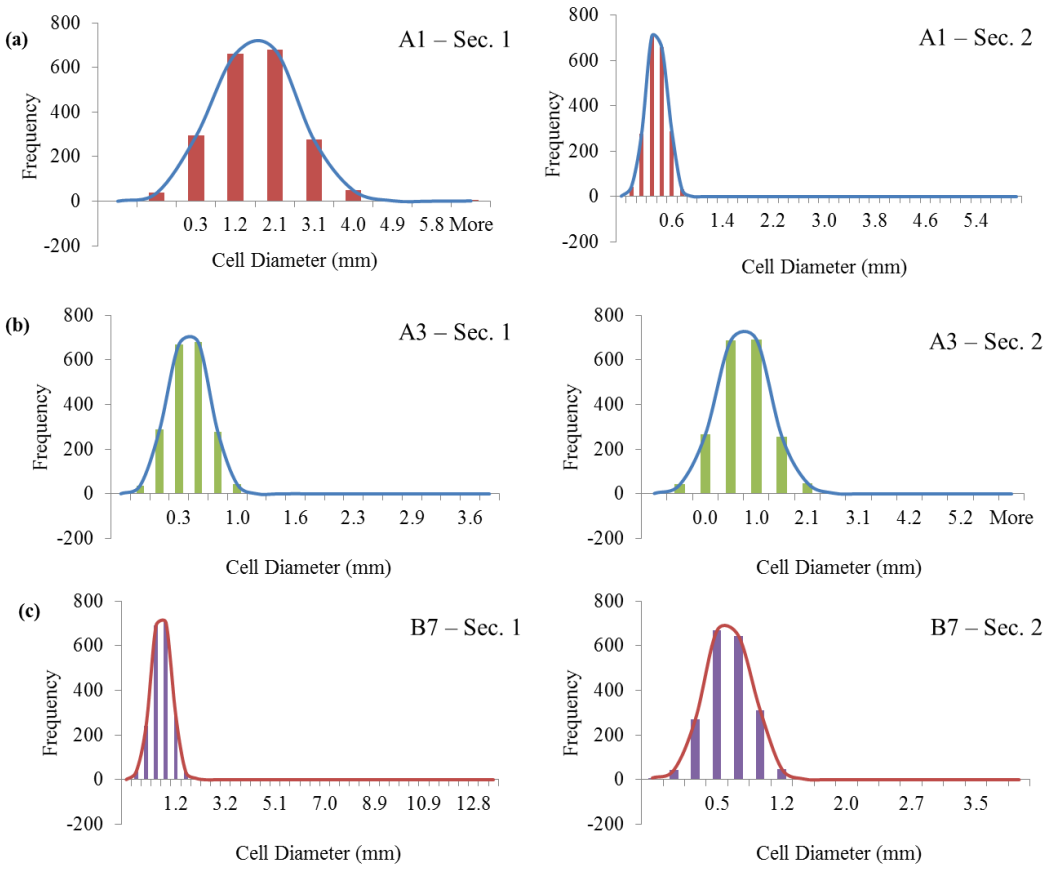

Figure 45: Pore-size-distribution histograms of (a) Control foam, A1 (b) Functionalized flexible foam, A3 (c) Functionalized rigid foam, B7

The B7 foam sample had a very rigid structure and, compared to A3, contained the same amounts of BES and DMSO, but higher amounts of TDI, in its composition. However, from the bell-curves shown in Figure 45c, the pore-size distributions look similar to that of A1. From the foam composition given in Table 4, it is clear that the presence of more TDI enhances the production of CO_2 gas during foaming, which aids in the formation of more pores. However, some of these pores become entrapped with no room for expansion due to the rigorous reaction, while others expand and collapse; eventually [84]. While this is a major factor for the rigidity in

the foam, the presence of BES and DMSO, or the lack thereof in appropriate ratios, seem to influence the pore size distribution to some extent.

If a histogram was generated for any foam using the pore data for multiple cross-sections, the distribution data will be more reasonable in determining the average pore size of the foam samples. Histograms generated by combining the measurements from two different field of views for each of the foams are shown in Figure 46. The average pore size determined by this method is summarized in Table 7. Comparing the combined histograms of each foam sample alongside each other shows that the pore size distribution of the foam samples does not vary significantly and the average pore diameters of the foam samples are in the range of 0.4 to 0.5 mm.

Table 7: Pore diameters based on the combined pore-size distribution histograms of the three foams

Foam Sample	**Cell Diameter (mm)**	
	Average	**Median**
A1	0.49	0.31
A3	0.40	0.28
B7	0.45	0.36

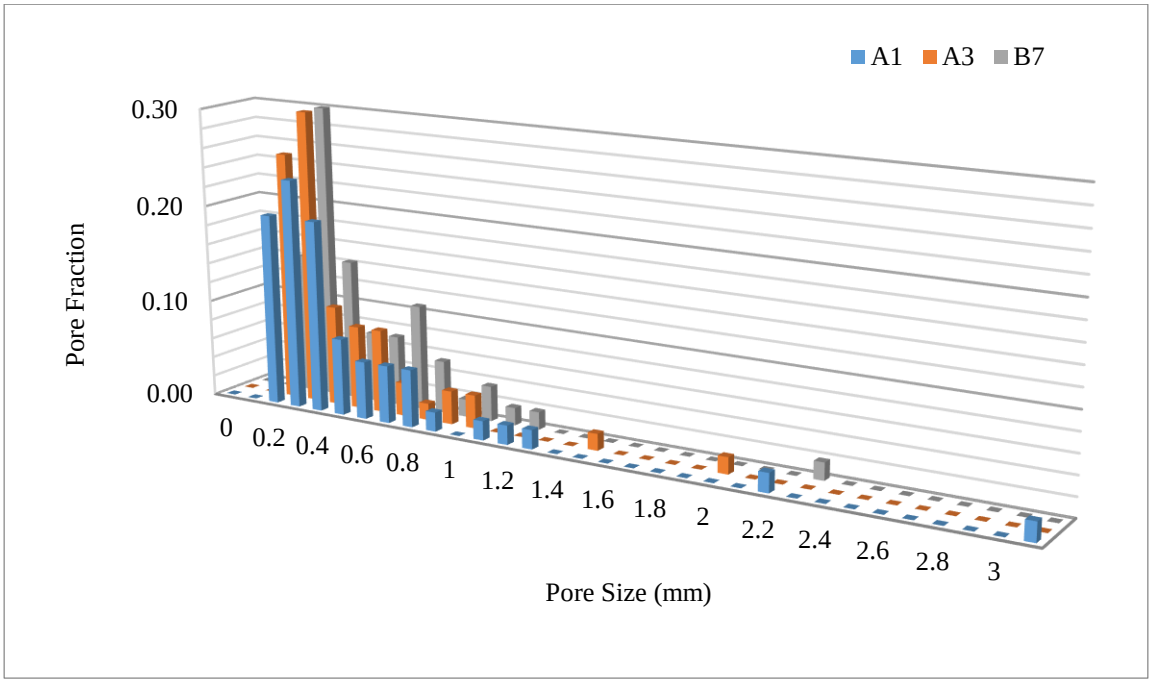

Figure 46: The combined pore-size histograms of A1, A3 and B7 foams

To determine the effect of conditioning (i.e. soaking) on the structure of the foams, 3D micrographs of the unconditioned (dry) and conditioned (wet) samples of A3 foam were obtained using a Keyence Microscope, shown in Figure 47. The micrographs show the distribution of pores and some pore-connectivity at the surface of the foam. Among all the three foams considered in this study, A3 was chosen for the 3D surface analysis as it had the highest density of open cells.

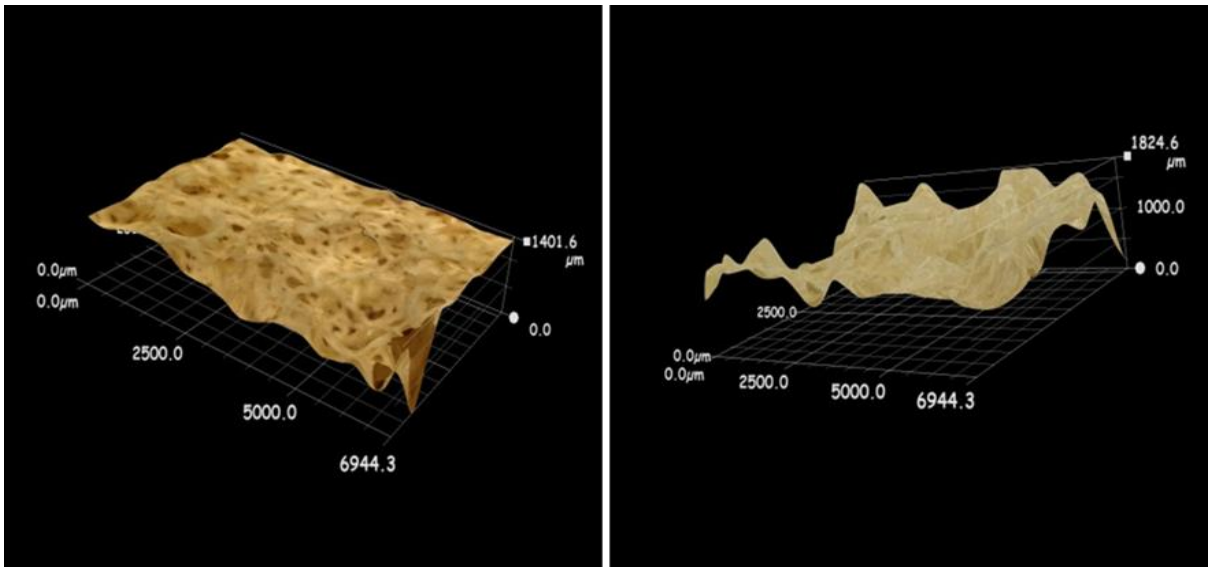

Figure 47: 3D surface micrographs of (Left) dry and (Right) wet foam A3

4.2.3 Physical Structure Analysis by Micro-CT

Micro computed tomography is simply an X-ray imaging in 3D**,** which is based on the same technology used in medical CT scans. However, Micro-CT is performed on a much smaller scale with a massively increased resolution. It is a non-destructive imaging technique which can generate 3D micrographs showing very fine scale internal structure of the objects [85]. An Xradia Versa 410 micro CT by Carl Zeiss Microscopy was used to analyze the microstructure of the PU Foams. XMReconstructor program was used for 3D reconstruction and the reconstructed images were viewed and analyzed through the XM3D viewer software.

Although statistical analysis of the optical micrographs is useful to understand the pore size distribution of the foam samples, it does not give the complete picture of the pore distribution in the bulk of the foam sample. Optical micrographs are restricted by the top views of the foam

samples. This top view depends on the way the samples are cut, so the data based on the optical micrographs alone is rather insufficient to characterize the bulk structure of the foam samples. Therefore, micro-CT was considered to characterize the bulk structure of the foam samples. Micro-CT uses x-rays to scan every section of the sample, along all three dimensions to recreate the 3D and 2D skeletal structure of the sample by combining 100's of projections from the scanned images.

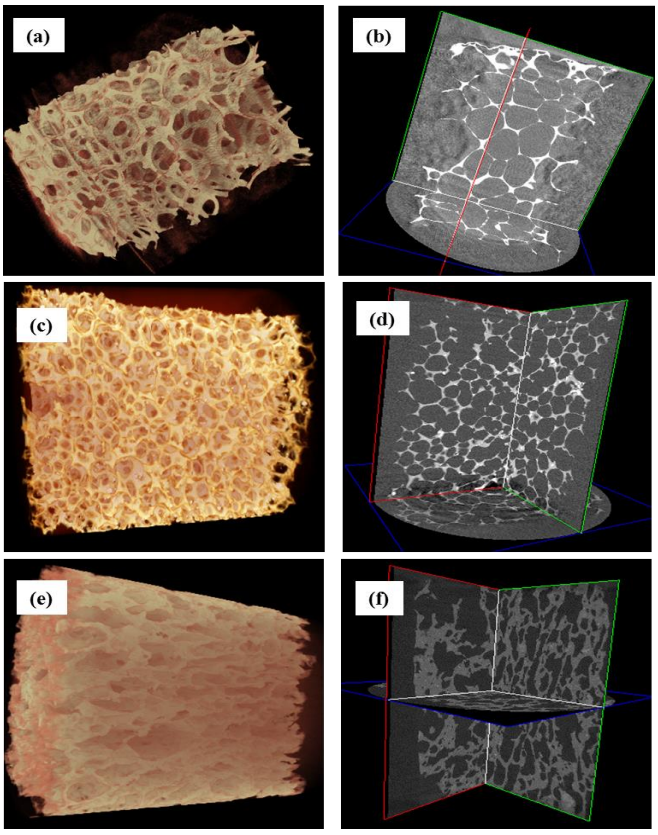

Figure 48: (a) 3D reconstruction and (b) 2D reconstruction of control, A1 foam sample; (c) 3D reconstruction and (d) 2D reconstruction of functionalized flexible, A3 foam sample; (e) 3D reconstruction and (f) 2D reconstruction of functionalized rigid, B7 foam sample

The 3D and 2D reconstructions of the control (A1), functionalized flexible (A3) and rigid (B7) PU foam samples are shown in Figure 48. The 3D micro-CT images, in Figures 48a, 48c, and 48e, clearly show significant differences in the skeletal structures, pore sizes and pore size distribution in the bulk of the three foam samples. The control and rigid foams, A1 and B7 seem to have rather larger pores compared to the flexible foam, A3. This reaffirms the effect of the foam formulation on the structure of these foams; such as, the presence and lack of DMSO in their foam formulation. It is clearly evident that DMSO acts as a plasticizer and influences the foaming process, pore formation and pore size distribution of the PU foams. 2D images also show a higher pore/cell density in A3 foam sample compared to A1 and B7 foam samples.

Visual examination of the samples revealed that the foams swell slightly upon conditioning. In water filtration operations, the amount of swelling has to be low to ensure that fluid flow is not disrupted and the efficiency of the filtration media remains unaltered. In order to determine the effect of swelling on the structure of the PU foams, micro-CT analysis was repeated on foam samples conditioned in DI water for 24 hrs. The water used for soaking the rigid foam started to turn yellow and turbid after 6 to 8 hours; whereas, the water used to soak A1 and A3 foam samples remained clear. Hence, B7 foam sample was considered unsuitable for drinking water filter applications. The micro-CT images of the dry and conditioned, control and flexible foam samples, A1 and A3 are shown in Figures 49 and 50; respectively.

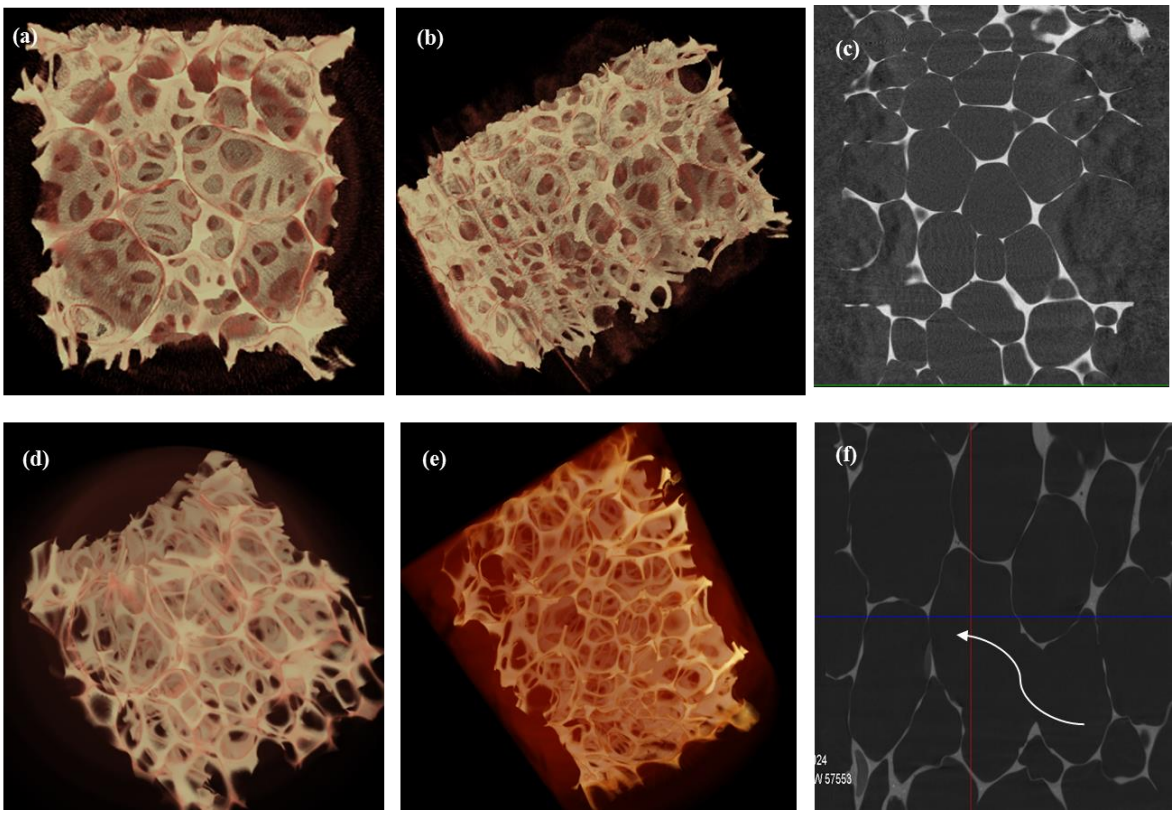

Figure 49: 3D and 2D reconstruction images of control PU foam, A1: (a) top view, (b) side view, (c) 2D view of unconditioned foam, (d) top view, (e) side view and (f) 2D view showing interconnected pores after conditioning in water for 24 hours

The size of the pores seemed to have expanded slightly in the control foam, A1, compared to the functionalized flexible PU foam, A3. The 2D images of the control foam show large pores throughout the bulk of the structure with some interconnected pores. Conditioning the foam did not seem to affect the structure or the pore size distribution of either foam types. A3 foam sample, seemed to exhibit higher swelling compared to the control foam sample, A1. However, the structure remained intact upon conditioning and a few channels for fluid flow were available in the conditioned foam compared to the unconditioned one (Figures 50c and 50f).

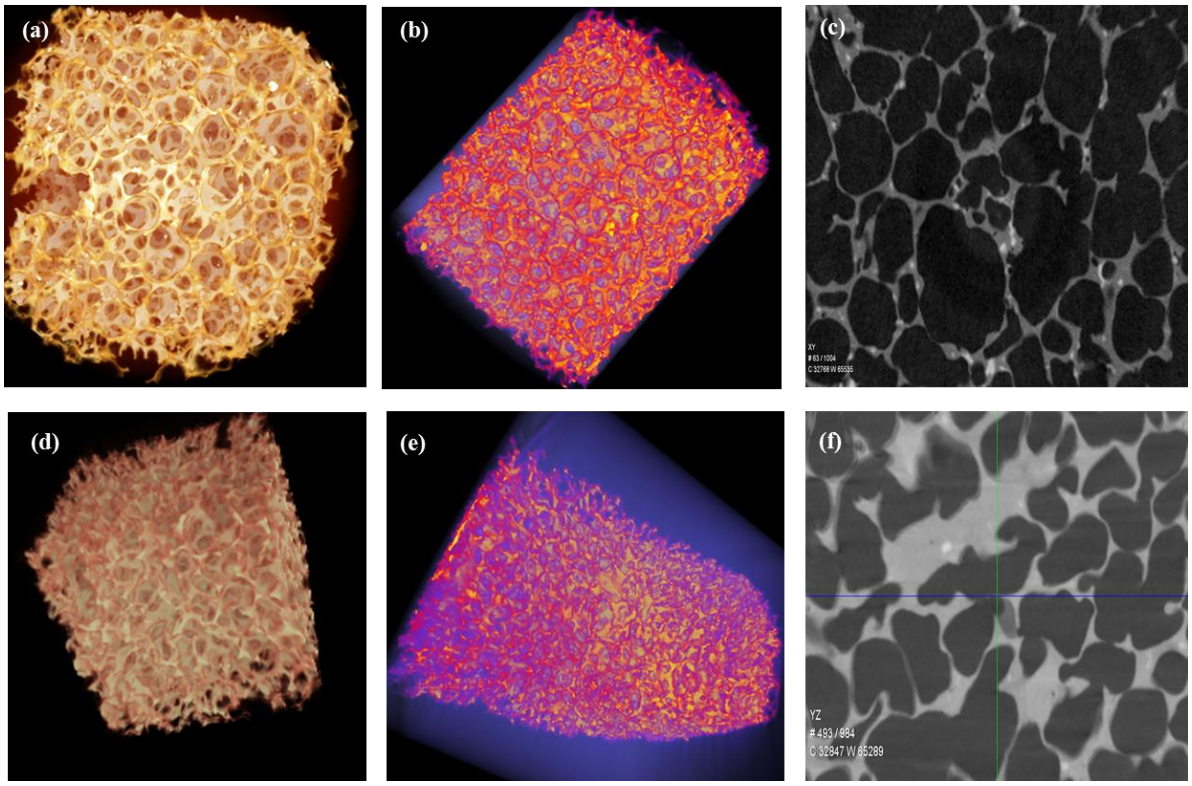

Figure 50: 3D and 2D reconstruction images of flexible functionalized PU foam, A3: (a) top view, (b) side view and (c) 2D view of unconditioned foam; (d) top view, (e) side view and (f) 2D view of foam after conditioning in water for 24 hours

4.3 Properties Evaluation

4.3.1 Physical Properties of Functionalized PU Foam

4.3.1.1 PU foam Density

Density of PU foams is a function of the chemistry and process used to produce the foam [86]. The presence of additives; such as the chain extender and the solvent, the molar ratio of the isocyanate and polyol, can influence the density of the final foam. Foam samples from the core

were cut into cubes and their dimensions and weights were recorded to determine the density according to the standard test method, ASTM D3574-01. This test method is used for the flexible polyurethane foams in slab, bonded, or molded forms, and is based on the weight to volume ratio of the foam specimens. The density is determined by dividing the mass of the sample by its measured volume and the results are reported in the relevant units [87].

The core densities of the samples were determined according to the method described in ASTM D3574-01. In general, the density of foam samples A1 to A4 increased gradually as the amount of chain extender increased in the foam formulations. The unfunctionalized foam A1 showed a density of 160.2 kg/m^3. The density of functionalized foam samples A2, A3 and A4 were 195.5, 230.9 kg/m^3 and 432.1 kg/m^3; respectively. Increasing the amount of TDI for the same amount of BES and increasing the chain extender reaction time (CERT) did not seem to affect the foam density considerably. The density of sample B7 with the highest amount of isocyanate content was 355.1 kg/m^3, which is lower than A4 with lower amounts of isocyanates and higher amounts of chain extender dissolved in DMSO. This may be due to the increase in crystallinity in the functionalized foam with the incorporation of the chain extender. The density of foam samples C9 and C10 with higher CERT were 279.3 kg/m^3 and 341.6 kg/m^3 respectively (Figure 51).

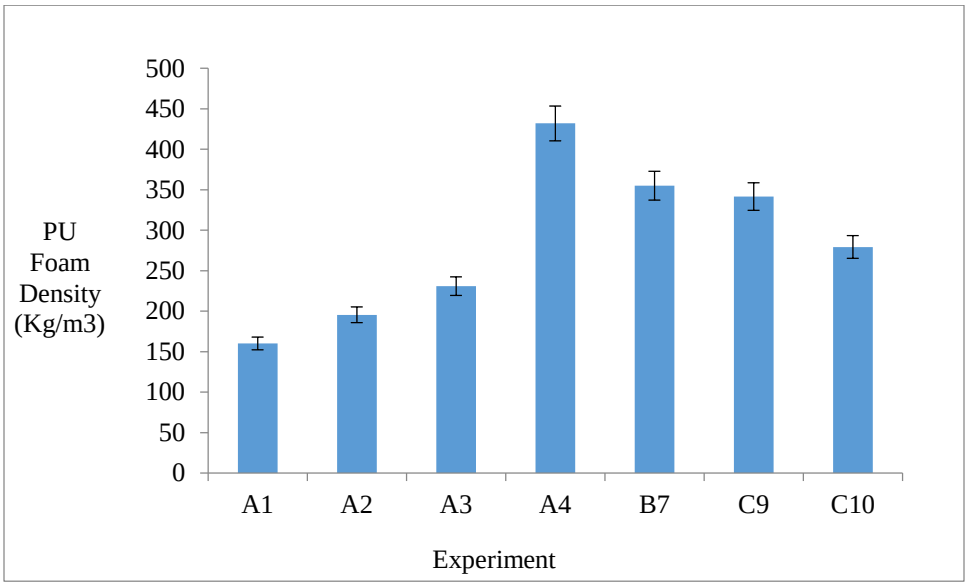

Figure 51: Density of functionalized PU foams as a function of process variables

Based on the physical and chemical characteristics of the synthesized foams, three foam samples were chosen for a thorough analysis of the foam properties. Samples from experiments A1, A3 and B7 were considered as they represent the unfunctionalized control foam, functionalized flexible foam with good structural stability, and functionalized rigid foams; respectively.

4.3.1.2 Hardness

A Shore-A durometer (ASTM D2240) was used to determine the hardness of the foam samples and quantitatively differentiate the types of foams synthesized by each formulation. The hardness values were measured in between the pores and in regions (membranes) with the least pore density and the average of four such measurements were recorded. The hardness of the control, i.e., unfunctionalized, polyurethane foam sample, A1, was 12 Shore-A. The functionalized polyurethane foam samples, A3 and B7, had a hardness of 7 and 41 Shore-A; respectively. These

values allow us to quantitatively characterize A3 as flexible and B7 as rigid functionalized PU foams.

4.3.1.3 Open Cell Content

Fluid flow in open cell foams takes place through the interconnected open cells only; hence it is important to determine the ratio of the open cells vis-a-vis the total number of cells in the foam. The open-cell content of the foam samples was evaluated according to the standard test method C described in ASTM D6266. AccuPyc II 1340 FoamPyc v1.07 instrument was used for this purpose. This technique uses nitrogen gas to fill the sample chamber and the difference in gas volume to the sample volume is used as a measure of the open cells volume in the foam sample.

The Open cell content of unfunctionalized foam sample, A1, was determined to be 89%. This shows that the molar ratio and type of polyol (PPG) and isocyanate (TDI) used in the formulation, as well as the synthesis method and reaction conditions, are suitable for the production of open cell foams. Functionalization of the foam samples using a sulphonic acid chain extender, BES, seems to improve the open cell content. The flexible foam samples, A3 showed a 91% open cell content. However, increasing the molar ratio of TDI and PPG seemed to affect the open cell content. The open cell % of B7 foam sample was found to be 70%. This can be attributed to the increased amounts of isocyanate groups in the foam formulation which lead to excessive foaming followed by foam collapse during molding, thus reducing the amount of open cells in the foam.

4.3.1.4 Porosity

An AutoPore IV 9500 V1.09 porosimeter was attempted to determine the foam porosity using the mercury intrusion method. However, the results were inconclusive due to the reaction of the foam samples with mercury (see Appendix A). Hence, another method based on the void volume was used to determine the porosity of the foam samples. A polyurethane polymer with the composition of A1, the control/unfunctionalized composition, was cast without foaming and was allowed to set in a glass mold.

Porosity is defined as the ratio of the volume of pores in a sample to the total volume of the sample. The latter was determined by dividing the mass of the foam sample by the density of the polymer used. The difference in the sample and polymer volumes yields the void or pore volume of the foam sample, which is used to determine the porosity of the sample. The porosity, ε, was hence determined using equation (6) below:

$$\varepsilon = \frac{V_{sample} - V_{polymer}}{V_{sample}} \qquad (6)$$

where, V_{sample} is the volume of the foam sample and $V_{polymer}$ is the volume of the un-foamed polymer.

Based on the volume of the polymer and the foam samples, the porosity of A1, A3 and B7 was estimated to be 89%, 85% and 90%; respectively. The porosity of the un-functionalized (A1) and the rigid functionalized (B7) foams seem to be similar in comparison to the flexible functionalized foam (A3) sample. This suggests two possibilities: the first is that the solvent,

DMSO, which is used to dissolve the chain extender BES in A3, acts as a plasticizer, thus improving the flexibility of the foam compared to the sample A1, which does not contain any DMSO or BES in its formulation. On the other hand, higher amounts of TDI present in the formulation of B7 sample seems to lower the plasticizing effect of DMSO by rendering the foam more rigid with a higher porosity. Several reactions between DMSO and diisocyanate's such as TDI have been reported which prove the above observation [88].

4.3.2 Flow Properties of the Functionalized PU Foam

A falling-head permeameter setup, shown in Figure 52, was used to determine the permeability of the foam samples. A graduated cylinder with open ends was fitted to a burette stand and a cylindrical foam sample with the same diameter as the graduated cylinder was placed inside it.

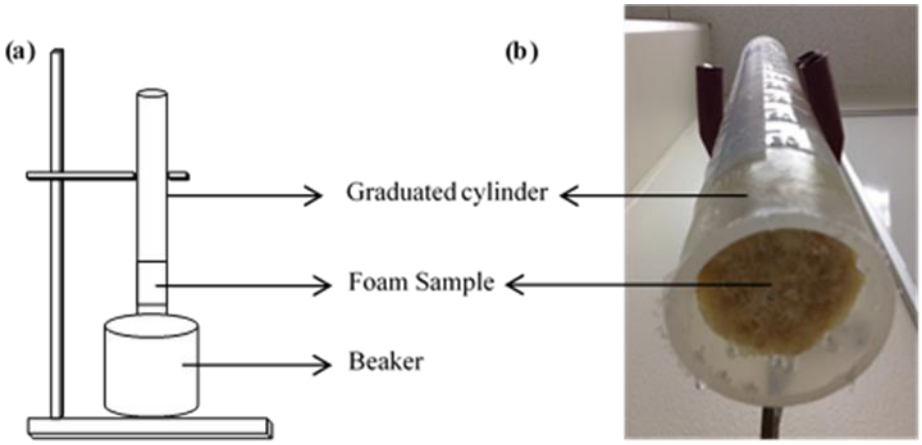

Figure 52: Falling head permeameter (a) Schematic diagram (b) Experimental setup

To ensure that the wall effect is nullified, the space between the sample and cylinder walls was sealed using a silicon caulking agent. Water was run through the foam several times before

starting the experiment to ensure that there were no leaks through the foam walls and the water was indeed flowing through the foam samples. The main principle behind this method is that a certain volume of water is allowed to flow through the foam, and the time lapse for the flow-through is directly related to the permeability of the foam; the higher the permeability, the lower the time lapse [88]. The test column was filled with water to the maximum height and the time lapse for the head to come down to a final, lower height was recorded. The permeability, *K* was then determined by equation (7) as the following:

$$K = \frac{\mu a L}{\rho g A t} \ln \frac{h_1}{h_2} \qquad (7)$$

where μ is the viscosity and ρ is the density of water at room temperature, g is the acceleration due to gravity, *a* is the cylinder cross-sectional area, A is the cross-sectional area of the foam sample (in this case, *a* is equal to *A* as the foam sample is placed within the graduated cylinder), *L* is the length of the foam sample, *t* is the time of flow, h_1 is the initial height of water in the column, and h_2 is the final height of water in the column [89].

As the functionalized PU foams are intended for water filtration applications, the permeability, *K*, of the porous medium is an important property to characterize as it can be used to predict fluid flow in any porous medium [90]. Several theoretical models are available to predict the permeability *K* of porous media. Of these, many were developed to analyze air-flow through open-cell and partially open-cell polyurethane foams [91], and were also used for water flow predictions through these foams. The theoretical permeability models are often a function of the

mean cell diameter and porosity of the compressed, fully open-cell, polyurethane foams. However, there are some deviations from these model predictions when applied to low density foams subjected to compressive strains [92, 93].

The *K* of the functionalized and non-functionalized polyurethane foams were determined using a falling-head permeameter experiment. It has been shown that *K* varies as the square of the mean cell diameter, *D*, for open-cell polyurethane foams [94], i.e.

$$K \propto D^2 \qquad (8)$$

Most of the models developed on permeability incorporate this primary relationship. As shown in Table 9, the experimental *K* values of the chain extended polyurethane foams are in the range of 0.45×10^{-11} m^2 to 2.62×10^{-11} m^2. The permeability values obtained from literature range from 0.6×10^{-9} to 1.65×10^{-9} m^2 for the slow-recovery polyurethane foams [91, 94]. Hence, the experimentally measured values of the permeability are lower by 2 orders of magnitude compared to the values in literature for polyurethane foams. However, the literature values for the permeability are for air flow. (Due to fluid slippage at very small length-scales, the air-flow permeability is usually higher than the fluid-flow permeability for any given porous medium [95].)

To compare the experimental values to the conventional theoretical models for liquid flow, some well-known models that are predominantly used to determine *K* for liquid (water, oil, etc.) flow

through porous media, which are based on the mean particle diameter (D) and porosity (ε) of the porous medium, were chosen. These models have been found to be suitable for particulate porous media and are of the general form:

$$K = D^2\phi(\varepsilon) \tag{9}$$

Here the porosity function, $\phi(\varepsilon)$ is a function determined by the theory used to predict liquid flow in porous media. Though several such theoretical models are available in literature, the equations developed by Kozeny and Carmen and Duplessis and Masliyah described in [96] were considered in this study. The corresponding porosity functions for these two models are:

Kozeny and Carmen: $\phi(\varepsilon) = \frac{1}{180}\frac{\varepsilon^3}{(1-\varepsilon)^2}$ (10)

Duplessis and Masliyah: $\phi(\varepsilon) = \frac{\varepsilon\,[1-(1-\varepsilon)^{0.33}][1-(1-\varepsilon)^{0.66}]}{63(1-\varepsilon)^{1.33}}$ (11)

Since the foam-based porous media are not made of particles but cells, the mean cell diameter was used for *D* to determine the theoretical permeability. The average cell diameter was obtained from the statistical analysis of the micrographs (see Figure 46 and Table 7). The experimental and theoretical *K* values along with other foam properties are summarized in Table 8. The theoretical *K* values obtained from the particulate media models are close to the ones reported in

literature [91, 92] for Polyurethane foams, however the former (like the latter) deviate from the experimental *K* values by two orders of magnitude.

The permeability shown in Eq. 8 is directly proportional to the square of particle (cell) diameter. The theoretical permeability listed in Table 8, follow this relationship with the cell diameters for A1, A3 and B7. Foam A3, with the lowest cell diameter, has the lowest theoretical permeability; whereas, foam A1, with the highest cell diameter, exhibits the highest theoretical permeability. However, this trend is not reflected by the actual measured permeability: although A1 does have the highest permeability, B7 shows the lowest permeability rather than A3.

Table 8: Permeabilities of the functionalized polyurethane foams

Foam	**Open Cell %**	**Porosity %**	**Effective Porosity ε_{eff} %**	**Avg. Cell Dia. (mm)**	**Permeability, $K_{experimental}$ (m^2)**	**Permeability, $K_{theoretical}$ (m^2)**		**Effective Permeability, K_{eff} (m^2)**	
						Kozeny and Carmen	*Duplessis and Masliyah*	*Kozeny and Carmen*	*Duplessis and Masliyah*
A1	90	89	79	0.49	2.62×10^{-11}	77.8×10^{-9}	25.3×10^{-9}	17.1×10^{-9}	6.9×10^{-9}
A3	91	85	77	0.40	1.08×10^{-11}	24.2×10^{-9}	8.9×10^{-9}	7.7×10^{-9}	3.3×10^{-9}
B7	70	90	63	0.45	0.45×10^{-11}	82.0×10^{-9}	25.7×10^{-9}	2.1×10^{-9}	1.0×10^{-9}

In order to explain this anomalous behavior, another parameter that pertains to the interconnectivity of the cells or pores has to be considered. Open-cell content, gives the percentage of the pores that are interconnected and will take part in the forced flow of a fluid through the sponges. The values listed in Table 8, show that the percentages of interconnected pores are higher (around 90%) in foams A1 and A3, and lower (around 70%) in foam B7. If we define an effective porosity, ε_{eff}, as the ratio of volume of interconnected pores (open cells) to

the total volume, then ε_{eff} is the product of the open cell % and the porosity. The new effective permeability K_{eff}, using the two theoretical models were obtained by using ε_{eff} in Eqs. 10 and 11 as listed in Table 8. After this modification, the trends in the theoretical permeability follow the trend seen in the experimentally measured permeability: A1 has the highest permeability, while B7 has the lowest permeability. Hence it is important to take into account the interconnectivity of pores while estimating any theoretical permeability. However, despite this improvement, the theoretical permeability values are higher than the experimental permeability values by two orders of magnitude.

Typically, the theoretical models are capable of predicting the permeability within an order of magnitude for the particulate and fibrous porous media. The large deviation between the experimental results and the theoretical predictions for the functionalized foams comes as a surprise and is a cause of serious concern. The possible causes for such a big divergence are speculated to be:

(1) The theoretical models consider porosity and the average cell diameter, and do not take into account the cell connectivity during water flow through the foams. The small pores connecting the large cells may be responsible for the unusually low permeability values observed experimentally in the functionalized PU foams. (Since the maximum pressure drops occur in the smallest cross-sections of the flow channels.) A form of 3-D network model, where the larger cells are connecting to their neighbors through the smaller pores, will be able to predict the permeability values more accurately.

(2) The foams seem to be swelling when exposed to water, this may lead to the disappearance of some pores during the permeability experiments. Since the foam micrographs shown in Figures 47a-47c were taken from dry foam samples, the mean cell diameter and porosity values listed in Table 8 may be higher than the actual values during the flow of water through the foams.

Let us discuss a consequence of the lower-than-expected permeability of the foam samples. The pressure drop of the foam can be determined using Darcy's equation [91, 97]:

$$Q = \frac{KA\Delta P}{\eta L} \qquad (12)$$

Where, ΔP is the pressure drop applied to a parallelepiped shaped piece of foam, Q is the volumetric flow-rate through a cross-section of the geometry that is normal to the flow direction, A is the corresponding cross-section area, L is the length of the foam in the parallelepiped, and η is the viscosity of water.

For a given flow rate, this equation relates the permeability to the applied pressure drop inversely. Due to the lower-than-expected experimental K values, larger applied pressures are required for higher (practical) flow rate—applications. Such high pressures may deform the foam structure during the proposed filtering operation, thus lowering the efficiency of the

functionalized PU foams. However, since the water flow in the permeameter experiment was gravity-fed, there is a good chance that the permeability and pressure drop through the PU foams will change when water is pumped at a constant flow rate against gravity. Hence, the permeability values will be compared to the ones evaluated under operating conditions during the performance analysis of the PU foams through column tests in the subsequent section.

4.4 Performance Evaluation

The sulfonic acid functional groups present in the chain extender (BES), used in the synthesis of functionalized PU foams are capable of selectively removing lead ions (Pb^{2+}) by exchanging H^{+} ions from the sulfonic acid group with Pb^{2+} ions. Since the goal of this research work was to design a filtration media capable of removing lead ions at very low concentrations, i.e., at parts per billion (ppb) levels, the variables affecting the lead ion removal capacity of the foam were studied thoroughly as detecting and removing lead ions at such low concentrations is a challenge in itself.

ICP-MS is a powerful analytical technique which allows detection of trace elements in a wide variety of samples. Trace elements detection limits are at ppb and parts per trillion (ppt) levels. Hence, this analytical technique was chosen to determine the lead removal efficiency fo the functionalized PU foams. An ICP-MS combines a high-temperature ICP source with a mass spectrometer. The ICP source converts the atoms of the elements in the sample to ions. The analyte ions are then focused by a series of ion lenses into a quadrupole mass analyzer, which

separates the ions based on their mass/charge ratio to be detected by the mass spectrometer. The block diagram of an ICP-MS is shown in Figure 53 [98].

ICP-MS analysis was performed using a Micromass Platform ICP-MS, connected to a computer-controlled, multi-purpose autosampler. The autosampler automates standard and sample introduction processes for instrument calibration and sample analysis [99].

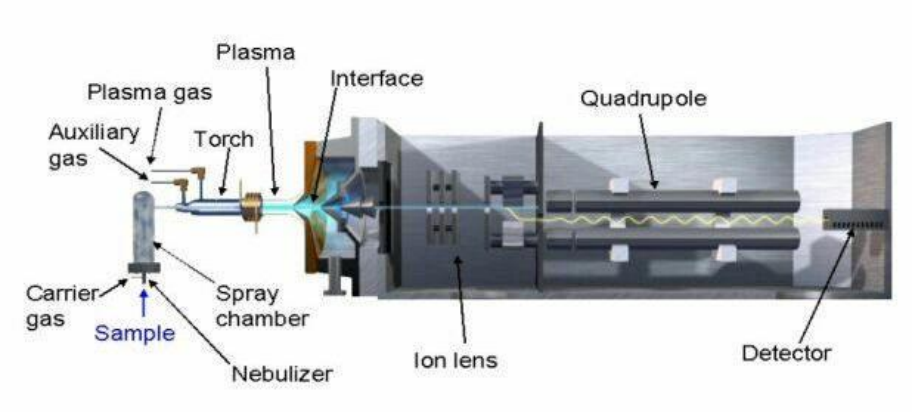

Figure 53: Block diagram of an ICP-MS [98]

The concentration of Pb^{2+} ions in the standard solution was measured and compared to the sample solutions, which were filtered after soaking the foam samples for a predetermined time by constantly agitating the lead solution by stirring or shaking. The difference between the measured standard and sample solution was used to calculate the lead removal efficiency of the foam.

4.4.1 Variables Affecting the Lead ion Removal Efficiency of Functionalized PU Foams

4.4.1.1 Foam Conditioning

Commercial ion exchange resins are usually dry and are not capable of exchanging ions unless they are conditioned in water. In the same way, PU foams need to be conditioned in water or 2N sodium chloride (NaCl) solution to homogeneously realign the polymeric bonds for ion exchange as the foams do not experience stress-free conditions after synthesis [58]. Figure 54 shows the effect of conditioning on the Pb^{2+} exchange capacity of the foam. Foam samples from experiment A3 were considered for this analysis. Foam samples conditioned in 2N NaCl for 4 hours showed higher Pb^{2+} removal capacity compared to the foam samples which were unconditioned. This confirms that conditioning rearranges the polymeric bonds [58] in the foam and exposes the functional groups for ion exchange. The Initial lead concentration in the standard solution was 100ppb. Conditioned foam samples showed a 40% increase in lead removal capacity compared to unconditioned foams over a period of 12 hours.

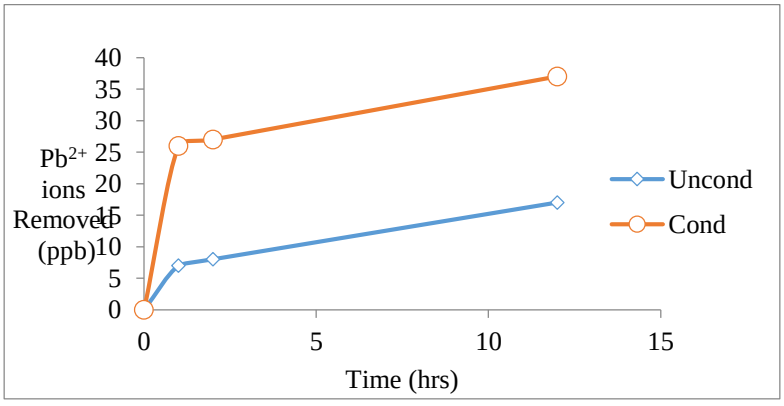

Figure 54: Effect of foam conditioning on lead ion removal capacity

4.4.1.2 Initial Lead Ion Concentration

The initial concentration of lead ions in the solution plays a crucial role in the lead removal efficiency of the foam as shown in Figure 55. The test solution containing higher amounts of lead (100ppb) has a higher lead removal capacity in comparison to the one with a low initial concentration (40 ppb). This is due to the low probability of lead ions which effectively seek ion exchange sites in a solution containing very few ions.

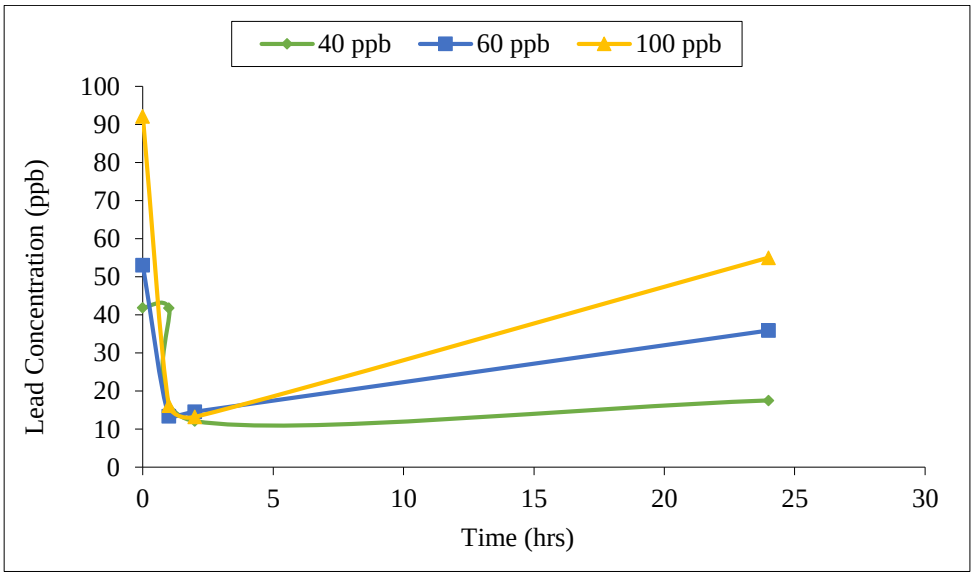

Figure 55: Effect of initial lead ion concentration on the lead removal efficiency of A3 foam sample

4.4.1.3 Process variables

(i) Effect of chain extender-solvent content

The solvent (DMSO) considered to dissolve BES for foam synthesis is a strong organic solvent which is capable of dissolving PU foams as well. So the amount of BES used during synthesis

was limited by the amount of solvent required to dissolve it. BES is soluble in water and is insoluble in most organic solvents. Dissolving BES in water is not a viable method for bulk functionalization of the PU foam since the addition of BES-water mixture to the pre-polymer will initiate the blowing reaction as water molecules will start reacting with the isocyanate groups. On the other hand, the functional groups will not have enough time to react with the isocyanate groups which are present in the pre-polymer. This will hinder the bulk functionalization of the PU foam at the molecular level.

The effect of BES content on Pb^{2+} removal (samples A1-A4) at various exposure time intervals is shown in Figure 56. The initial concentration of the lead solution was chosen to be 100ppb based on previous experiments and NSF/ANSI 53 test standards. One gram of each foam sample was soaked in 25ml, 100ppb lead solution and the solution was stirred using a magnetic stirrer for the duration of the test.

Foam samples with A1 composition showed some Pb^{2+} removal in the absence of sulfonic functional groups, this suggests that the mechanism of Pb^{2+} removal is not solely by ion exchange and it may be due to adsorption as well [100]. Polyurethane foams are well known for their strong adherence properties and it may have contributed to some Pb^{2+} removal. Observations also indicate that this behavior changes with time, suggesting that the initial exposure at lower time intervals allows the Pb^{2+} to adhere to the foam surface or pores and on prolonged exposure, to maintain thermodynamic equilibrium, some Pb^{2+} ions leach back into the solution from the foam surface as they do not form any complexes with the PU foam.

Foam samples with A2 composition showed a steady increase in Pb^{2+} removal efficiency with time. This can be attributed to the lower amounts of BES used during synthesis. The availability of fewer functional groups for ion exchange along with surface adsorption may be the main reason for this behavior. Foam samples, A3, exhibited an opposite trend in Pb^{2+} removal efficiency. As shown in Figure 56, the Pb^{2+} removal was high initially at lower time intervals and reached a saturation limit between 2 to 12 hours, further exposure beyond 12 hours did not show any significant increase in Pb^{2+} removal capacity.

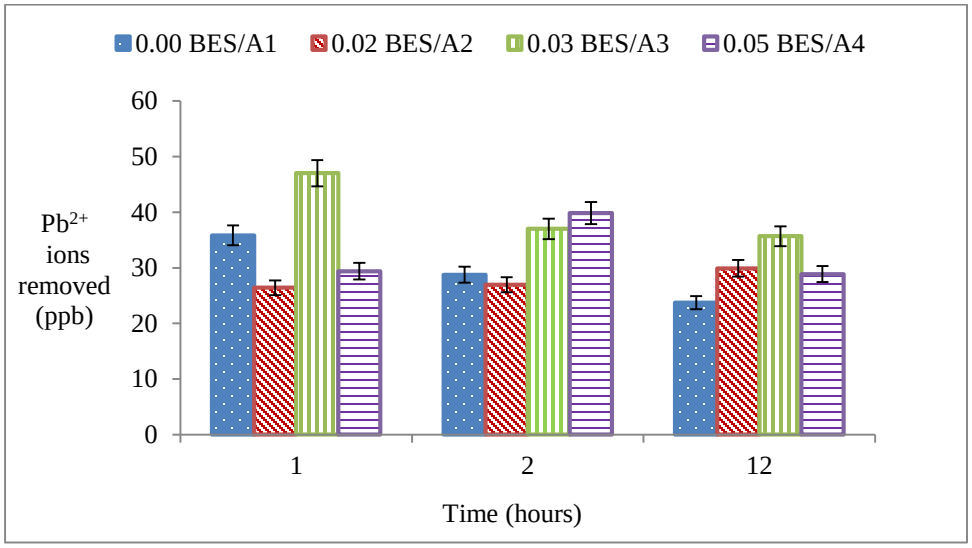

Figure 56: Lead removal efficiency based on BES/DMSO molar content

Foam with A4 composition showed a rather unique trend in comparison to A2 and A3. With higher BES content, one would expect the foam to have higher and faster Pb^{2+} removal capacity due to the higher number of sites for ion exchange. But the experimental results contradict this

expectation and the foam shows a sinusoidal performance, instead. Pb^{2+} removal seemed to increase steadily at lower time intervals and was observed to be much lower than the samples from A3 at 1 hour time interval, meaning higher amounts of BES does not contribute to faster Pb^{2+} removal as one would expect. However over a period of 2 hours, A4 performed better than A3. This may be due to adsorption coupled with ion exchange mechanism. Finally the Pb^{2+} removal capacity tapered down and saturated on prolonged exposures even when higher amounts of BES in the foam formulation. This behavior may be due to the effect of excess DMSO in the formulation which disintegrates the molecular structure of the PU foam, limiting the surface availability of functional groups for ion exchange in the foam.

Preliminary results indicate that the composition of the foam from experiment A3 has the best performance efficiency as it showed a Pb^{2+} removal capacity of 47ppb/g of foam in 60 minutes; hence the BES/DMSO content from this composition will be maintained constant in the remaining set of experiments while varying other process parameters.

(ii) Effect of polyol-isocyanate (PPG/TDI) content

As discussed earlier, the amounts of PPG and TDI play a very important role in determining the type of PU foam produced. Figure 57 shows the effect of PPG–TDI molar ratio on the Pb^{2+} removal capacity of the functionalized foam. The composition of sample B5 was not suitable to synthesize the foam and hence there are no results on Pb^{2+} removal capacity from this experiment. Sample B6 is similar in composition to that of A3 and the Pb^{2+} removal capacity results are the same as discussed earlier. The characteristic feature observed from this set of

variables is the Pb^{2+} removal capacity exhibited by the rigid foam with composition B7. The rigid foam, compared to its counterparts, was difficult to handle during sample preparation due to its brittle structure. This led to the assumption that it may have a lower Pb^{2+} removal capacity.

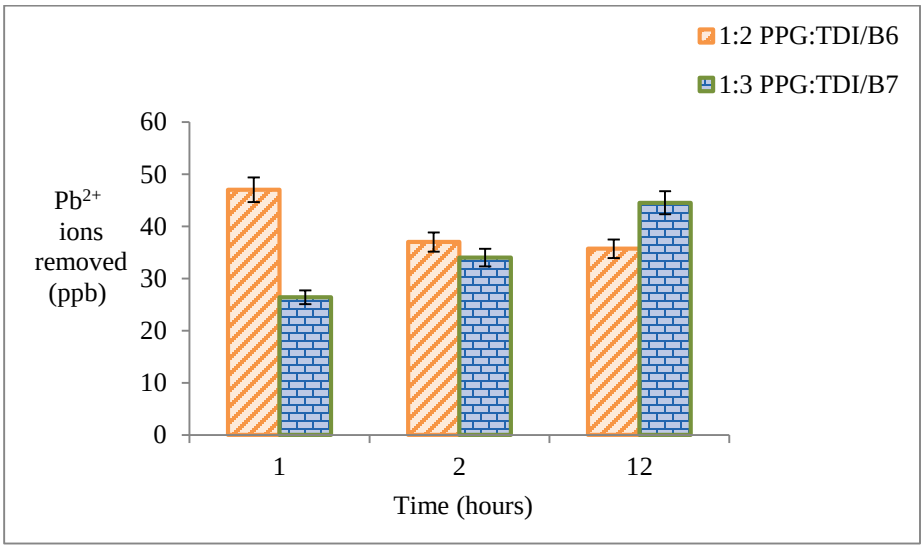

Figure 57: Lead removal efficiency based on PPG/TDI molar content

However, ICP-MS analysis showed that the rigid foam with higher TDI content (hard segments) exhibited a steady increase in Pb^{2+} removal from the standard solution. This can be attributed to the availability of excess isocyanate groups for the chain extender (BES) to react and form additional sites for ion exchange. Since the lead removal efficiency is better after prolonged exposure, it also indicates that rigid foams need more conditioning/soaking to realign the polymeric bonds for ion exchange. From the results shown in Figure 57, one can conclude that flexible foams are suitable for faster Pb^{2+} ion removal whereas rigid foams are best suited for prolonged exposure.

(iii) Effect of Chain Extender Reaction Time (CERT)

The last process variable investigated was the effect of chain extender reaction time (CERT) on Pb^{2+} removal capacity for a given composition. Figure 58 shows the ICP-MS results for samples C8 to C10. The compositions of PPG/TDI and BES/DMSO were maintained the same as in A3 (C8) in all the experiments and the CERT was increased from the initial 40 minutes used in A3 to 60 and 90 minutes in C9 and C10; respectively. Foam sample A3 (C8) showed the fastest Pb^{2+} ion removal capacity of 47 ppb/g of the foam for an exposure period of 1 hr. For an exposure of 2 hours, foam sample C10 showed the maximum Pb^{2+} removal capacity of 42ppb/g; followed by C9 at 44ppb/g. The Pb^{2+} ions removal capacity of C8 over extended time periods is similar to that of A3.

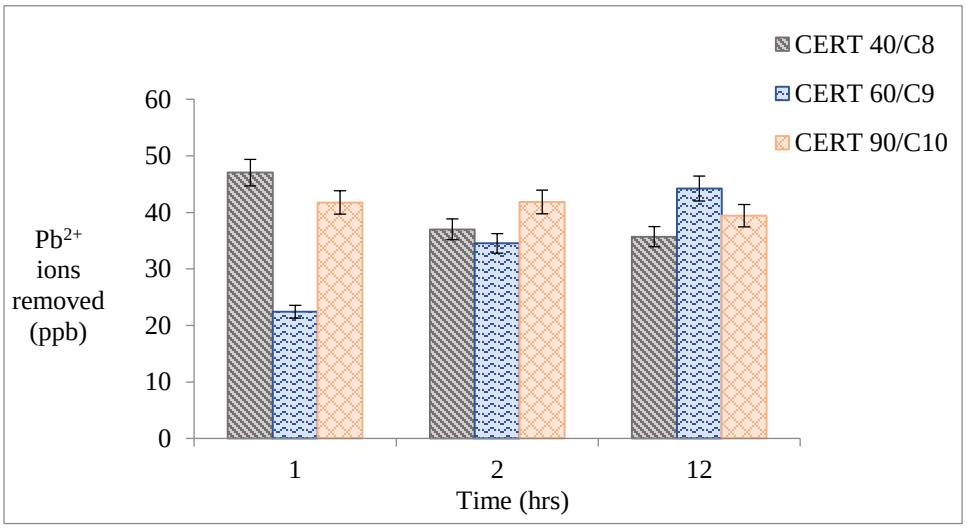

Figure 58: Lead removal efficiency with variable CERT

C9 showed a steady increase in Pb^{2+} removal efficiency over the time periods. This may be due to the additional bonding of the –OH groups from BES to the –NCO groups in TDI leading to a

higher degree of functionalization of the polymer back bone on prolonging the CERT. Although the experimental results are encouraging, the foam shows slower initial Pb^{2+} removal efficiency which increases steadily. However, the foam structure, color, and odor are not appealing when compared to A3 (C8). C10 foam showed a behavior similar to A3 in Pb^{2+} removal capacity and performed better than A3 at longer exposure times. However the higher CERT affected the foam structure, color and odor and made it less appealing, this is due to the presence of DMSO in the composition as it tends to disintegrate the foam structure similar to sample A4.

4.4.1.4 Lead Solution pH

Based on the above results, A3 foam samples were analyzed at 6.5 and 8.5 pH levels over a period of 2 days, the results of which are presented in Figure 59. Since the foam is considered for drinking water applications, it was not tested at higher, or lower, pH levels. The lead removal capacity of the foam seemed to be higher at a pH of 6.5; with a maximum lead removal capacity of 51 ppb/g, after soaking the foam in lead solution for 2 hours. The lead removal capacity of the foam seemed to taper down and saturate after 2 hours. Lead removal capacity of the foam also seemed to decrease as the pH of the solution increases to 8.5. This may be due to the neutralization of sulfonic acid groups at higher pH levels which in turn diminishes the availability of functional groups for ion exchange. The foam seems to have a better lead removal capacity at lower pH values for the same reason.

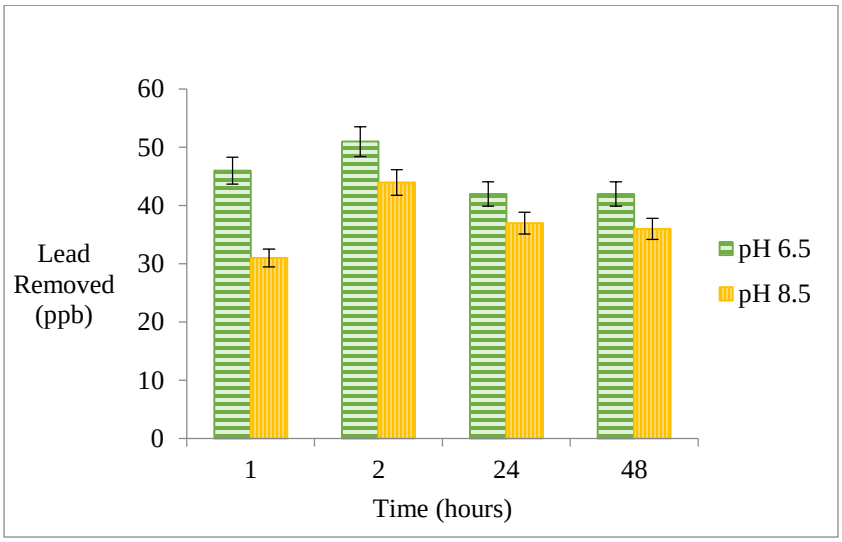

Figure 59: pH analysis of functionalized PU foam, A3

4.4.1.5 PU Foam Weight

The lead removal capacity of the foam is supposed to increase based on the availability of functions groups. Foam samples of different weights were soaked in a 100ppb standard lead solution for 2 hours and the lead removal capacity was investigated by ICP-MS. The lead removal capacity of the foams increased when the weight of the foams exposed to the lead solution was increased from 1 to 2g (Figure 60). This is a clear indication that an increase in foam surface area increases the efficiency of the foam making it suitable for scaled applications.

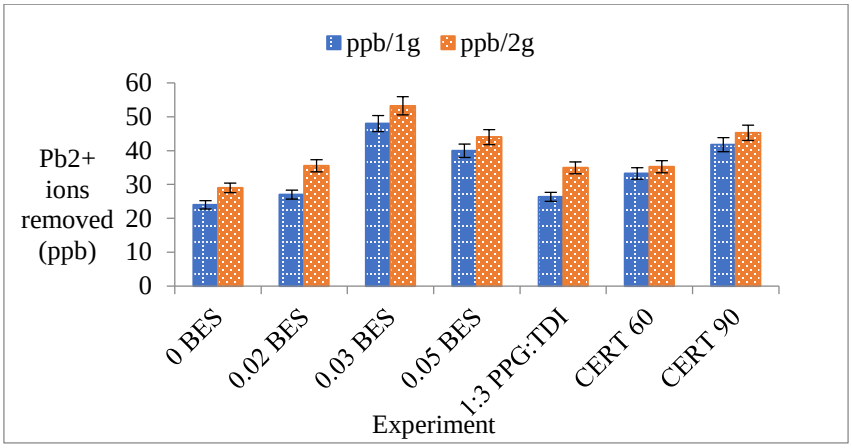

Figure 60: Lead ion removal efficiency based on foam weight

4.4.1.6 Multistage Batch Filtration

In order to improve the Pb^{2+} removal capacity of the foam, a multi stage batch filtration method was setup as shown in Figure 61. Foam samples with compositions A3 and C10 were selected for this study as they had different CERT and had previously exhibited the highest lead removal capacities. In this method, based on the number of stages, multiple pieces of virgin foam were soaked in 50ml of standard Pb^{2+} solution for a period of 30 minutes consecutively as opposed to a single piece of foam soaked in a 25ml for a period of 1, 2 and 12 hour time intervals. This setup improved the Pb^{2+} removal efficiency of the A3 foam to 50ppb and the C10 foam to 54ppb over a period of 1.5 hrs. The results are shown in Figure 62. One would expect this process to be more efficient and render the solution Pb^{2+} free after multiple runs; however the Pb^{2+} removal efficiency of the foams seems to slow down as the Pb^{2+} concentration decreases in the solution. This may make it difficult for the few Pb^{2+} ions to efficiently seek ion exchange sites or merely adsorb on the foam surface as the results from initial lead ion concentration have shown that the

Pb^{2+} removal capacity of the foam is lower and much slower in solutions containing less than 50ppb of Pb^{2+} ions.

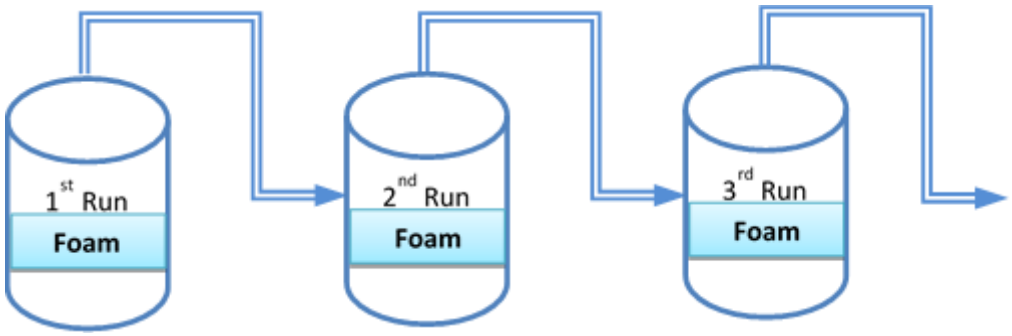

Figure 61: Multi stage batch filtration process setup

The time required to reach equilibrium is another parameter which might have influenced the Pb^{2+} removal capacity of the functionalized PU foams. As the experiment was run for a total period of one hour and thirty minutes, with an individual exposure time of 30 minutes, the foam samples and the lead solution might not have had a chance to reach equilibrium. Based on previous results, the time taken by the foam to be in equilibrium with the lead solution is estimated to be between 2 to 12hrs. Additional batch tests used to determine the adsorption isotherms may shed some light on the time taken by the foam to be in equilibrium with the lead solution. Additionally, based on the results from this setup, we can speculate to achieve higher Pb^{2+}ion removal capacity by using higher amounts of the functionalized polyurethane foam (ex: 50-100g) in a multistage setup based on the time the system takes to reach equilibrium.

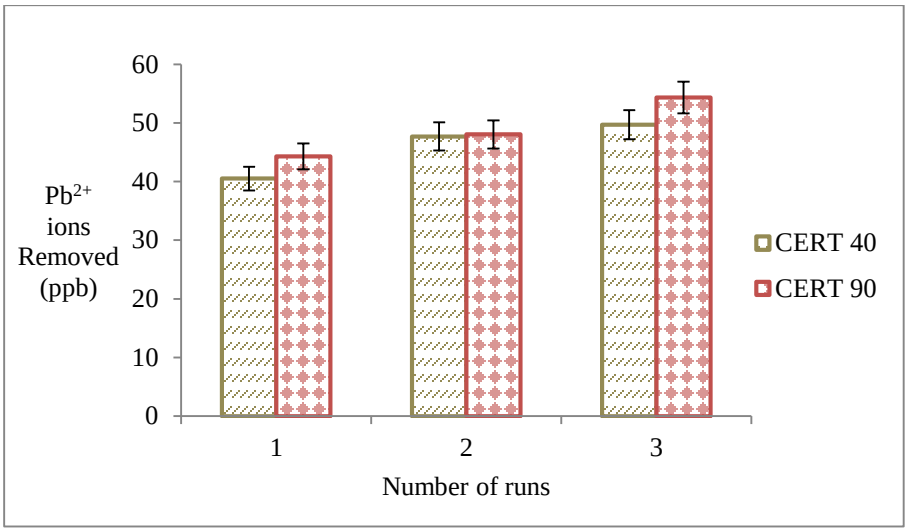

Figure 62: Lead removal capacity of functionalized PU foams from multi stage filtration process

4.4.1.7 Competing Ions

Natural waters usually contain several essential and non-essential metal ions. The efficiency of filtration media are usually affected if a similar metal/heavy metal ion is present in water which has a higher affinity to the surface of the media in comparison to the target contaminant. Hence analyzing the lead removal efficiency in the presence of other competing ions is crucial to ensure the performance of the functionalized PU foams remain unaltered.

Cadmium ions (Cd^{2+}) have a similar atomic radius (161 pm) and charge as lead ions and were chosen along with Calcium (Ca) and Sodium (Na) which are usually present in water to determine the effect of competing ions on the lead removal efficiency of the functionalized PU foam samples. Five standard solutions, the concentrations of which are described in Table 9, were prepared. A1 and A3 foam samples were soaked in the solutions and shaken for 2, 4 and 24

hours; respectively. At the end of each time interval, the solutions were filtered and analyzed by ICP-MS to determine the impact of other metal ions on the lead ion removal efficiency of the functionalized PU foam.

Table 9: Standard solutions used for competing ion analysis

Solution Code	Lead (ppb)	Cadmium (ppb)	Calcium (ppb)	Sodium (ppb)
S1	100	0	0	0
S2	0	100	100	100
S3	100	100	100	100
S4	50	100	100	100
S5	100	50	50	50

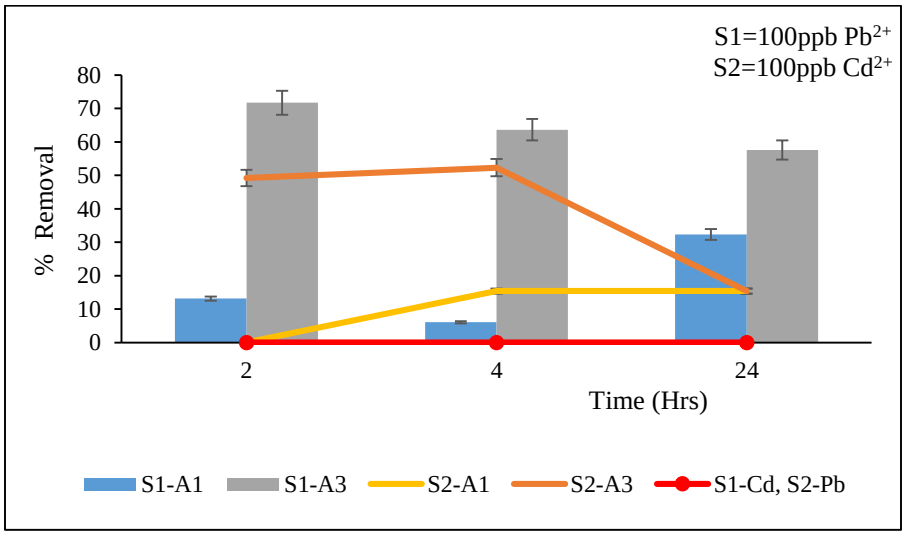

Figure 63: Lead and Cadmium Ion removal efficiency A1 and A3 foam samples in standard solutions containing lead and cadmium ions respectively

Sodium and calcium ions were undetectable by ICP-MS and are hence not part of the analysis. Additionally, solution S5 showed unusual levels of cadmium and lead ions in the test solution and hence the results from this batch are also not included in the analysis. Solutions S1 and S2 had equal amounts of lead and cadmium, respectively, and the percent of each ion removed by the control and functionalized PU foam samples is shown in Figure 63.

In the absence of other ions in solution S1, A3 foam sample showed a lead removal efficiency of 72% while the control sample showed a mere 13% lead removal efficiency after 2 hour exposure. However, the lead removal efficiency of A3 foam decreased slightly as the exposure time increased. This behavior of A3 has been observed in other tests discussed earlier indicating the time required to reach equilibrium is between 2 and 4 hours for A3 in a 100% lead solution. On the other hand, in the absence of lead ions in solution S2, which contains only Cd^{2+} ions, A1 did not show any ion removal at the end of 2 hrs. However, on prolonged exposure, the Cd^{2+} ion removal efficiency increased slightly and remained at around 20%. A3 foam sample exhibited a 50% Cd^{2+} ion removal efficiency at the end of 2 hours and prolonged exposure decreased the Cd^{2+} ion removal efficiency even though it had removed higher amounts of Cd^{2+} compared to A1.

When the foam samples were soaked in the standard solution S3, containing both the metal ions in equal concentrations (100ppb each), the functionalized PU foam, A3 retained its lead removal efficiency in the presence of competing cadmium ions while additionally removing around 50% of cadmium ions from the solution. The control foam A1, had a lower efficiency compared to

A3, however, the lead and cadmium ions removal efficiency had improved when both the ions were combined in the solution in comparison to them in individual solutions as seen in Figure 64.

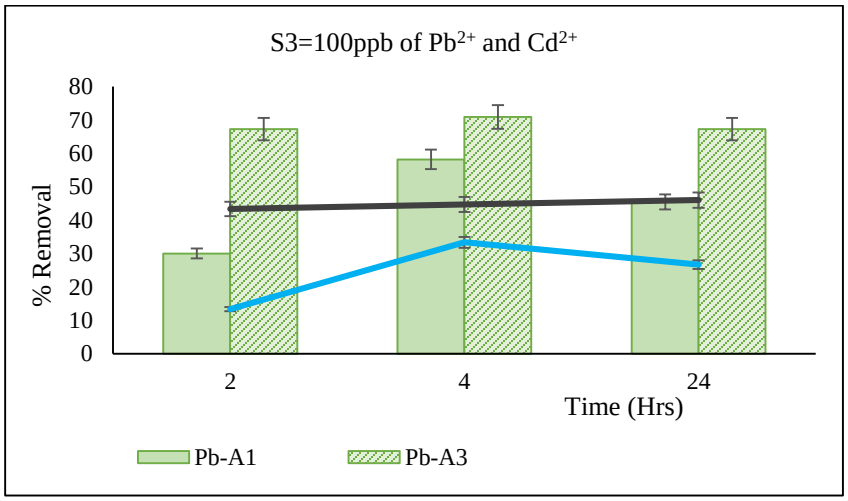

Figure 64: Lead and Cadmium Ion removal efficiency of A1 and A3 foam samples in a standard solution containing equal amounts of lead and cadmium ions

Solution S4, had a lower concentration of lead ions and high concentration of cadmium ions. A3 foam samples soaked in this solution showed around 20% lead removal and 15% cadmium ion removal capacity initially which started to decrease as the exposure time increased as shown in Figure 65. On the contrary, A1 foam sample showed a slightly higher lead removal capacity at longer exposure times in the presence of excess cadmium ions. A1 also showed a stable cadmium ion removal efficiency of around 7% irrespective of the time the foam was soaked in the solution.

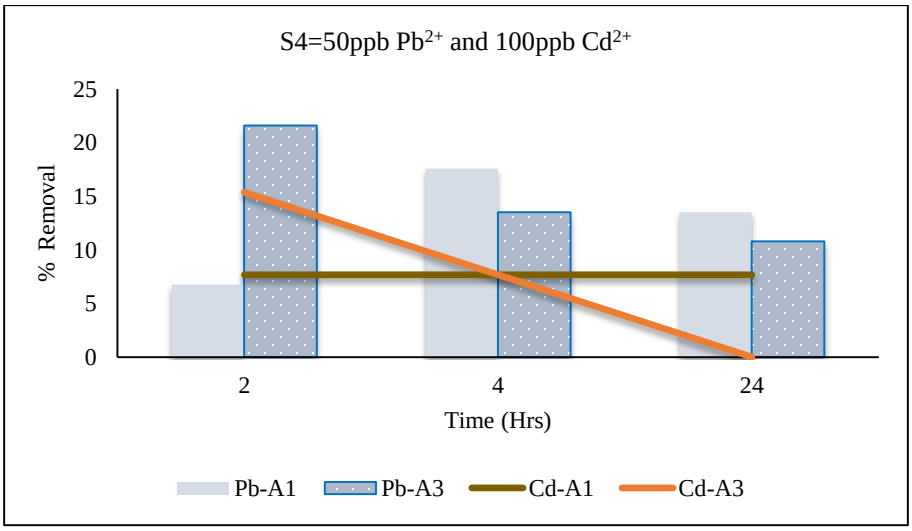

Figure 65: Lead and Cadmium Ion removal efficiency of A1 and A3 in a standard solution containing low amounts of lead and higher amounts of cadmium ions

The results from competing ion analysis, indicate that lead has a higher affinity to sulfonic acid groups in comparison to cadmium ions and confirm the choice of chain extender used to functionalize the PU foam is suitable to selectively remove lead ions from water in the presence of cadmium.

4.4.2 Lead Ion Removal Mechanism in Functionalized PU Foams

PU foams functionalized by BES were reported by Moon et al. as capable of exchanging cations from water and were intended for use as continuous electro deionization systems. However, the low deionization capacity exhibited by the functionalized PU foams might have discouraged the researchers from pursuing it further. Commercial ion exchange resin beads containing sulfonic acid functional groups are used to exchange heavy metal ions from contaminated water. Based on the above factors, the functionalized PU foam was considered for lead ion removal as PU

foams have a few advantages over polymer resin beads and granulated activated carbon in terms of increased surface area, lower fouling, and ease of handling and tailoring of the synthesis process.

Based on the ion exchange chemistry, as shown in equations 13a and 13b below, sulfonic acid groups form complexes with lead ions by exchanging hydrogen ions:

$$SO_3H = {SO_3}^{2-} + H^+ \qquad (13a)$$

$$2SO_3H + Pb^{2+} = Pb(SO_3)_2 + 2H^+ \qquad (13b)$$

This can be confirmed by measuring the pH of the standard lead solution before and after a batch test. An increase in the solution pH will indicate that ion exchange process is active in the functionalized PU foam. Figure 66 shows the change in pH of the lead solution before and after a batch test run for 4 hours using the control PU foam A1, functionalized PU foam A3 and GAC, a well-known commercial adsorption media used for heavy metal ion filtration.

The pH of Sample A1 remains almost the same throughout the test indicating that lead ion removal mechanism is not exclusively by ion exchange mechanism in the unfunctionalized foam. The pH of GAC starts to decrease at lower amounts of the media in the lead solution and then start increasing as the amount of media is increased in the lead solution. The change in pH can be attributed to the change in surface charges, H^+ and OH^- ions at the GAC-water interface. Functionalized PU foam sample A3, shows a sudden drop in pH as the foam is exposed to lead

solution and remains at the same pH irrespective of the amount of media in the lead solution. This indicates that the ion exchange mechanism is in progress in the system as depicted by equations 13a and 13b.

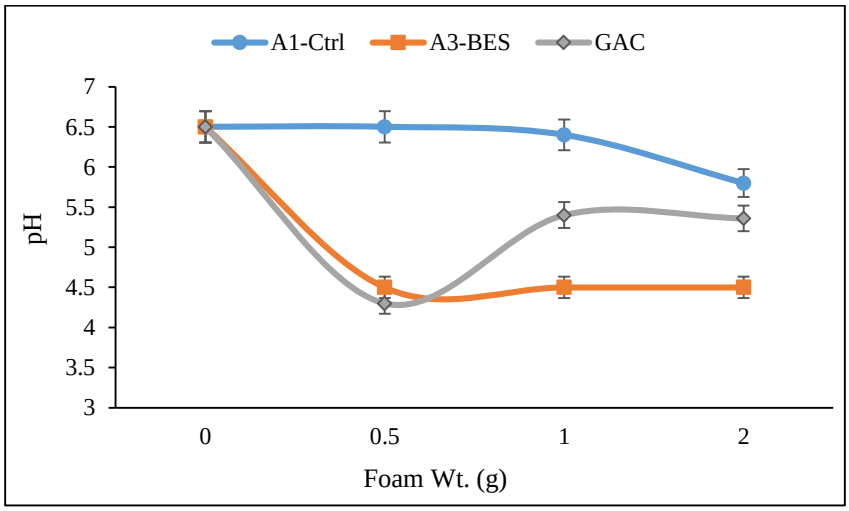

Figure 66: Change in pH as a function of foam weight indicating the ion exchange mechanism in functionalized PU foam sample, A3

Since the control foam, A1, has shown some lead removal capacity, and pH analysis indicate that it is not by ion exchange mechanism, adsorption may also play a role in the lead ion removal capacity of the PU foams. Adsorption isotherms can help us understand the mechanism of adsorption in both functionalized and unfunctionalized PU foams.

4.4.2.1 Adsorption Isotherms

Adsorption isotherms were used to determine the lead removal capacity of the PU foam samples using a batch test. Variable amounts of foam samples were shaken in a Heathrow Scientific Sea

Star Multipurpose Digital Orbital Shaker (Figure 67) at 200rpm for 4 hours in 50ml centrifuge tubes containing 50ml of 100ppb lead solution at a pH of 6.5.

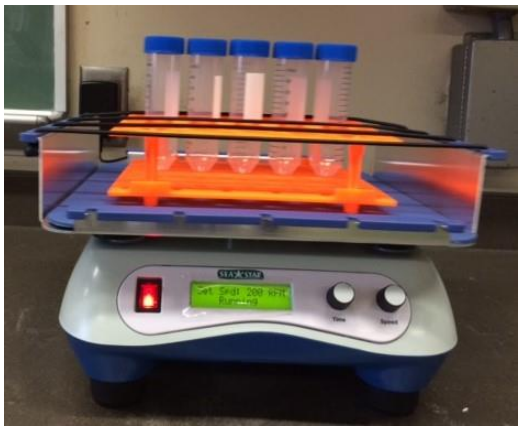

Figure 67: Shaker used to determine the adsorption isotherms by batch test

The samples were filtered after 4 hours and analyzed by ICP-MS to determine the concentration of lead in the solution. Adsorption isotherms were determined by plotting the equilibrium concentration of lead ions on the foam surface (q_e), which was determined using equation 1, versus the equilibrium concentration of the lead solution (C_e).

The adsorption capacity and parameters determined from the batch tests are shown in Figures 68 and 69, respectively. Batch test results, which were run for 24 and 48 hours, were inconclusive and the data could not be used to predict the adsorption isotherms. This confirms that it takes around 4 hours for the functionalized PU foam to attain equilibrium in the lead solution and it explains the high lead removal capacity of the functionalized PU foam soaked for shorter time

intervals. One can speculate that once equilibrium is reached, the remaining lead in the solution starts to precipitate on to itself increasing the concentration of lead in the effluent.

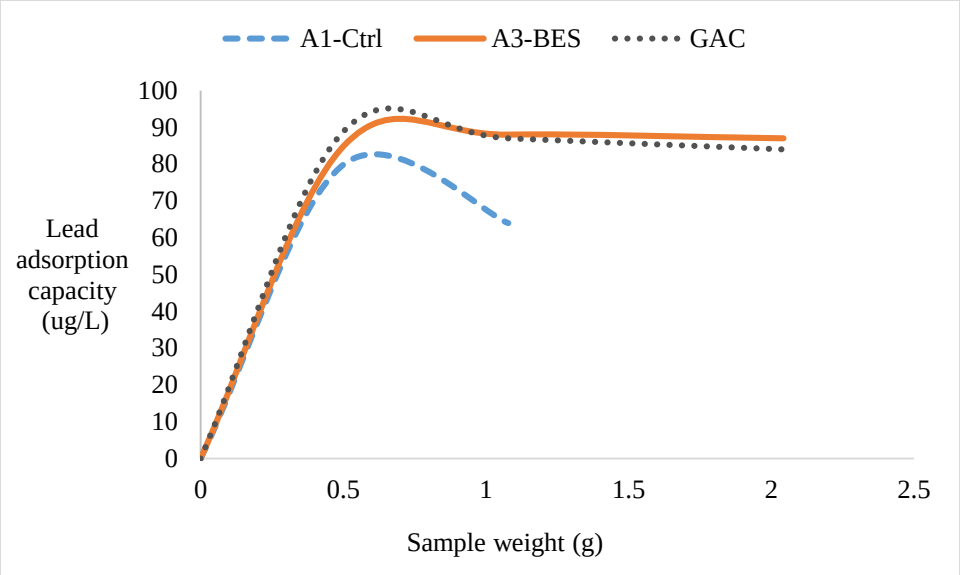

Figure 68: Lead ion adsorption capacity of PU foams and GAC determined by batch test

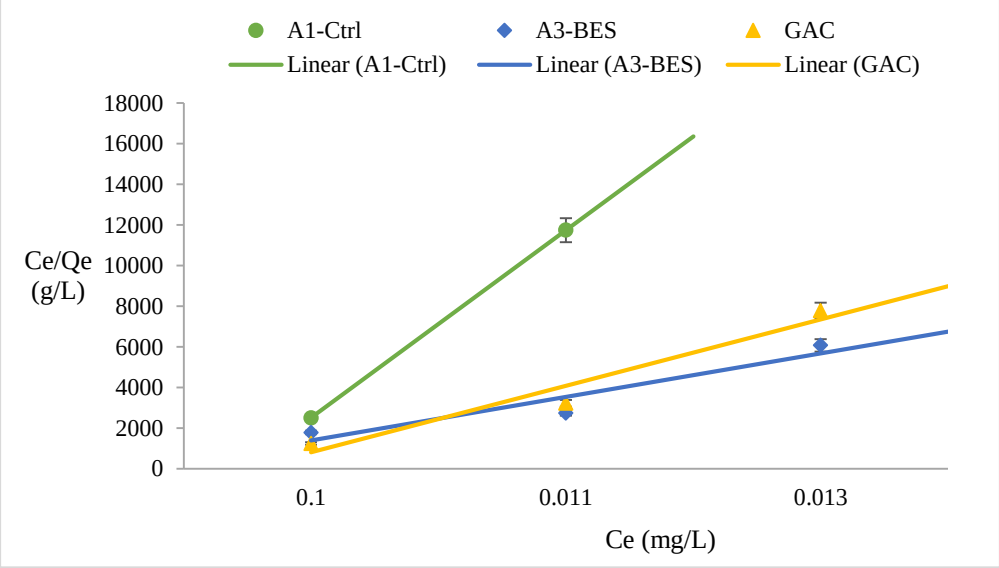

Figure 69: Langmuir adsorption isotherm of PU foams and GAC

Based on the adsorption isotherms, it is evident that the adsorption of lead ions on the PU foam is mono-layer. The adsorption capacity of the control foam A1 is 7.97µg/L or 0.038 µmol/L, followed by the functionalized foam with a capacity of 8.41µg/L or 0.041 µmol/L. The adsorption capacity of GAC was found to be 8.85µg/L or 0.043 µmol/L.

4.4.2.2 Column Tests

The kinetics of fluid flow were determined by setting up a column test. Column tests were carried out at the global water center, courtesy of AO Smith, to study the lead ion removal kinetics of the PU foams. The test water was prepared according to NSF/ANSI 53 standard at 6.5 pH; the test water was spiked with 100ppb lead. The test water characteristics are reported in Table 10. The column test was scaled down to determine the lead removal capacity of a 10″ filter for 1000 gallons of water. The test was run for 5 days at a flow rate of 15-16 ml/min with a bed contact time of 20 minutes repeated in 36 cycles per day. The column test setup, fitted with a pressure gauge and the pump, is shown in Figure 70.

A pre-weighted amount of PU foam was placed at the center of the column in between two metal meshes. Small glass beads were filled on both sides of the metal mesh in the column and sealed to regulate the water flow through the foam in the column. Once the test started, fluid samples were collected every hour for four hours on the first day to determine the remaining lead in the effluent as batch tests showed that it took 4 hours for the foam to be in equilibrium with the lead

solution. To determine the long-term capacity of the foam samples, the test was continued for five more days and fluid samples were collected every 24 hours for analysis.

Table 10: Lead test water characteristics for column test according to NSF/ANSI 53 standard [101]

Alkalinity (as $CaCO_3$)	10-30 mg/L
Hardness (as $CaCO_3$)	10-30 mg/L
pH	6.5 ± 0.25
Polyphosphate (as P)	< 0.5 mg/L
TDS	< 100 mg/L
Temperature	20 ± 2.5° C (68 ± 5° F)
Turbidity	< 1 NTU
Lead (as Pb)	0.1 mg/L or 100ppb

(a) (b)

Figure 70: (a) Column test station with automated pump (b) close-up images of the PU foam in the column and the pressure gauge

The test was scheduled to run for 5 consecutive days, since the PU foams under investigation are saturated by the lead solution within four hours, samples were collected at the end of every hour,

for four hours on the first day. Thereafter, samples were collected once every 24 hours. The concentration of the lead ions in the effluent started to increase as time progressed. A3 foam sample showed the highest lead removal of 87% as the challenge water started to flow through the foam and decreased to 71% at the end of four hours. A1 foam sample exhibited a 79% lead removal efficiency at the start of the test, however the lead removal capacity started to decrease and reached 54% after four hours.

Since lead removal in the A1 foam sample is by mere adsorption, the amount of functionalization or the ion exchangeability of the functionalized foam A3 was determined by taking the difference in the performance efficiencies of both the foam samples and plotting it against time as shown in Figure 71. The slope of this differential curve can be used to determine the functionalization efficiency, which is an indirect measure of the percent functionalization of the A3 foam sample. The slope of the differential curve was determined as 5.17%, indicating that ion exchange is also an active mechanism and BES was successfully integrated into the backbone of the PU foam as confirmed by other structural analysis.

The lead ion concentration in the samples collected after 24 hours for 5 consecutive days show a steady decrease in the lead removal capacity of A3 foam from 70% after 24 hours to 11% after 96 hours. Similarly, in A1 foam sample, the efficiency decreased from 60% to 5% (Figure 72).

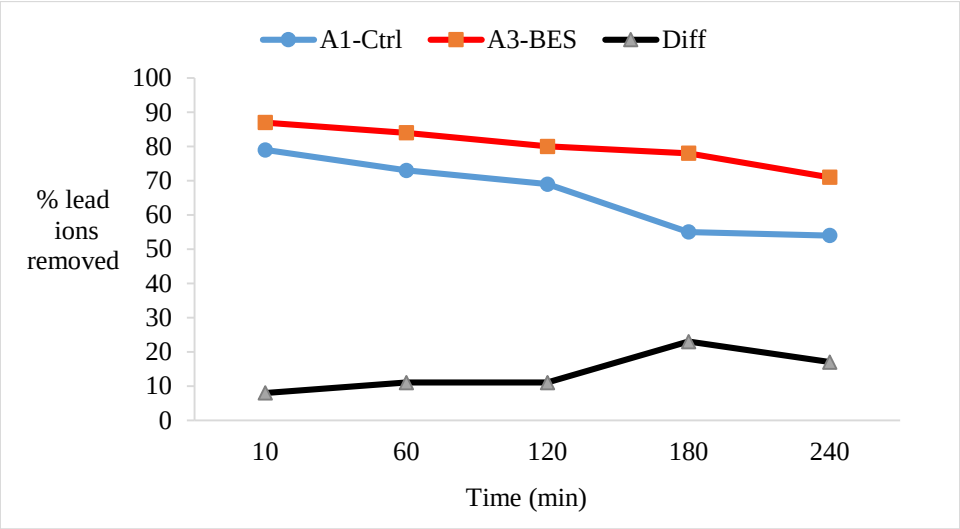

Figure 71: Lead ion removal efficiency and functionality (difference in their lead ion removal efficiency of A1 by adsorption and A3 by ion exchange mechanisms) of PU foams as determined by the column test

We can speculate that the combination of adsorption and ion exchange mechanisms in the PU foam samples are probably affecting the performance of the foam samples as they seem to be saturated within a few hours. Based on the adsorption isotherms and the fluid flow kinetics from column tests, it appears that both ion exchange and adsorption mechanisms are dominant in the A3 foam sample. However, since the adsorption is limited by a single layer, the saturation of lead ions on the surface of the foam seems to prevent further ion exchange in the bulk of the foam sample.

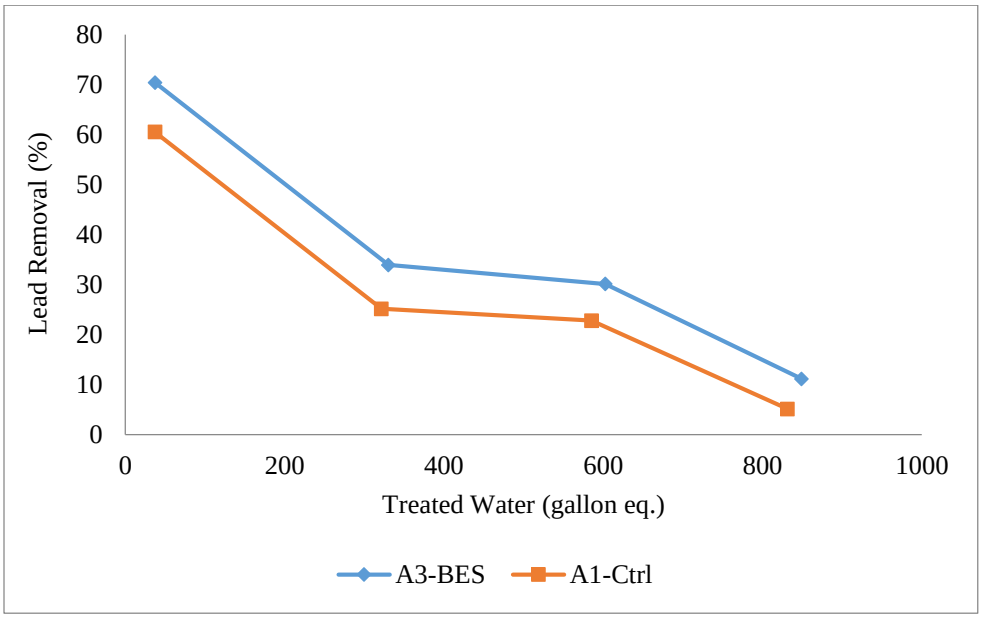

Figure 72: Lead ion removal capacity per 1000 gallon eq. of A1 and A3 foam samples

4.4.3 Functionalized PU Foam Structure-Property-Performance Relationship Analysis

4.4.3.1 Effect of lead ions on the chemical structure of the functionalized PU Foam

To determine the effect of lead ions on the chemical structure of the functionalized PU foam samples, A1 and A3 foam samples, which were previously used in the 4 hour batch test, were characterized by FTIR. The FTIR spectrum of the A1 foam samples show a slight shift in the peak intensities of the O-C-O groups as shown in Figure 73. The peak intensities of the A1 foam sample seems to change from 20 to 68% after exposure to lead ions in the solution. This can be attributed to the adsorption of lead ions on the foam surface which can alter the IR frequencies caused by vibration of bonds at the molecular level.

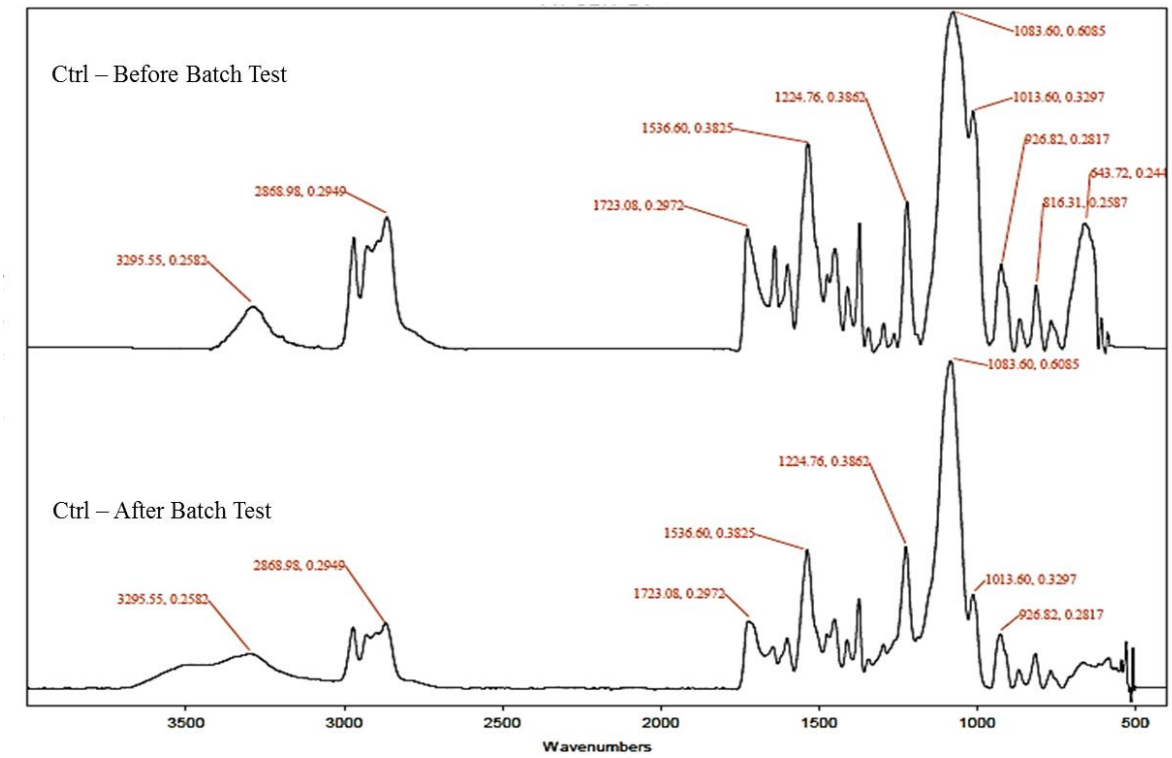

Figure 73: FTIR spectrum of A1 foam samples before and after exposure to lead ion solutions

In A3 foam sample, the shift in peak intensities of the O-C-O and O-S-O is more prominent compared to that of foam sample A1. The intensities of 1013 and 1088 peaks have shifted in the sample after the batch test (Figure 74). The area under the peaks were determined using the peak intensities (height) and the width of the peaks, the initial O-S-O and S=O peaks were then quantified by determining the ratio of the areas of the respective bonds to the entire area under the peaks in the spectrum. The initial amount of O-S-O and S=O bonds determined by the above said method were 17.36% and 5.63% respectively. When the foam contacts the lead solution, the hydrogen ions in the sulfonic acid groups are replaced by the lead ions, forming a lead sulfate complex.

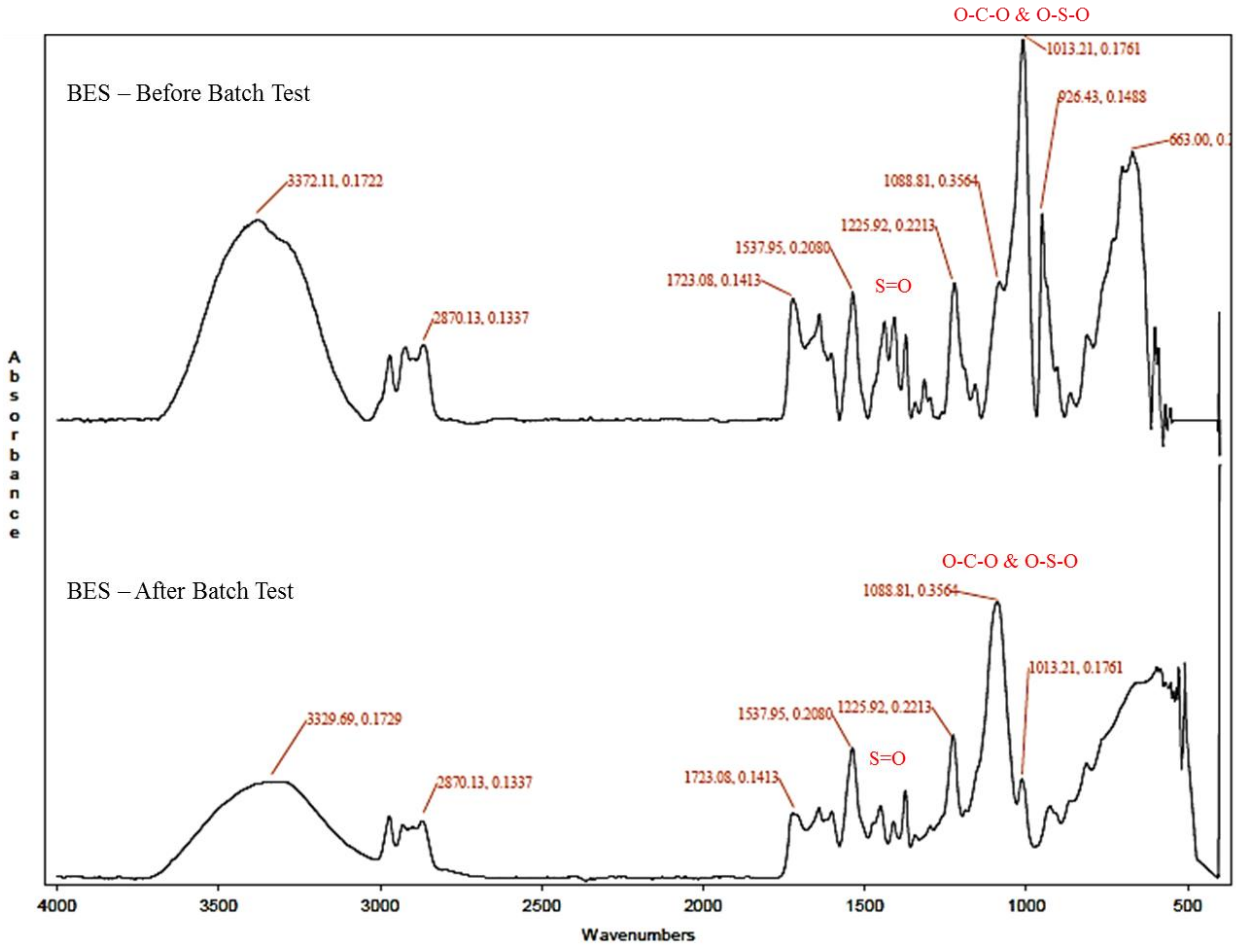

Figure 74: FTIR spectrum of A3 foam sample before and after exposure to lead solution

The presence of a heavy metal such as lead, tends to sway the bending and stretching vibrations of the O-S-O groups, which is visible as a shift in the peak intensities of the A3 foam sample containing lead ions. In addition, the intensity of the S=O peaks in the A3 sample has decreased after the batch test which reaffirms the presence of a heavy metal element in the vicinity of the S=O group. Alternatively, quantifying the O-S-O and S=O bonds in the foam samples using the areas under the peaks in the FTIR spectrum as described earlier, shows a 71% and 12% decrease in the O-S-O and S=O bonds respectively. Around 5% of the initial 17.4% of the O-S-O bonds

were found in the sample after exposure to lead solution. This may be due to the formation of the lead sulfate complexes, which are bulkier and tend to vibrate or rotate at a lower frequency resulting in peaks with lower intensities, compared to the S=O and O-S-O bonds.

4.4.3.2 Lead ions in the structure of PU Foams

SEM/EDS was used to confirm the presence of lead ions in the bulk of the A3 foam sample after batch tests. The EDS spectrum shows the presence of Pb^{2+} in the bulk of the foam sample along with sulfur and various other elements, as shown in Figure 75. Though the amount of lead could not be quantified by EDS due to the low concentrations. Microstructural analysis confirming the presence of lead indicates that lead ions have bound chemically to the sulfonic acid functional groups present in the functionalized foam sample.

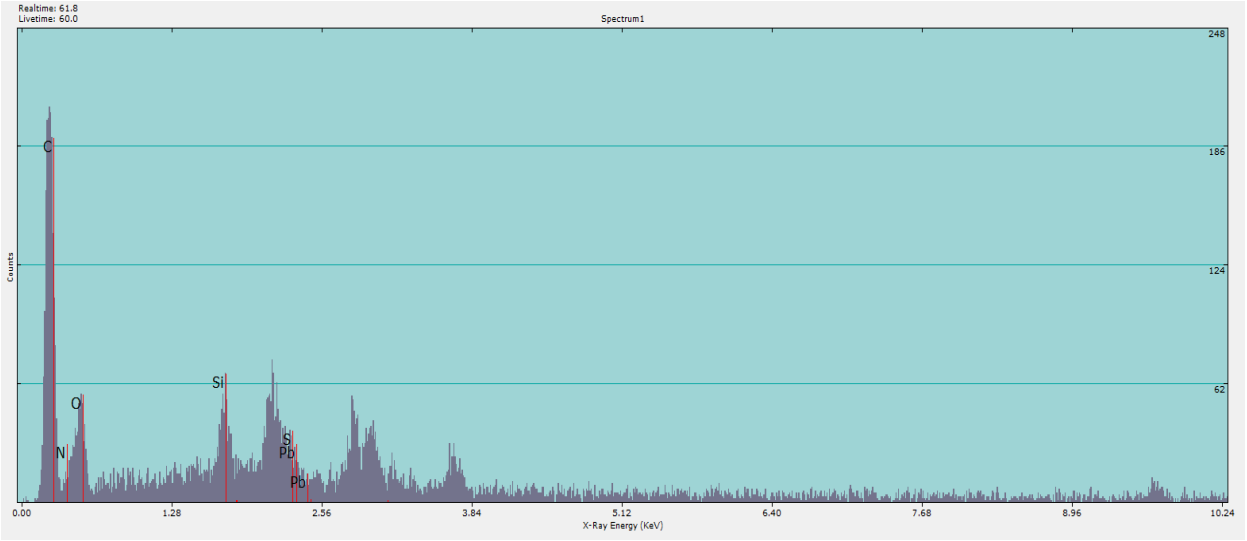

Figure 75: EDS spectrum of A3 foam sample showing lead in the bulk of the foam

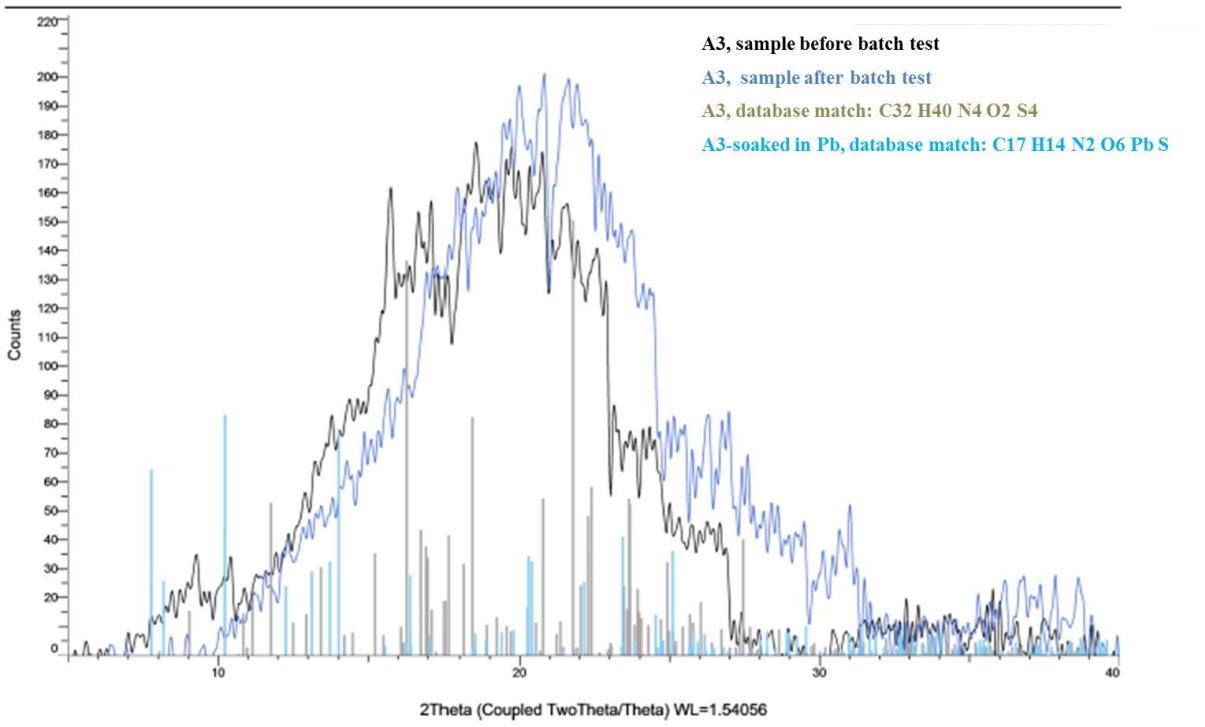

Figure 76: XRD spectrum of A3 foam sample before and after batch test showing the lead in the bulk structure of the foam

The presence of lead in the bulk of the A3 foam sample after the batch test was also identified by XRD as shown in Figure 76. The intensity and the number of crystalline peaks seem to have increased in the sample exposed to lead solution indicating that the crystallinity of the A3 foam sample has increased slightly as lead forms a crystalline salt complex with the sulfonic acid moieties. A database search revealed several complex chemical compounds containing lead and sulfur along with other basic elements present in the functionalized PU foam A3. Quantifying the amount of lead by the structural analysis is challenging due to the low concentration of lead in the foam structure. These results, however, serve as another means to correlate the foam structure to its performance and vice-versa.

Chapter V: Product Development Case Study

5.1 The Water Industry: An Overview

Freshwater, a natural resource, which was once abundant is becoming a scarcity making it the most valuable commodity in recent times. The demand for freshwater now, is similar to what oil was in the past few decades as multinational corporations and investors are trying to capitalize on the new 'liquid gold'! Growing population, climatic changes, pollution, aging infrastructure and water regulations has created a tremendous imbalance between supply and demand of freshwater all over the world. Only 2.5% of the water on our planet is potable of which less than 1% is accessible surface water. Though the freshwater supplies are relatively stable, the global population is expected to increase to nine billion by 2050 [102]. Moreover, the fresh water sources are not evenly distributed which tips the supply-demand balance. For example, in India, approximately, 100000 cubic feet of water is available per person where as in Israel, it is a mere 8750 cubic feet! Water pollution and the lack or cost of water treatment has denied access to safe drinking water for at least 1/3rd of the world's population [103].

This growing imbalance between the supply and demand has made the water sector an attractive investment, which is currently estimated to be a USD 450-500 billion global market. The high growth potential of the water sector has thus led investors to develop business models which can address the supply-demand imbalances. Water infrastructure, water treatment and water utilities are the major investment categories in the water industry which play a pivotal role in balancing the supply and demand applications [102] as shown in Figure 77.

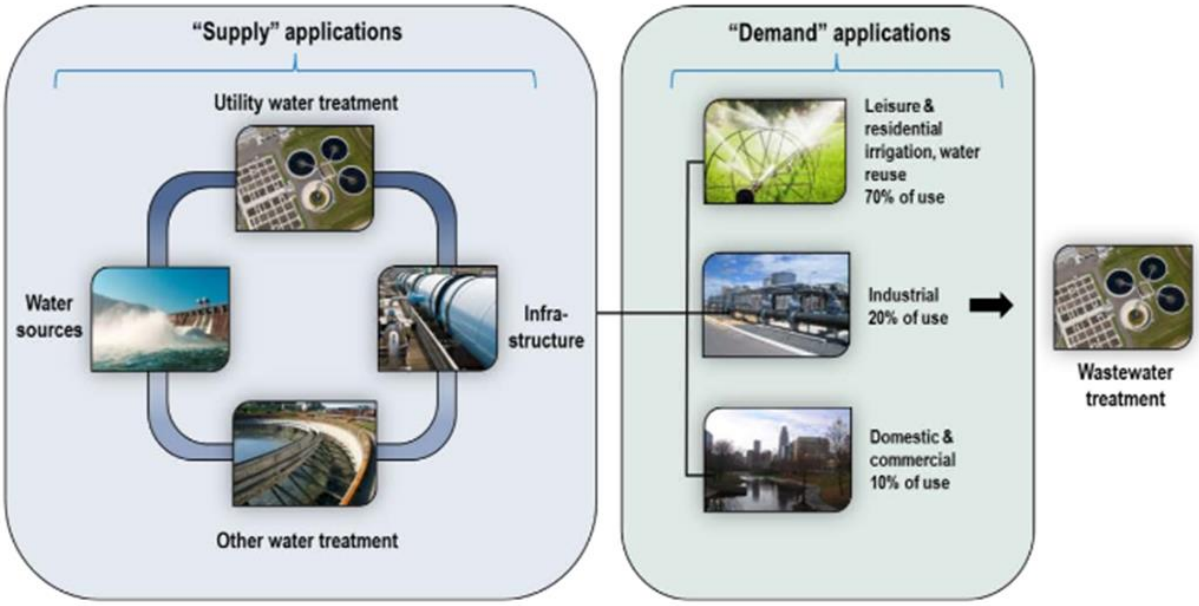

Figure 77: Global supply and demand applications in the water industry [102]

Pumps, pipes, valves, irrigation, water conservation and reuse equipment make up a major chunk of the water infrastructure with a steady global growth potential of up to 12%, while emerging markets in Asia have a growth potential of up to 16%. In the US, the Environmental, Protection Agency (EPA) plays a key role in providing tools and knowledge to ensure the investments on water infrastructure are sustainable. The path to sustainable water infrastructure depends on the technologies available and the financing options to ensure the efficiency of the sustainable practices improve as shown in Figure 78. However, the lack of a governing body in several developing countries and underinvestment in repairs and upgrades in developed countries can significantly stress the aging infrastructure and hinder the path to sustainability. Water leakage is a direct consequence of failing infrastructure, it has been found that around 25% of residential water is lost to leakage in London where in the infrastructure is over 150 years old. In addition,

studies have shown that reducing the leakage in London by 1% could provide enough water for 224,000 people [102, 104]!

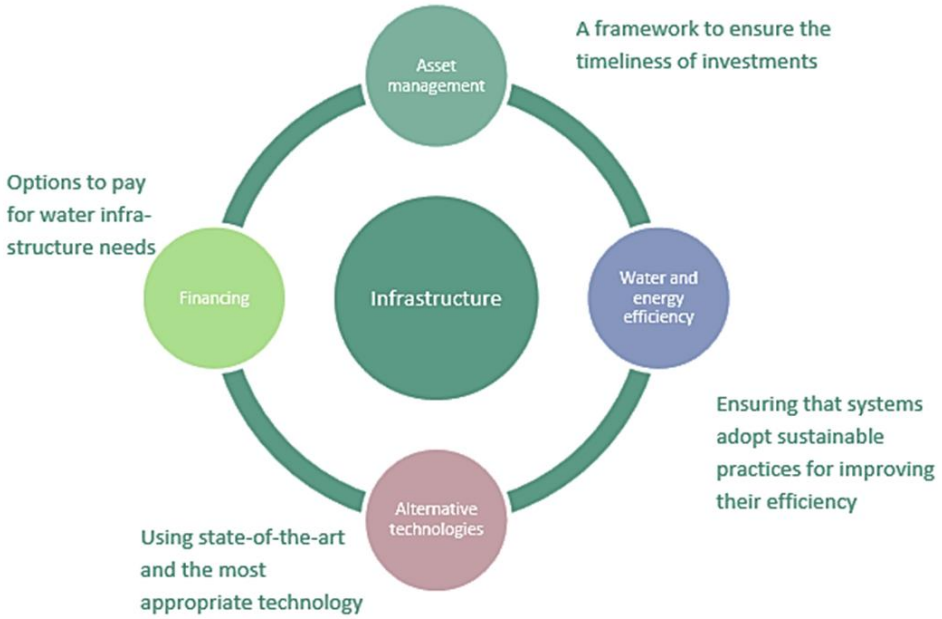

Figure 78: The path to sustainable water infrastructure [102]

The water utility sector is made up of domestic companies which are responsible for the safe and timely distribution of water and other related services, such as wastewater treatment. Most water systems are local or regional. With tight regulations from the federal, state and municipal jurisdictions, the water utilities sector is mature and capital intensive with no product differentiation. Water utilities usually seek to enlarge operations either by way of merger and acquisition activities or by venturing into non-regulated markets to benefit from greater economies of scale [105, 106].

The water treatment sector is an integral component of the water industry as it is the key to sustain the infrastructure and the utilities. Strict government regulations including that of the United Nations on the quality of water has increased the demand for water and wastewater treatment techniques and equipment's globally. Chemicals, filters, membranes, desalination equipment and physical disinfection treatments, comprising niche applications such as, UV and ozone treatment are aiding the demand in the water industry and are forecast to reach $53.4 billion by 2020 [107]. The chemicals used in water treatment operating expenditure items and are often characterized as having relatively low monetary value, but high importance in the treatment process. On the other hand, filters wear out and need replacing, hence all membrane or filtration-based businesses are lucrative as investors earn above-average earnings generated by the recurring consumables. The global growth rate of filters or membranes alone are around 15 to 20% with annual growth forecast in China and India to be 26% and 20% respectively. The physical water treatment products tends to have high margins, providing investors the pricing power due to specialized technologies. While the global growth rate of physical treatment s methods remains at 2-4%, the annual growth rate in China and India are forecast to 13.5% and 15-20%, respectively [102]. Let us now take a closer look at the membrane filtration systems to benchmark the bulk functionalized PU foam.

5.2 Filtration Systems

Increasing health concerns and the environmental impacts of biological contaminants, chemicals, and disinfection byproducts in supply water and wastewater, has elevated the requirement for stringent manufacturing practices to process water. Water and/or waste water treatment is crucial

in extracting resources such as oil, minerals etc., in addition to the increasing demands of the commercial and residential markets. The demand for water treatment equipment alone is forecast to grow at the rate of 5.9% in the US by 2017 [108]. The emerging markets are forecast to grow at a much higher rate either due to the increasing quality of life or due to the depleting freshwater sources in the regions. Though the commercial and residential markets are continuing to recover from the recession, the resource extraction sector has seen tremendous gains as water recycling and treatment are vital in sustaining extraction activities, which may be in the form of hydraulic fracturing to extract oil and natural gas or for mining minerals.

5.2.1 Filtration Systems and Membranes

Conventional water filtration systems continue to dominate the water treatment sector and are differentiated by their capacities in treating water for the above said markets. Residential water filtration systems are of two types: point of entry (PoE) and point of use (PoU) based on the condition and the contaminants present in water.

- PoU water filters purify water right before it is used and are hence usually restricted to cooking and/or drinking. They are portable and can be mounted to faucets or under the sinks, PUR and Brita faucet mounts filters and filtering pitchers are some of the most commonly used PoU filters. From a consumers perspective, the downside of PoU filters are their low handling capacities, and continued operational costs as they have to be replaced often.
- PoE filters purify water before it enters the house, the purified water runs through the pipes and comes out through the faucets. PoE filters are usually housed in the basements

or outside the house. They are designed to handle larger volumes and filters are usually replaced annually. Water which is either very hard or contaminated and unfit for cleaning and washing can benefit from PoE filters due to their cost effectiveness [109].

Several filtration methods are employed in PoE and PoU filters, some of the popular filtration methods along with their respective commercial products are compared in Table 11. Most of the filters used in residential or commercial units employ more than one filtration method as they are either limited by the target contaminant or the efficiency, for example, the RO and carbon filters are used in conjunction with each other for better performance efficiencies and to handle larger volumes, similarly, the UV filters are used with other RO or carbon filters to treat a broad range of contaminants.

Table 11: Comparison of water treatment methods which are routinely used for commercial and residential purposes [110 - 117]

Sl. No.	Filtration Method	Benefits	Limitations	Cost[3]
1	*Adsorption Media:* Ex: Carbon filters using activated charcoal, filters using activated alumina etc.	- Suitable as both PoE and PoU filters - Capable of removing chemicals, heavy metals, organics and some bacteria	- Filters prone to fouling by bacterial growth - Require constant replacement - Better performance efficiencies when used in conjunction with other filtration methods	PoE filters from $400 - $1500 PoU filters from $15 onwards

[3] Residential filters, excludes cost of replacement filter cartridges and filter parts

Sl. No.	Filtration Method	Benefits	Limitations	Cost
2	*Membrane Filters:* Ex: Reverse Osmosis filters	- Capable of removing chemicals, heavy metals, organics or other contaminants missed by carbon filters - PoU and PoE models are available	- 4 to 9 gallons of water is wasted for every gallon of water filtered - Better performance efficiencies when used in conjunction with other filtration methods	PoE filters from $1500 - $8000 PoU filters from $200 onwards
3	*Ion Exchange Media:* Ex: Ion Exchange Resins	- Suitable for desalination or water softening, heavy metals removal and chlorination - Regenerable	- pH dependent - Resins prone to fouling by bacteria - Requires constant backwashing to maintain its efficiency - High maintenance costs	PoE filters from $600-$2000 PoU filters from $25 - $150
4	*Disinfection Filters:* Ex: UV, Ozone filters	- Suitable to remove bacteria - No harmful residues or byproducts formed after treatment	- Costly - Other filtration methods are required to target broad range contaminants	PoE filters from 700 - $1300 PoU filters from $100 - $400

A multistage RO filtration system is shown in Figure 79 to help understand the components and the water treatment process. The unit usually consists of several pre-filters to filter sediments, heavy metals and some chemicals that cannot be removed by the RO membrane. A

polypropylene (PP) or polyethylene (PE) foam pre-filter is usually used to filter sediments, rust and silt in the first stage. Other contaminants such as chlorine which can mar the taste and odor of water along with other chemicals and heavy metals are removed in the second stage by two (or three) carbon cartridges. Water treated through the pre-filters flows through the RO semi-permeable membrane, which continues to remove heavy metals such as arsenic, lead, chromium, copper, and other metals and chemicals such as, sodium, TDS (total dissolved solids), perchlorates, along with parasytic cysts. The treated water is then stored in the RO tank, the stored water passes through the final GAC (granulated activated carbon) polishing filter before coming out through the faucet. The GAC filter enhances the taste of the water while removing other residual contaminants that may have escaped the pre-filters and the RO membrane. Similarly, pre-filters and GAC are used with ion exchange and UV filtration systems in most PoE or PoU residential and commercial units.

Figure 79: Multistage residential RO filtration system [118]

5.2.2 Functionalized PU Foam as a Filtration Media

With the current insight on water treatment and filtration methods, we will now analyze and evaluate the capabilities of the functionalized PU foam media to position it for suitable filtration applications.

- Based on the performance evaluation of the functionalized PU foam, it is clear that the novelty of the media lies in the fact that it is capable of treating heavy metal ions such as, lead via both adsorption and ion exchange mechanisms (recall Figure 24) in comparison to other commercial filters which function on only one of the above-said mechanisms.
- The short range efficiency of the functionalized PU foam is similar to that of PoU carbon filters. In addition, the PU foam media is not prone to bacterial fouling due to its physical structure and chemical nature as opposed to the carbon filters.
- The lab-scale production cost of functionalized PU foam is approximately $10-$12/oz. (Figure 80a), which is lower than the current carbon or ion exchange filters used in PoU systems. The production costs can be optimized further by following proper lean manufacturing practices.
- The ease of processing and tailoring the structure of the PU foam makes it a viable replacement to the current PP or PE foam sediment pre-filters which are used with RO, carbon, ion exchange and UV filters. The functionalized PU foam filters will be able to remove heavy metal ions in addition to the sediments when used as a pre-filter and extend the life of the filtration system.

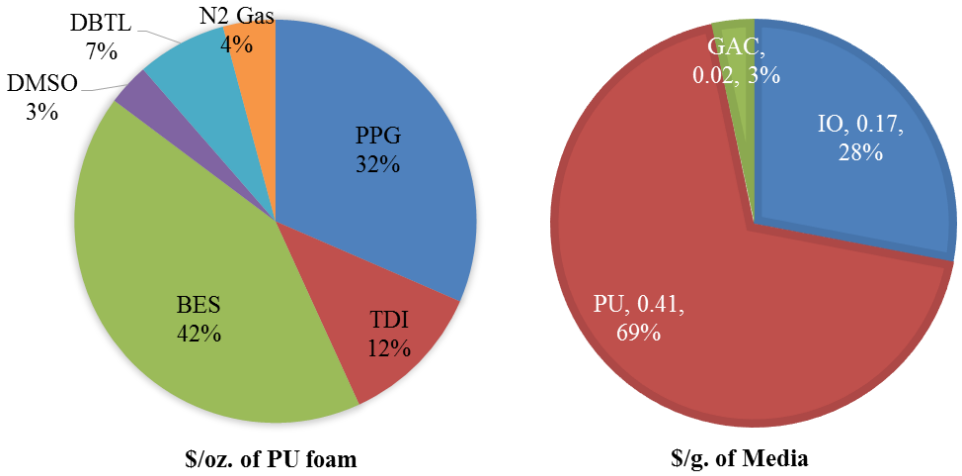

Figure 80: Cost estimation of (L) functionalized PU foam and (R) cost benchmarking estimate with respect to popular commercial media

5.3 Market Outlook: Porters Five Forces

Development of any new product requires a thorough market analysis to formulate strategies to suitably position a product in the market. The Porter's five forces analysis is an excellent framework for industry analysis and business strategy development. Three of the five forces in the model deal with competition from external sources while the rest deal with internal threats [18]. We will now analyze the porter's five forces for the water treatment industry in general and compare the functionalized PU foam to the industry requirements to formulate strategies for product development.

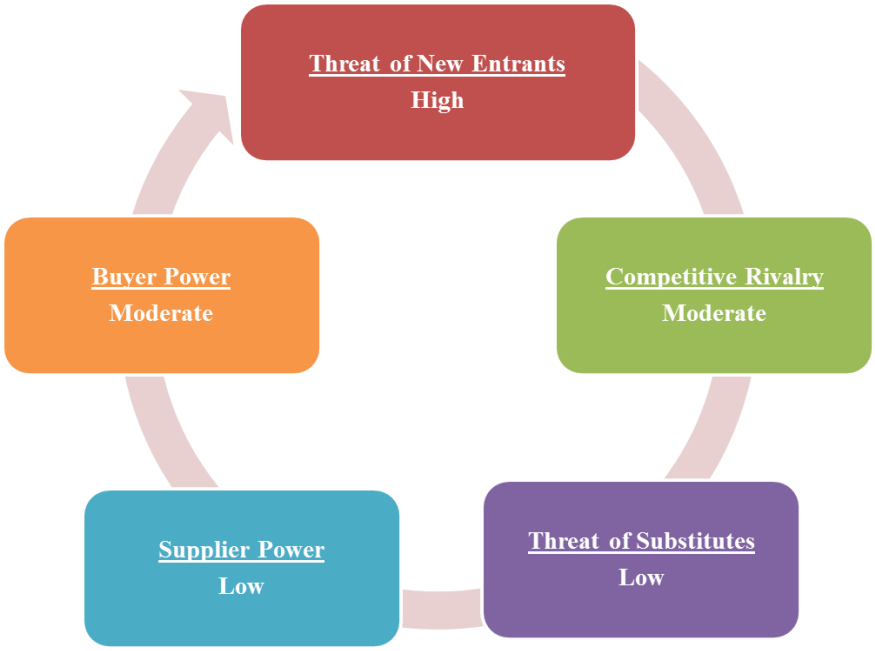

Figure 81: Porter's five forces analysis for the water treatment industry

1. *The threat of substitutes* is low for water treatment products in general as there are no substitutes or alternatives for water treatment.
2. *The threat of new entrants* is fairly high as the scarcity of water around the globe is key to driving investments in this sector! Companies are either looking to expand their product lines by spending a fair amount on R & D to modify existing systems or introducing newer products to gain a cost or performance advantage or by acquiring niche and small scale water treatment companies as a means to enter the business.
3. The *threat of competitors* is moderate as not all water treatment techniques are suitable to treat all types of water and contaminants. The type of water and contaminants in general, vary depending on the geography and the regulations in place to treat the local water

supply. These factors determine the type of filtration system required for a particular region which in turn drives the product availability. Brand recognition is the only other factor which would set the competitors apart driving the risk due to competitive rivalry to moderate.

4. *The threat from the buyer* is low to moderate and depends on several factors such as, the water condition and availability, the geography and living standards which determine the spending power. In regions where water treatment is inevitable, either due to the quality of water or due to water scarcity, the buyer has no choice than to use suitable water treatment products to sustain a healthy lifestyle. Most of the emerging markets, (in developing countries) such as China and India are in this situation, pollution and water scarcity has increased the demand for water treating and recycling products in the region. On the other hand, for example, in developed countries, where regulations maintain the quality of water, scarcity in the future, will bring down the buyer power from moderate to low.
5. *The threat from suppliers* is low as there are only a handful, conventional water filtration methods which have proven to be consistent and efficient to treat water. Of all the materials used in water treatment products, activated carbon comes from a natural source while the membranes and ion exchange resins, etc. are synthetic. Since most of the water filtration systems, employ more than one of these materials, the supply chain remains unaffected when the demand for a specific material, say activated carbon increases. Even in that case, other synthetic materials can easily be used as a substitute to activated carbon. Major water treatment industries are also investing in R&D to upgrade existing

products or to develop novel materials to stay ahead as the demand for water treatment increases. All the above factors, leave the supplier with very less or no power on the supply chain in case of water treatment products.

The functionalized PU foam, follows suit in most cases: The *threat from substitutes* is low, as the market lacks, foam based, multifunctional water treatment products. The *threat from new entrants* is high, as firms are aggressively seeking to introduce novel materials for competitive advantage or to enter the market to capitalize on the booming water industry. The *threat from buyer power* is low to moderate, and depends again on the geography, need for water treatment and the standard of living. The *threat from suppliers* is also low, as the functionalized PU foam is a tailor made synthetic media, which can be easily produced using a few chemicals that are commonly available. The *competitive rivalry* is rather high, as there are several well established water treatment products in the market which are constantly being upgraded in addition to the introduction of other clean, novel water treatment products.

5.4 Product Development: Strategies and Implementation

Based on the current state of the water industry, the type of focal firm will determine whether new product development is a business level or a corporate level strategy. We will restrict our discussion to the business level strategies assuming that the focal firm considering to develop functionalized PU foam is a front runner in the water industry. Formulating strategies for product development depend on leveraging the internal and external resources, to ensure it is within the

WACC (weighted average cost of capital) for the said division with promises of a good ROI (return on investment) and add ‘value’ to both the investors and the focal firm.

Strategies based on *cost leadership* and *product differentiation* to target various markets will be suitable to develop the functionalized PU foam into a filter. The focal firm can leverage its internal and external resources to keep the manufacturing and marketing costs to a minimum. The product, can be a *complementarity* to an existing system used for residential and commercial purposes in matured or emerging markets. In addition, the chemistry of the functionalized PU foam can be exploited, to develop a *multipurpose filter* targeting the resource extraction market; PU foam can be tailor-made to have either oil resistance or sorption based on its chemical structure in addition to treating water.

The above-said strategies can be implemented by focusing on developing the PU foam filter as a complementarity or a multipurpose filter media.

- The target audience in case of development as a complementarity should be the residential and commercial markets using RO, UV, Ion exchange and/or Carbon filtration systems.
- The functionalized PU foam can be developed as a pre-filter to replace the existing PE or PP pre-filters, which are used to filter sediment and silt from the influent in RO, UV and carbon filtration systems.
- The equipment used to produce PE and PP foam pre-filters can be modified to produce the functionalized PU foam pre-filters.

- Addition of new minor equipment, can be categorized as upgrades, which will maintain the existing operating costs and labor (the process is not labor- intensive) without affecting the WACC.
- In addition, the production technology can be patented to avoid imitation and competitive rivalry.
- The functionalized PU foam pre-filter will be able to filter both silt and sediment along with lead ions, this multi-functionality will extend the life of the carbon pre-filters and the RO membrane, and this feature could be used as a marketing strategy to gain a competitive advantage in residential markets.
- To foray into the industrial and municipal markets, the product development process can be modified to produce a multi-purpose filter for specialty applications as in oil refineries or industrial waste treatment.
- The additional cost to tailor the foam for specialty applications can be offset by pricing the filter appropriately.
- Cost leadership and brand recognition are two factors, which will continue to drive the growth in either emerging or mature markets. This creates opportunities for economies to scale and geographical expansion eventually.

The increasing population, improving living standards and scarcity of fresh water sources render the water industry lucrative to investors. Water treatment is an integral part of the water industry, and the risk of developing a new product (for water treatment), is marginally low compared to other industries. The development of a product depends on the strategies in place and effective

implementation of these strategies without losing the ‘value’ of the product in the process. Careful planning and execution by exploiting the market vulnerabilities can contribute to the success of a new product in the market. The functionalized PU foam has a fair chance to succeed and add value as a water filter if the afore mentioned strategies are implemented and executed carefully.

Chapter VI: Conclusions and Future Work

6.1 Research Summary and Conclusions

Functionalized, open-cell PU foams were synthesized using PPG, TDI and BES as a chain extender dissolved in DMSO to remove Pb^{2+} ions from aqueous solutions. The effect of various process parameters, such as the BES/DMSO content, PPG/TDI ratio, and chain extender reaction time (CERT), on the structure, properties and performance of the functionalized foam were analyzed. The foams were conditioned in 2N NaCl solution to improve the ion exchange capacity and to realign the polymeric bonds. ICP-MS was used to determine the lead removal capacity in ppb levels of the functionalized PU foam samples. The analysis led to the following conclusions:

1. The functionalized PU foam is capable of removing Pb^{2+} ions by both adsorption and ion exchange mechanisms.
2. The optimum molar composition to formulate a structurally stable, high efficiency foam is: 1 mole of PPG for 2 moles of TDI with 0.6 moles of BES dissolved in 4 moles of DMSO, which is reacted with the pre-polymer for 40 minutes (CERT).
3. The density of the foam produced using the above composition was found to be 230.9kg/m^3 with an open cell content of 91%. The lead removal efficiency of this foam sample was 88% per gram of foam as determined by batch adsorption tests.
4. DMSO, used to dissolve BES, is the rate limiting factor in functionalized PU foam formulation and synthesis as seen from the structure-property-performance relationship.
5. It was observed that, higher amounts of BES in the foam formulation does not necessarily improve the lead removal capacity of the foam due to structural degradation at a molecular level, due to the inherent nature of DMSO.

6. Higher amounts of BES may be added to the foam formulation by increasing the molar ratio of PPG/TDI to 1:3. Experimental results show that the presence of excess isocyanate groups negate the derogatory effects of DMSO in the foam formulation.
7. FTIR characterization of the foam samples confirmed the presence of sulfonic groups (O-S-O and S=O) in the polyurethane backbone.
8. GPC characterization confirmed disintegration of polymer chains in samples containing high amounts of DMSO and longer chain extender reaction times.
9. EDX analysis confirmed the presence of Pb^{2+} in the foam samples soaked in a standard lead solution.
10. **S**tatistical analysis of the optical micrographs of cross-sections using normal distribution curves has proved to be a good method to characterize the structure and cell size distribution of functionalized open cell polyurethane foams.
11. Micro-CT analysis shows fluid flow in the foam is through interconnected pores and permeable channels between pores. Swelling of the foam due to conditioning or fluid flow does not seem to hinder the fluid flow pathways.
12. The permeability, measured experimentally by a permeameter experiment is two orders-of-magnitude smaller than the theoretically-predicted permeability, none of the available theoretical permeability models (including the particulate porous-media models by Kozeny-Carman and Duplessis-Masliyah) can be directly applied to predict the permeability of these foams.
13. The multiplication of the open cell percentage with the overall porosity results in effective porosity, which is the ratio of interconnected pores (that permit liquid flow

through them on the application of an external pressure) to the total volume. Use of the effective porosity instead of the overall porosity not only brings the theoretical models for permeability closer to the experimental value, but also brings in the same trend as seen in the experiments. This clearly means that the effective porosity is the right porosity for estimating the foam permeability.

14. The pressure drop recorded during column tests is between 1 to 2.5psi, the structural stability of the functionalized PU foam remained undeterred under operating conditions.
15. The initial lead ion concentration and the pre-conditioning of the functionalized PU foam significantly influence the lead removal efficiency of the foam.
16. pH analysis of the foam showed reduction in its lead removal capacity at higher pH levels due to neutralization of sulfonic acid groups, which lowers the number of functional sites available for ion exchange.
17. The presence of competing ions such as cadmium in variable measures along with the lead ions in the test solution, did not affect the lead removal capacity of the functionalized foams. The foams were capable of treating 40-45% of the cadmium ions present in the test solution along with the lead ions.
18. Adsorption isotherms show that the structure of the synthesized PU foams render them suitable for monolayer adsorption. However, this partly affects the ion removal mechanism of the PU foams as the surface of the foam approaches saturation, the ion exchange sites in the bulk of the foam become inaccessible to the lead ions.
19. The functionality of the PU foam was determined as 5% based on the lead removal capacity of the control and the functionalized PU foams from column tests. This may be

used as a measure to quantify the actual amount of BES available for ion exchange after foam synthesis. In addition, this also explains the drop in lead removal capacity after the equilibrium is established between the solid (foam) and liquid (lead solution) phases.

20. Batch tests show that it takes 4 hours, for the equilibrium to be established as the functionalized PU foam comes in contact with the lead solution.
21. The lead removal efficiency of the functionalized PU foam is comparable to that of commercial activated carbon filter cartridges. However, the foam has a limited capacity due to the aforesaid reasons.
22. The lab-scale production cost of the functionalization PU foams is around $11-$12 per ounce of foam, which is slightly lower than that of commercial activated carbon filters. The production costs can further be lowered by use of proper lean manufacturing practices.
23. The structure and functionality of PU foams renders them with the potential to replace the PE or PP foam pre-filters used in RO, UV and ion exchange water filtration systems.
24. If they were to be developed as alternative pre-filters, the functionalized PU foams will complement the existing water filtration systems by prolonging the life of the RO membrane or the GAC cartridges, the PU foam pre-filters can be replaced periodically at a fraction of the current operating cost of the water filtration unit.

6.2 Future Outlook

A thorough analysis of the structure-property-process-performance relationship of the functionalized, open cell PU foam has provided the scientific community the merits and limitations of the system. This knowledge can be applied to further the lead ion removal capacity of the functionalized PU foam by one or a combination of the following methods:

- Synthesizing a foam with higher PPG/TDI content, say in a 1:3 molar ratio. This will allow the addition of more than 0.6 moles of BES to the foam formulation, without deterring the chemical and physical structure of the PU foam. This may be a means to increase the functionality (currently at 5%) of the PU foams.
- Introducing suitable, titanium or zirconium based nanomaterials to the existing foam formulation to improve the lead ion removal capacity of the foam.
- Additional surface functionalization of the foam by treating it with suitable sulphonic moieties to render it regenerable for continued usage by periodic backwashing, as is practiced in current ion exchange systems.

The additional production costs incurred by the above said methods can be offset by the improved performance and capacity of the PU foams as the need for water treatment product is on the rise as water and waste water treatment are becoming inevitable around the globe due to increasing population, higher living standards, climatic changes and depleting water resources.

In addition, tailor made polyurethane foams can also benefit from the development of newer permeability models to optimize the pore size and structure for fluid flow as there is a large

difference between the experimental and theoretical permeabilities determined from conventional models. Studies on determining the surface area and tailoring the pore size distribution of the foam samples to target contaminants ranging from silt and cysts to heavy metal ions will make it easier to manufacture pre-filters for appropriate water filtration systems.

References

1. Lead Toxicity, accessed Mar 2012, http://allabouttoxins.org/

2. Heavy metal toxicity, accessed Mar 2012, http://emedicine.medscape.com/article/814960-overview

3. Chemistry in the community: ChemCom - By American Chemical Society

4. Lead poisoning, http://bigstory.ap.org/article/lead-poisoning-toll-revised-1-38-young-kids

5. G. Wilke, R. Bunke, R. Buchholz, Removal of heavy metal ions from waste water by adsorption immobilized microalgae, TU Berlin, Inst. of Biotechnology, Dept. Bioprocess Engineering, Ackerstraße, Germany.

6. V. Anand, et al., Ion exchange resin complexes, DDT, vol. VI, No. 17, Sept. 2005, pg. 905-914

7. HPLC separation modes, ion exchange chromatography, accessed Apr 2013, http://www.waters.com/waters/en_US/HPLC-Separation-Modes/nav.htm

8. C. E. Harland, Ion exchange: theory and practice, Royal Society of Chemistry, 1994

9. Ion exchange an introduction, accessed Nov 2011, http://www.lenntech.com/Data-sheets/Ion-Exchange-RH.pdf

10. Puretec, Basics of Deionized Water by Ion Exchange, accessed Nov 2011, http://puretecwater.com/resources/basics-of-ion-exchange.pdf

11. F. G. Helfferich, Ion exchange, Courier Dover Publications, 1995, chapter 5.

12. J. Clark, Physical Chemistry, chemguide.co.uk (2002)

13. Water Treatment Gel-Type Polystyrene Strong Cation Exchange Resin (SQ-60 C), Jiangsu Suqing Water Treatment Engineering Group Co., Ltd.

14. How ion exchange resins work, Puring learning center, accessed Nov 2011, http://www.ccdpy.com/ENLCAHIXRW.html

15. Ion exchange resin fundamentals, accessed Nov 2011, http://msdssearch.dow.com/PublishedLiteratureDOWCOM/dh_0032/0901b803800326ca.pdf

16. D. Uhríková, Adsorption, pp 1-2, accessed March 2015, https://www.fpharm.uniba.sk/fileadmin/user_upload/english/Physical_Chemistry/5-Adsorption.pdf

17. Adsorption, accessed March 2015, http://www.rpi.edu/dept/chem-eng/Biotech-Environ/Adsorb/adsorb.htm

18. Product summary, accessed March 2015, http://www.kze.co.jp/english/spex.html

19. Goldberg, Adsorption equations and models, Ch 10 pp 489-491

20. Adsorption Equilibria, accessed Feb 2015, http://mimoza.marmara.edu.tr/~zehra.can/ENVE401/3.%20Adsorption%20Equilibria.pdf

21. Langmuir adsorption isotherm, accessed Feb 2015, http://infohost.nmt.edu/~jaltig/Langmuir.pdf

22. GAC, accessed Mar 2015, http://carbonair.com/granular-activated-carbon-gac/

23. Accessed Mar 2015, http://www.health.state.mn.us/divs/eh/hazardous/sites/washington/oakdalewell.html

24. Accessed Mar 2015, http://www.usbr.gov/pmts/water/publications/reportpdfs/Primer%20Files/07%20-%20Granular%20Activated%20Carbon.pdf

25. S. T. Lee, N. S. Ramesh, Polymeric Foams: Mechanisms and Materials, CRS Press, 2004

26. R. McBryer, Polyurethane foams formulation and manufacture, Technomic Publishing – 1999, 100 pages

27. M. Szycher, Szycher's handbook of polyurethanes, CRC Press, 1999

28. K. Ashida, Polyurethane and related foams – chemistry and technology, CRC press, Sep 22, 2006.

29. L. Zhang, Structure-property relationship of polyurethane flexible foam made from natural oils, Dissertation, University of Minnesota (2008)

30. M. Chanda, S. K. Roy, Plastics Technology Handbook, Third Edition, CRC Press, Apr 10, 1998, Chapter 2.

31. Merquinsa, what is polyurethane? Accessed Nov 2011, http://www.merquinsa.com/whats/whatsaPU.pdf

32. Understanding Chain Extenders and Crosslinkers, SpecialChem - Jul 21, 2004

33. G. Woods, Flexible polyurethane foams, chemistry and technology, Appl Sci Pub Ltd, Essex, England, 1982.

34. Aneja, Polyurethane foams review, chapter 2, 2002, vt.edu, http://scholar.lib.vt.edu/theses/available/etd-12032002-170009/unrestricted/03.pdf

35. D. Eaves, Handbook of Polymer Foams, iSmithers Rapra Publishing, Jan 1, 2004 - Technology & Engineering - 289 pages

36. H. J. M. Bowen, Absorption by polyurethane foams: new method of separation, J. Chem. Soc., A 1082 (1970)

37. D. C. Venerus and N. Yala, Transport analysis of diffusion-induced bubble growth and collapse in viscous liquids, AIChE Journal, 43(11), 2948–2959, 1997

38. J. G. Lee et al, A refined approach to bubble nucleation and polymer foaming process: dissolved gas and cluster size effects, Journal of Colloid & Interface Science, 184(2), 335–348, 1996.

39. S. T. Lee, N. S. Ramesh, Polymeric Foams: Science and technology, CRS Press, 2007

40. Blowing Agents and Foaming Processes, iSmithers Rapra Publishing, Jan 1, 2004 - Foam rubber - 212 pages

41. H. D. Gesser, A. Chow, F. C. Davis, J. F. Uthe, J. Reinke, The extraction and recovery of polychlorinated biphenyls (PCB) using porous polyurethane foam, Anal. Lett. 4 (1971) 883.

42. T. Braun, A. B. Farag, Foam chromatography, solid foams as supports in column chromatography, Talanta 19 (1972) 828.

43. T. Braun, A. B. Farag, Reversed-phase foam chromatography - Separation of palladium, bismuth and nickel in the tributyl–phosphate–thiourea–perchloric acid system, Anal. Chim. Acta 61 (1972) 265.

44. T. Braun and A. B Farag, Polyurethane foams and microspheres in analytical chemistry: Improved Liquid–Solid, Gas-Solid and Liquid-Liquid contact via a new geometry for the solid phase", Analyticachimicaacta, 99(1) (1978) 1-36

45. V. A. Lemos et al., Application of polyurethane foam as a sorbent for trace metal pre-concentration — A review, Spectrochimica Acta Part B 62 (2007) 4–12.

46. D. W. Lee, M. Halmann, Selective separation of nickel (ii) by dimethyl-glyoxime-treated polyurethane foam, Anal. Chem. 48 (1976) 2214 – 2218.

47. A. Ramesh, K. R. Mohan, K. Seshaiah, N. D. Jegakumar, Determination of trace elements by inductively couple d plasma-atomic emission spectrom-etry (ICP-AES) after preconcentration on a support impregnated with piperidine dithiocarbamate, Anal. Lett. 34 (2001) 219 – 229

48. Cellular plastics, Proc. Conf., Natick, Massachutessetts, 1996, National Academy of sciences, National research Council, Washington, D.C., 1967.

49. E. A. Moawed, M. A. A. Zaid, M. F. El-Shahat, Analytical application of polyurethane foam functionalized with quinolin-8-ol for preconcentration and determination of trace metal ions in wastewater, J Anal Chem+, September 2006, Volume 61, Issue 5, pp 458-464

50. J. G. A. Terlingen, Introduction of functional groups at polymer surfaces by Glow discharge techniques, Europlasma tech paper, Ch 2

51. V. A Lemos, L. N. Santos, A. P. Alves, G. T. David, Chromotropic acid-functionalized polyurethane foam: A new sorbent for on-line pre-concentration and determination of cobalt and nickel in lettuce samples, J. Sep. Sci. 2006 Jun;29(9):1197-204

52. S. V. S Rao et al. treatment of low level radioactive liquid wastes using composite ion-exchange resins based on polyurethane foam, J. Radioanal Nucl Chem (2010) 283:379-384

53. D. Fournier, B.G. De Geest, Filip E. Du Prez, On-demand click functionalization of polyurethane films and foams, Polymer, Volume 50, Issue 23, 3 November 2009, Pages 5362-5367

54. R. J. Krupadam, M. S. Khan, S. Das, Adsorption of fluoride from water by surface-functionalized polyurethane foam, Water Sci Technol. 2010;62(4):759-65. doi: 10.2166/wst.2010.190

55. G. A. Meligi, Removal of Some Heavy Metal Ions Using Grafted Polyurethane Foam, Polym-Plast Technol, 2008, 47: 106–113

56. S. H. Jang, B. G. Min, Y. G. Jeong, W. S. Lyoo, S. C. Lee, Removal of lead ions in aqueous solution by hydroxyapatite/polyurethane composite foams, J Hazard Mater. 2008, 152(3), 1285-92

57. H. Sone, B. Fugetsu, S. Tanaka, Selective elimination of Pb(II) ions by alginate/polyurethane composite foams, J Hazard Mater. 2009, 162(1), 423-9

58. S. H. Moon et al., Preparation and characterization of cation-exchange media based on flexible polyurethane foams, J. of applied polymer science, 86 (2002) 1773-1781

59. N. M. K. Lamba, K. A. Woodhouse, S.L. Cooper, Polyurethanes in Biomedical Applications, CRC Press, Medical; 1997, pp 74-79.

60. D. C. Allport, D. S. Gilbert, S. M. Outterside, MDI & TDI: Safety, Health and the Environment, John Wiley & Sons, May 2003, pp 298

61. N. Mills, Polymer Foams Handbook: Engineering and Biomechanics Applications and Design Guide, Butterworth-Heinemann, Mar 23, 2007 - Technology & Engineering

62. P. X. Ma and J. Choi, Biodegradabel polymer scaffolds with well-defined interconnected spherical pore network, Tissue Eng, Vol 7, No. 1, 2001

63. S. K. Annapragada, Mechanism of foaming on polymer-paperboard composites, PDH thesis, Georgia institute of technology, Dec 2007

64. Cellular Polymers, iSmithers Rapra Publishing, 1993 – Foamed materials – 200 pages

65. TDI, accessed Oct 2013, http://en.wikipedia.org/wiki/Toluene_diisocyanate

66. PPG, accessed Oct 2013, http://en.wikipedia.org/wiki/Polypropylene_glycol

67. BES, accessed Oct 2013, http://www.chemblink.com/products/10191-18-1.htm

68. DMSO, accessed Oct 2013, http://en.wikipedia.org/wiki/Dimethyl_sulfoxide

69. R. Vignes, DMSO-A new clean, unique, superior solvent, American Chemical society, 2000, accessed February 2014, http://www.ac-limoges.fr/physique-chimie/IMG/pdf/vignes-acs.pdf

70. R. Borchardt, Pharmaceutical Profiling in Drug Discovery for Lead Selection, springer science & business media, 2005 pp 110-115

71. R. Vignes, DMSO-A new clean, unique, superior solvent, American Chemical society, 2000, accessed February 2014, http://www.ac-limoges.fr/physique-chimie/IMG/pdf/vignes-acs.pdf

72. R. Borchardt, Pharmaceutical Profiling in Drug Discovery for Lead Selection, springer science & business media, 2005 pp 110-115

73. C. G. Zimba and J. F. Rabolt. Raman Spectroscopic Characterization and Molecular Force Field Development of a Synthetic Polyamide: Nylon 66. Macromolecules 1989, 22, 2863-2867

74. P. J. Hendra et al, The Laser-Raman Spectra of some Nylons, Chem. Comm. (1970)

75. M. Gharg et al, FTIR analysis of high energy heavy ion irradiated kapton-H polyimide, Indian Journal of Pure & Applied Physics, Vol. 45, July 2007, pp 563-568

76. S. Gunashekar, N. Abu-Zahra, Synthesis of Functionalized Polyurethane Foam using BES Chain Extender for Lead Ion Removal from Aqueous Solutions, J. Cell. Plast.,0,0 (2014) pp 1-18

77. Why is GPC important? Accessed Apr 2012, http://www.waters.com/waters/en_US/GPC---Gel-Permeation-Chromatography/nav.htm?cid=10167568&locale=en_US

78. S. Gunashekar, N. Abu-Zahra, Characterization of Functionalized Polyurethane Foam for Lead Ion Removal from Water, International Journal of Polymer Science, (2014) doi:10.1155/2014/570309

79. Accessed Mar 2015, http://web.pdx.edu/~pmoeck/phy381/Topic5a-XRD.pdf

80. XRD, accessed Mar 2015, http://www.chem.sc.edu/faculty/zurloye/xrdtutorial_2013.pdf

81. SEM, accessed Mar 2015, http://serc.carleton.edu/research_education/geochemsheets/techniques/SEM.html

82. Reticulate PU foams, accessed Mar 2015, http://www.ufpt.com/materials/foam/reticulated-polyurethane-foam.html

83. V. Mittal, Polymer Nanocomposite Foams, CRC Press, Oct 18, 2013 - Technology & Engineering - 264 pages, ch 6

84. K. Boomsma, D. Poulikakos, The effects of compression and pore size variations on the liquid flow characteristics in Metal foams, ASME J Fluids Eng. 124 (2002) pp 263-272.

85. Micro-CT, accessed Mar 2015, https://www.bruker.com/products/x-ray-diffraction-and-elemental-analysis/x-ray-micro-ct.html

86. Importance of Density, accessed Mar 2015, http://www.pfa.org/intouch/new_pdf/lr_IntouchV1.2.pdf

87. ASTM D 3574 - Standard Test Methods for Flexible Cellular Materials—Slab, Bonded, and Molded Urethane Foams, ASTM Volume 08.02 Plastics (II): D3222 D5083.

88. S. Gunashekar, K. M. Pillai, B. C. Church, N. H. Abu-Zahra, Liquid flow in polyurethane foams for lead-ion filtration: A study on their characterization and permeability estimation, Journal of Porous Materials, 2015, 10.1007/s10934-015-9948-2

89. A. N. Gent, K. C. Rusch, Permeability of open-cell foamed materials, J. Cell. Plast., 2, 1 (1966) pp 46-51

90. R. Masoodi, K. M. Pillai, Wicking in Porous Materials: Traditional and Modern Modeling Approaches, CRC Press, Technology & Engineering; 2012, pp 80-81

91. N. J. Mills, The wet kelvin model for air flow through open-cell polyurethane foams, J. Mater. Sci., 40 (2005) pp 5845-5851

92. M. A. Dawson, J. T. Germaine, L. J. Gibson, Permeability of open-cell foams under compressive strain, Int. J Solids Struct., 44, 16 (2007) 5133-5145, ISSN 0020-7683.

93. P. Pichat, Photocatalysis and Water Purification: From Fundamentals to Recent Applications, John Wiley & Sons - Technology & Engineering, 2013, part II, ch -6

94. N. C. Hilyard, P. Collier, A structural model for air flow in flexible PUR foams, Cellular Polymer, 6, 6 (1987) pp 9-26.

95. J. Bear, Dynamics of Fluids in Porous Media, American Elsevier, New York; 1972.

96. T. W. Lambe, Soil Mechanics, John Wiley & Sons, Technology & Engineering; 1969, pp 281.

97. H. Darcy, Les Fontaines Publiques de ville de Dijon., Dalmont, Paris, (1856).

98. D. Edouard, M. Lacroix, C. Pham, M. Mbodji and C. Pham-Huu, Experimental measurements and multi-phase flow models in solid SiC foam beds. AIChE J 54, 11 (2008) pp 2823-2832

99. ICP-MS , accessed Mar 2015, http://eecelabs.seas.wustl.edu/ICP-MS.aspx, http://em-.stanford.edu/Schedule/ICP/MakingICPStd.asp

100. Z. Alfassi, C. M. Wai, Preconcentration Techniques for Trace Elements, CRC press, Dec 1991.

101. D. W. Van-Krevelin, Chapter 13 - Properties of Polymers, 3rd Edition, Elsevier, New york, 18, 1990.

102. Investing in Water, accessed Mar 2015, http://www.impaxam.com/sites/default/files/investing_in_water_global_opportunities_in_a_growth_sector_all_final.pdf

103. Accessed Mar 2015, http://www.theguardian.com/environment/2012/nov/30/climate-change-water

104. Accessed Mar 2015, http://legacy.london.gov.uk/assembly/reports/pubserv/water.pdf

105. Water Utilities, accessed Mar 2015, http://www.lucintel.com/reports/energy/water_utilities_industry_2012_2017_trends_foreacast_april_2012.aspx

106. Accessed Mar 2015, http://www.prnewswire.com/news-releases/global-water-utilities-industry-2012-2017-trend-profit-and-forecast-analysis-177480341.html

107. Accessed Mar 2015, http://www.waterworld.com/articles/2014/07/rising-industrial-production-drives-the-global-water-and-wastewater-treatment-equipment-market.html

108. Accessed Mar 2015, http://www.freedoniagroup.com/industry-study/3052/water-treatment-equipment.htm

109. Accessed Mar 2015, http://livehealthy.aquasana.com/2010/08/what-is-the-difference-between-a-point-of-entry-and-a-point-of-use-water-filter-system/

110. Accessed Mar 2015, http://environment.nationalgeographic.com/environment/green-guide/buying-guides/water-filter/shopping-tips/

111. Accessed Mar 2015, http://www.health.state.mn.us/divs/eh/water/factsheet/com/pou.html

112. Accessed Mar 2015, http://www.purewaterproducts.com/reverse-osmosis/

113. Accessed Mar 2015, http://www.isopurewater.com/product.asp?itemid=3580&gclid=CP-9oJ7o_8QCFQqSaQodlEIArA

114. Accessed Mar 2015, http://www.crystalquest.com/whole-house-water-filters.htm

115. Accessed Mar 2015, https://www.google.com/search?q=PoE+RO&ie=utf-8&oe=utf-8#tbm=shop&q=PoU+ion+exchange+resins

116. Accessed Mar 2015, https://www.google.com/search?q=PoE+RO&ie=utf-8&oe=utf-8#tbm=shop&q=PoE+carbon+filters&spd=8784507455555212364

117. Accessed Mar 2015, https://www.google.com/search?q=PoE+RO&ie=utf-8&oe=utf-8#q=PoU+carbon+filters+cost

118. Accessed Mar 2015, http://www.amazon.ca/Watts-Premier-WP5-50-Five-Stage-Treatment/dp/B000E77I04

Appendix A

Mercury porosimetry was attempted to estimate the porosity of the foams. In this method, the sample is dipped in a pool of mercury and the latter is gradually pressurized. As a result, the non-wetting mercury is progressively forced into the pores of the porous (sponge) sample with larger pores getting filled up before the smaller ones. The total volume of mercury thus pushed into the porous medium equals the total pore volume. The porosity is estimated by dividing the pore volume by the sample volume. Due to the relation between mercury pressure and pore size, it is also possible to estimate the pore size distribution in the sample.

The porosity measured by mercury porosimetry showed that the porosity of F0 foam sample was 65.3% while the pore size varied from 100μm to 20μm. Samples F1 and F2 returned considerably lower porosities values of 13.4% and 10.2%, respectively. All of the mercury test samples were of similar size and geometry; visual examination suggested similar porosity levels. A mercury intrusion test should result in a penetrometer stem volume change between 33 and 90%. Samples F1 and F2 showed a penetrometer stem volume change of 2 and 3% respectively indicating that mercury did not enter the samples as pressure was applied during the test. The mercury test assumes that mercury is non-wetting on the sample surface; such that upon initial filling of the sample penetrometer, the mercury comes into contact with the sample but does not penetrate into the structure. The low porosity numbers obtained from the F1 and F2 samples suggest that the functionalized foam increases the wettability of mercury by reacting with its sulphonic groups, thus making the mercury porosimetry method unsuitable for porosity measurements with these samples.

Curriculum Vitae

Subhashini Gunashekar

Place of Birth: Mysore, India

Education:

BE, Sri Jayachamarajendra College of Engineering, June 2004
Major: Polymer Science and Technology

MS, University of Wisconsin – Milwaukee, December 2012
Major: Materials Science and Engineering

PHD, University of Wisconsin – Milwaukee, May 2015
Major: Materials Science and Engineering, Minor: Business Management

Dissertation title: A Study on the Synthesis – Structure – Property – Performance Relationship of Bulk Functionalized Polyurethane Foams for Water Filtration Applications

Internship: AO Smith Corporate Technology Center, Milwaukee, WI, June 2014 – August 2014

Peer Reviewed Journal Publications:

1. Manasa Nayani, Subhashini Gunashekar, and Nidal Abu-Zahra, *Synthesis and Characterization of Polyurethane-Nanoclay Composites*, International Journal of Polymer Science, vol. 2013, Article ID 717895, 5 pages, **2013**. doi:10.1155/2013/717895

2. Subhashini Gunashekar and Nidal Abu-Zahra, *Synthesis of Functionalized Polyurethane Foam for Lead Ion Removal from Water*, Journal of Cellular Plastics, **2014**, 0(0), 1-18

3. Subhashini Gunashekar and Nidal Abu-Zahra, *Characterization of Functionalized Polyurethane Foam for Lead Ion Removal from Water*, International Journal of Polymer Science (IJPS), vol. 2014, Article ID 570309, 7 pages, **2014**. doi:10.1155/2014/570309

4. Nidal Abu-Zahra and Subhashini Gunashekar, *Structurally functionalized polyurethane foam for elimination of lead ions from drinking water*, Journal of Research Updates in Polymer Science (JRUPS), **2014**, 3(1), 16-25, DOI: http://dx.doi.org/10.6000/1929-5995.2014.03.01.3

5. Subhashini Gunashekar, Krishna Pillai, Ben Church, Nidal Abu-Zahra, *Liquid flow in polyurethane foams for lead-ion filtration: A study on their characterization and permeability estimation*, Journal of Porous Materials, 22(3), **2015**, pp 749-759, doi:10.1007/s10934-015-9948-2

6. Subhashini Gunashekar and Nidal Abu-Zahra, *Studies on the structure – performance relationship of bulk functionalized polyurethane foams designed for lead ion removal from water*, Water Science and Technology, **2015** (in preparation)

7. Parisa Khoshnoud, Subhashini Gunashekar, Murtatha M. Jamel, Nidal Abu-Zahra, *Comparative Analysis of Rigid PVC Foam Reinforced with Class C and Class F Fly Ash*, Journal of Minerals and Materials Characterization and Engineering, **2014,** 2, 554-565 doi:10.4236/jmmce.2014.26057

8. Parisa Khoshnoud, Murtatha M. Jamel, Subhashini Gunashekar, Nidal Abu-Zahra, *Characterization of Rigid PVC Foam Composites Reinforced with Fly Ash*, Journal of Applied Polymer Science, **2015** (in press)

9. Aruna P. Wanninayake, Subhashini Gunashekar, Shengyi Li, Benjamin C. Church, Nidal Abu-Zahra, *CuO Nanoparticles Based Bulk Heterojunction Solar Cells: Investigations on Morphology and Performance*, J. Sol. Energy Eng. 137(3), 031016, **2015,** 7 pages; Paper No: SOL-14-1293; doi:10.1115/1.4029542

10. Aruna P. Wanninayake, Subhashini Gunashekar, Shengyi Li, Benjamin C. Church, Nidal Abu-Zahra, *Performance Enhancement of Polymer Solar Cells using Copper Oxide Nanoparticles*, Semicond. Sci. Technol. ,Special Issue on Organic Photovoltaics, **2015** (in press)

11. Aruna P. Wanninayake, Subhashini Gunashekar, Shengyi Li, Benjamin C. Church, Nidal Abu-Zahra, *Effect of Thermal Annealing on the Power Conversion Efficiency of CuO-Bulk Heterojunction P3HT/ PC70BM Solar cells*, Journal of Sustainable Energy Engineering, **2015** (in press)

12. Murtatha M. Jamel, Parisa Khoshnoud, Subhashini Gunashekar, Nidal Abu-Zahra, *Enhancement of Dimensional Stability of Rigid PVC Foams using E-Glass Fibers*, Journal of Minerals and Materials Characterization and Engineering, **2015**, Vol 3, No. 2, 65-75. doi: 10.4236/jmmce.2015.32009

13. Murtatha M. Jamel, Parisa Khoshnoud, Subhashini Gunashekar, Nidal Abu-Zahra, *Mechanical Properties and Dimensional Stability of Rigid PVC Foam Composites Filled with High Aspect Ratio Phlogopite Mica*, Journal of Minerals and Materials Characterization and Engineering, **2015** (in press)

14. Murtatha M. Jamel, Parisa Khoshnoud, Subhashini Gunashekar, Nidal Abu-Zahra, *Effect of E-Glass Fibers and Phlogopite Mica on the Mechanical Properties and Dimensional Stability of Rigid PVC Foams*, Journal of Polymer-Plastics Technology and Engineering, **2015** (in Press)

Conference Papers:

1. Tribological properties of fly ash based green friction products, Pradeep K. Rohatgi, Pradeep L. Menezes, Subhashini Gunashekar and Michael R. Lovell, Proceedings of Third International Workshop on Advances in Asbestos Free Friction Composites (IWAAFC-III), Delhi, India, 2011, 63-69

2. Functionalized PU Foam for Water Filtration, Nidal H. Abu-Zahra, Subhashini Gunashekar, World Academy of Science, Engineering and Technology, International Journal of Chemical, Materials Science and Engineering (IJCMS) Lisbon, Portugal, 2014, 8(4), 241-245

3. Effect of Glass Fibers on the Dimensional Stability and Strength of Rigid PVC Foams, Abu-Zahra, N., Jamel, M., Khoshnoud, P., Gunashekar, S., World Academy of Science, Engineering and Technology, International Science Index, Materials Science and Engineering, 2014, 2(9), 486.

4. Effect of Fly Ash on the Mechanical and Thermal Properties of Rigid PVC Foams, Abu-Zahra, N., Khoshnoud, P., Jamel, M., Gunashekar, S., World Academy of Science, Engineering and Technology, International Science Index, Materials Science and Engineering, 2014, 2(9), 488.